RESERVOIR ANALYSIS BASED ON COMPOSITIONAL GRADIENTS

A DISSERTATION
SUBMITTED TO THE DEPARTMENT OF ENERGY RESOURCES ENGINEERING
AND THE COMMITTEE ON GRADUATE STUDIES
OF STANFORD UNIVERSITY
IN PARTIAL FULFILLMENT OF THE REQUIREMENTS
FOR THE DEGREE OF
DOCTOR OF PHILOSOPHY

By
Olubusola Thomas
February 2007

I certify that I have read this thesis and that in my opinion it is fully adequate, in scope and in quality, as a dissertation for the degree of Doctor of Philosophy.

Prof. Roland N. Horne
(Principal Adviser)

I certify that I have read this thesis and that in my opinion it is fully adequate, in scope and in quality, as a dissertation for the degree of Doctor of Philosophy.

Prof. L. Durlofsky

I certify that I have read this thesis and that in my opinion it is fully adequate, in scope and in quality, as a dissertation for the degree of Doctor of Philosophy.

Prof. H. Tchelepi

Approved for the University Committee on Graduate Studies.

Abstract

Variations in fluid composition as a function of location within a reservoir have been observed in oil and gas reservoirs around the world. This is usually referred to as compositional variation. Over the many years that is takes a reservoir to form, processes such as oil migration, fluid convection and diffusion play important roles in the development of compositional gradients particularly in reservoirs with horizontal and vertical temperature gradients.

This study used the general mass and energy balance equations to simulate fluid movement within a nonproducing reservoir with thermal gradients. The configuration of fluid components and heat within the reservoir is characterized using various metrics such as the Nusselt and Rayleigh numbers, as well as separation and density factors. These metrics are able to show, in a concise manner, the effect of changes in the reservoir and fluid properties on compositional variations.

It was observed in this study, that for multicomponent fluids in reservoir with compositional gradients, the movement of fluid components compensates for the drastic change in thermal gradients that is typically noticed in single-component, single-phase fluids, such as water, heated from below. Changes in different reservoir properties impact the compositional variation in different ways, for example, a change in the reservoir thickness results in a moderate change in the distribution of components, while a change in reservoir thermal gradients results in a drastic shift in the distribution of components.

Reservoir heterogeneity was found to play an important role in the variation of components, as well as the transfer of heat within the reservoir. It was also observed that because convection and diffusion in nonproducing reservoirs are slow processes and the diffusion terms are small in magnitude, the effect of variable diffusion coefficients was negligible. Other observations include a consistency in the results obtained irrespective of the grid size used, for example, the three-dimensional grids produced the same average pressure, temperature, composition and velocity profiles as the two-dimensional grids for certain reservoir configurations.

Acknowledgements

I am indebted to my family, my parents, Mr. and Mrs. Thomas, for laying the foundation and challenging me to always give my best in everything, my brothers, Dapo, for always looking out for me, and Kunle and Laolu. I am also thankful for my husband Godwin, for his support and for my little angel, Jason, for making me see the light at the end of the tunnel.

I would like to thank Professor Roland Horne, my advisor, for his guidance during my M.S. and Ph.D. programs. I am grateful to him for the flexibility in allowing me to explore areas that are of interest to me, for his ingenuity in looking at things from different perspectives and especially for his understanding during the last year of my program.

I am grateful to SUPRI-D, the Consortium on Innovation in Well Testing, for the financial support over the past six and a half years that I have spent at Stanford. This study was made possible by it.

Many thanks to the entire department of Energy Resources Engineering (formerly Petroleum Engineering) at Stanford University. To the faculty, students and staff, for sharing knowledge, great friendships and immense support. Thanks to Yuguang Chen, Josephina Schembre, Gracel Diomampo, Mark Habana, Yolanda Williams, Ginni Savalli, and Sandy Costa.

My internships at ConocoPhillips and Chevron were of great help to me particularly with respect to Well Testing and Reservoir Characterization.

Thanks to my friends Damilola Ogunlana, Tunde Oyenekan and Chineme Ekweani, my sisters Priscilla Ajao, Sike Akerele, Winifred Adams and Chioma Osondu, and Tola and Dapo Akerele. Ms. Holloway, thank you for all those candles you kept burning. Professors Oloko and Bello, thank you for your invaluable advice and prayers.

"All things work together for good to them that love God".
To my little angel

Contents

List of Tables

List of Figures

Chapter 1

Introduction

1.1 Background

During the initial appraisal and development of an oil or gas reservoir, the aim is to conceive a development strategy that will give maximum value in exchange for minimum expenditure. The main tool behind this development is the reservoir model, which comprises details of the reservoir in terms of rock and fluid properties. With all the technological advances that have been made in the oil and gas industry, the description of the reservoir now contains a lot more detail than the 'layer-cake', single-component, single-phase model of years gone by. Data obtained from wells is no longer limited to pressure only; data on temperature, in-situ stress, and fluid composition are also available. This increase in detail takes into account, to some degree, the presence of multicomponent mixtures, structures, heterogeneity and thermal gradients. In general, reservoir fluids in the preproduction stage are assumed to be static, while the temperature gradients in the reservoir are assumed to be negligible. These assumptions simplify computations but are not necessarily valid for all reservoirs. For example, the assumption of negligible thermal gradients does not hold for deep and tilted reservoirs.

Vertical and/or areal compositional variations have been found to occur in reservoirs around the world. Vertical compositional variations have been observed in many

reservoirs, and documented in the literature. Padua (1997, 1999) reported compositional variations in an oil-saturated sandstone reservoir in the Campos Basin in Brazil. Others including Metcalfe et al. (1988) and Schulte (1980) have noted vertical compositional variations in the Anschutz Ranch East field, and the Brent and Statfjord reservoirs of the North Sea Brent fields respectively. Horizontal compositional variations, in addition to those in the vertical plane, have also been documented, for example, Hamoodi et al. (1994) noted this occurrence in a reservoir in the Middle East, while Temeng et al. (1998) documented the decrease of condensate content and hydrocarbon compositions and the increase of acid gas content with depth and/or with temperature in the Ghawar Khuff reservoirs in Saudi Arabia.

The occurrence of vertical compositional gradients is generally believed to be caused by capillary forces, gravity and/or vertical temperature gradients, usually geothermal gradients. The presence of horizontal and vertical variations in fluid compositions may be attributed to a number of factors, the presence of additional driving forces, such as chemical reactions, diffusion and horizontal thermal gradients. Horizontal and vertical temperature gradients influence the distribution of fluid components greatly. In turn, the distribution of fluid components may be used for reservoir characterization, such as determining the presence of structures and the extent of a reservoir. This study seeks to gain a better understanding of these occurrences and develop a process by which such information can be used to improve the characterization of reservoirs, i.e. this study is concerned with the effect of thermal gradients on multicomponent reservoir fluids.

1.2 Problem Statement

The gathering of information about a reservoir at any stage of development is geared towards more accurate predictions of reservoir productivity. This study seeks to improve the understanding and characterization of reservoirs with vertical and horizontal compositional variations due to interplay of heterogeneity, diffusion, natural convection and other forces that may affect the distribution of fluids in porous media. The motivation behind this work lies in the desire to be able to:

1. portray the current and past states of fluid pressure and temperature,
2. delineate drainage areas accurately,
3. predict the chemical distribution,

in such reservoirs.

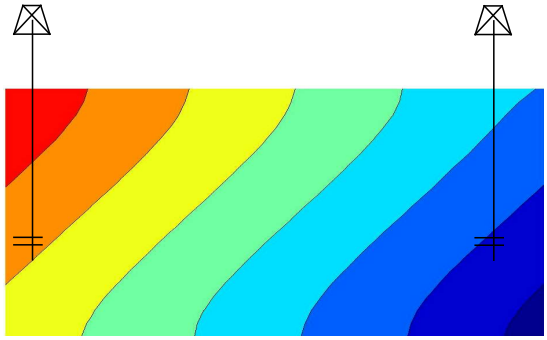

Figure 1.1: Composition profile in a reservoir with compositional variation.

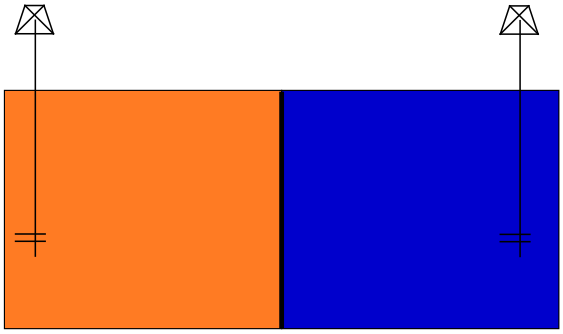

Figure 1.2: Composition profile in a reservoir with two drainage areas bounded by a fault.

When a reservoir is produced from two wells A and B and the fluid compositions at the wells differ, questions arise as to the reason why this would occur. Are the wells draining from different drainage areas, separated by a boundary as depicted in Figure

1.2 or is there some form of compositional variation that has not been accounted for, as depicted in Figure 1.1? Figures 1.1 and 1.2 show two conceptual reservoirs with different fluid distributions.

Questions about reservoir delineation and fluid distribution are important in determining not only hydrocarbon reserves but also in making decisions on well placement and recovery mechanisms. The analysis of compositional variation may also be applied to predicting the distribution of components in natural gas reservoirs. Although previous authors have tried to solve the problem of analyzing compositional variations, there are still limitations to be resolved.

Temperature distribution: the inclusion of the energy equation in problems such as these is important, particularly because the movement of fluids within the reservoir also results in the movement of energy. In general, most studies include the effect of temperature by imposing a linear temperature profile on the reservoir. The initial assumption of a linear temperature profile may be accurate, but there may be substantial changes as time goes on and fluids move within the reservoir. Since thermal gradients influence the distribution of components and due to these gradients fluids will move and in moving transport energy, the temperature profile of the reservoir will change continuously as the dynamic state of the reservoir keeps changing.

Fluid compressibility: fluids in reservoirs at high pressures are compressible. The assumption that the effect of pressure on fluid density is minimal (Boussinesq approximation) is not an accurate assumption to make particularly when dealing with hydrocarbons under high pressure. Therefore, a better approach through the use of an equation of state that incorporates this dependence would be advantageous.

The three-dimensional problem: reservoirs are three-dimensional entities. Most studies (Ghorayeb and Firoozabadi, 2000a, for example) have been limited to the x-z plane. The three-dimensional effect is particularly important in tilted reservoirs. Thus, there should be an extension to three dimensions. Although

the introduction of a third dimension increases the computational cost of the solution, to fully understand the interaction of the different processes, a three-dimensional reservoir model should be used.

Effect of boundaries: boundary here refers to any structures that impart heterogeneity, either faults or actual boundaries. The boundary conditions imposed on the system of equations are important and will affect the solution of the problem. The effect of faults and channels on compositional variation should be included in such studies so that reservoir characterization is not limited to 'simple' reservoirs.

Phase changes: depending on the range of temperature and pressure that fluids are subjected to, there could be phase changes. The quantity of heat transferred will increase when there is vaporization or condensation of the reservoir fluid. This should be taken into consideration particularly when the fluid lies in the retrograde region of its phase diagram.

There are other unresolved issues of less importance.

1.3 Scope of this Work

There are a number of areas in which more work is required in order to make better use of the information from compositional gradients to characterize oil and gas reservoirs. Some were listed in the previous section on the problem statement. In this study, a number of issues were addressed, namely;

Inclusion of the energy balance - This takes into account heat transfer in and out of the reservoir from and to the underburden and overburden. It also accounts for heat transfer due to convection as well as conduction.

Inclusion of fluid compressibility - The use of a cubic equation of state, such as the Peng-Robinson equations and a flash routine takes into account the change in composition and fluid density as a function of pressure and temperature which

are both dynamic variables. Also the fluid viscosities are computed based on fluid composition and reservoir pressure and temperature.

Effect of heterogeneity - So far in the literature, reservoirs with homogeneous permeability fields were used. In this work, the effect of heterogeneity on compositional gradients was investigated.

Use of three-dimensional grids - Three-dimensional grids were used to portray the reservoir in order to test the accuracy of representing the reservoir as a two-dimensional x-z entity.

Effect of variable diffusion coefficients - Diffusion coefficients like other fluid properties are functions of pressure, temperature and for multicomponent mixture, composition. The effect of this dependence on compositional gradients was investigated.

Chapter 2

Literature Review

There are various fields in which compositional variations have been observed. The application of this idea encompasses a variety of areas, from oceanography, chemistry, metallurgy and material science to geology, geophysics and petroleum engineering (Turner, 1974, 1985). A number of authors have looked at compositional variation in hydrocarbon reservoirs with a view to improving the characterization of such reservoirs. The relevant literature comprises research on natural convection, double-diffusive phenomena and multicomponent convection in porous media both in terms of numerical solutions and stability analysis.

2.1 Natural and Double-Diffusive Convection

Natural convection can be defined as the flow induced by density gradients caused by temperature differences. Double-diffusive convection is flow due to simultaneous heat and mass transfer. For this phenomenon to occur, the minimum requirements are:

1. The fluid must contain at least two components with different molecular diffusivities.

2. These components must make opposing contributions to the vertical density gradient (Turner, 1974).

It is this difference in diffusivities that generally produces differences in buoyancy that drive fluid motion. In this area, different scenarios have been studied, both numerically and experimentally, for example, a horizontal fluid layer being heated from below (referred to as the Rayleigh-Benard problem), thermohaline (heat and salt) convection, as well as isothermal ternary fluid systems. The Rayleigh-Benard problem may be applied to geothermal convection and heat transport due to the burial of nuclear waste in mountains or in a seabed.

Horne (1975) analyzed transient geothermal convective systems. In his work, Horne conducted experiments which showed that at Rayleigh numbers of approximately 1000 and 1600, two flow regimes persist. The first is steady convective and the second exhibits fluctuations with smaller circulation cells developing between the larger, more dominant circulations cells in two dimensions. From his numerical work on single-phase and thermohaline mixtures, in both two and three dimensions, Horne corroborated the experimental results and also concluded that the system configuration, such as boundary conditions, as well as the flow equations, is important in determining the flow regime prevalent in a reservoir under any set of conditions of temperature and pressure.

Wood and Hewett (1982) investigated convection as a mode of mass transfer with a view to explaining the processes that occur in rock diagenesis. They observed that although the velocities present under normal geothermal gradients are of the order of 1 meter per year, over a long period of time, changes in rock porosity may occur due to processes such as cementation of natural sandstones. Wood and Hewett also concluded that the eddies that arise in the reservoir due to temperature gradients persist because of the difficulty associated with establishing equilibrium conditions in reservoirs with temperature gradients.

Riley and Firoozobadi (1998) investigated the effect of natural convection and diffusion on a binary, single-phase fluid in a reservoir with a horizontal temperature gradient. This investigation appears to be the first in a series of works by Firoozobadi and others on the subject matter. The importance of this group of investigations is the inclusion of thermal, pressure and Fickian diffusion. Riley and Firoozobadi looked at the interplay of various parameters and concluded that increasing permeability does

not necessarily cause a decrease in the horizontal compositional variation and that the thermal diffusion influences the distribution of components particularly in the case where the permeability approaches zero.

2.2 Multicomponent Convection in Porous Media

The criteria for multicomponent convection to occur are very much the same as those for double-diffusive convection:

1. The fluid must contain at least two components with different molecular diffusivities, each of which affects the density of the fluid.

2. Differential or coupled diffusion can produce convective motions that are associated with a decrease in the gravitational potential energy of the system (Turner, 1985).

It is not necessary for the net vertical density gradient to change sign and become unstable for convection to occur. Double-diffusive convection can develop under less stringent conditions, which allow local density anomalies while the horizontally averaged vertical density gradient remains negative (Turner, 1985).

Moser (1986) studied the preproduction state of gas reservoirs with binary, incompressible mixtures, subject to geothermal temperature gradients (both vertical and horizontal). He concluded that the steady-state flow regime is nonunique. He also concluded that there are two stable fluid configurations, namely; the convection-dominated and the diffusion-dominated states. In the former, the composition of the gas mixture is approximately uniform and there is strong convection due to buoyancy while the latter is dominated by strong gradients in the gas composition and weak convection due to thermal gradients.

Jacqmin (1985, 1990) was one of the first people to investigate the interaction of thermally-induced convection and gravity segregation on hydrocarbon fluids in porous media with horizontal and vertical temperature gradients. He found that for a weak temperature gradient, the fluids redistribute themselves in the reservoir so as to compensate for the horizontal density differences. Jacqmin concluded that the natural

state of the fluids in a reservoir is a dynamic one and the compositional variation observed in some reservoirs is due to the interaction between gravity segregation and natural convection. Jacqmin, like Moser (1986) concluded that the solutions were nonunique.

Schulte (1980) investigated compositional variations in a hydrocarbon column due to gravity. Using well known cubic equations of state, such as the Peng-Robinson equation, Schulte solved the Gibb's sedimentation equation for compositional variations as a function of depth. He was able to use his results to explain the occurrence of natural miscibility in reservoirs as due to the gradually changing compositions in the hydrocarbon column. Schulte also noted that these compositional variations depend not only on pressure, but also on the presence of aromatic compounds and other parameters that depend on the nature of the fluid system. Other authors, such as Hamoodi et al. (1994), Metcalfe et al. (1988) have also approached this problem by looking at an equation of state model.

The works of Padua (1997, 1999) were prompted by the observation of significant fluid compositional variations in a large deep-water field in Brazil. Padua sought to look at the effect of thermodynamics, in terms of gravity and temperature, accumulations processes such as migration and reservoir characteristics, such as permeability and geological structures on the distribution of components in the reservoir. He developed a compositional model which was used to evaluate steady-state thermodynamic equilibrium. Padua concluded from his results that geological structures, permeability, porosity and capillarity could be important factors in the distribution of oil in a reservoir.

Temeng et al. (1998) investigated compositional variations in a gas reservoir. They proposed that the observed variation in hydrocarbon composition, condensate saturation and acid gas content with depth and temperature in a gas reservoir was due to the production of hydrogen sulfide by the thermochemical reduction of sulfates. This conclusion serves to buttress the point that accumulation processes, such as chemical reactions, serve to upset the effect of gravity-chemical equilibrium.

Ghorayeb and Firoozabadi (2000a) investigated the modeling of convection and diffusion of multicomponent mixtures in porous media. In this work, Ghorayeb and

Firoozabadi (2000a) included the effects of molecular, pressure and thermal diffusion. From this work, they concluded that the features of compositional variation could be due to either convection or thermal diffusion. These authors have also looked at the compositional variations in fractured porous media (2000c).

2.3 Stability Analysis

The classic problem in convective stability is the Rayleigh-Benard problem. In the case of a porous medium, it is referred to as the Horton-Rogers-Lapwood problem. This problem looks at the distribution of fluid in a porous layer heated from below. The convective stability limit of a fluid heated from below has been described by the Rayleigh number which was determined to be of the order of $4\pi^2$ for a homogeneous single-phase fluid (Lapwood, 1948). The stability limit determines the point at which convective instabilities may occur in the reservoir. This is important because when convective instability occurs, the rate of heat transfer is increased (Nield, 1991) and the fluid components redistribute themselves to balance the instability.

Jacqmin (1985) was one of the first authors to look at the stability of convection with respect to horizontal temperature gradients in hydrocarbon reservoirs. He sought to establish the bounds for which the horizontal gradients in composition served to nullify the effect of temperature on the horizontal density gradient in gas reservoirs. The results were for specific reservoir configurations, for example, in a channel, the critical temperature was found to be nine times the critical concentration.

Nield, in collaboration with other authors, has worked on various areas of convection in porous media. The basic equations are the continuity equation, the Boussinesq approximation, and mass and momentum balance equations. Using perturbation analysis and the Garlerkin method to solve the resulting eigenvalue problem, Nield investigated convection in a porous medium with an inclined temperature field (Nield, 1991). In a similar work (Lage and Nield, 1998), the conclusions are that for non-diffusive problems, Hadley circulation (a collection of circulation cells) on its own is unstable for sufficiently large horizontal Rayleigh numbers and for large values of the horizontal Rayleigh number the critical flow can consist of more that one layer of

rolls. Nonoscillatory longitudinal rolls are the favored configuration for the cells.

Manole et al. (1994), extending the works of Nield, looked at convection in a system with both thermal and solutal gradients, with horizontal mass flow. They concluded that an increase in the vertical solutal Rayleigh number is always destabilizing, an increase in the horizontal Rayleigh number is stabilizing for certain parameter ranges and determined that increasing the horizontal solutal Rayleigh number will result in a change from a stabilizing effect to a destabilizing one.

Manole (1995) looked at the linear stability of double-diffusive convection in a porous layer with a horizontal temperature gradient. He was able to conclude that increasing the positive vertical solutal Rayleigh number is always destabilizing while increasing the horizontal temperature gradient is stabilizing, over a specific range of parameters. Also noted is that an increase in the horizontal solutal Rayleigh number has a stabilizing effect, until the net flow of the system is zero, after which it decreases until the system becomes unstable.

Qiao and Kaloni (1997) investigated the effect of mass flow on the Rayleigh numbers (vertical and horizontal) of a porous system. They concluded that increasing the flow rate has a destabilizing effect of the horizontal and vertical Rayleigh numbers. At low flow rates, an increase in the horizontal Rayleigh number results in a destabilizing effect on the critical Rayleigh number.

2.4 Solution Techniques

Table 2.1 gives a summary of the techniques that have been used to evaluate double-diffusive and multicomponent diffusive systems numerically. The point here is to understand the various approaches that have been applied to the problem in the past and the successes and drawbacks of each approach.

The main drawbacks of many of the solution techniques that have been used are:

1. The fluid is assumed to be incompressible and thus may be described using the Boussinesq approximation. The Boussinesq approximation states that density differences are negligible, with the exception of gravity force.

2. The temperature field is constant, whereas the temperature in the reservoir is dynamic and should be computed as the flow evolves.

Table 2.1: Summary of solutions techniques

Author	**Approach**	**Assumptions**
Moser (1986)	Solution of Gibbs sedimentation equation including diffusion and Darcy's law.	Incompressible fluid following the Boussinesq approximation. Imposition of temperature field with horizontal gradient only.
Horne (1975)	Solution of conservation of mass, momentum and energy equations. Formulation based on stream functions.	Incompressible fluid whose density follows an equation of state. Boussinesq approximation.
Jacqmin (1990)	Solution of conservation of mass including diffusion and Darcy's law.	Boussinesq approximation, Negligible horizontal diffusion. Imposed fixed temperature field.
Riley and Firoozobadi (1998)	Solution of conservation of mass including thermal, pressure and Fickian diffusion for a binary mixture.	Imposed fixed temperature field and assumed steady state conditions.
Ghorayeb and Firoozobadi (2000a)	Solution of conservation of mass including thermal, pressure and molecular for a multicomponent mixture.	Imposed fixed temperature gradients, assumed Boussinesq approximation is valid.

Chapter 3

Theoretical Background

This study seeks to investigate the interaction between convection and diffusion in porous media and their effect on compositional variation in reservoirs with existing temperature gradients. In this chapter, the two processes are described, and the techniques used to solve the problem are presented.

3.1 Convection

Convection is fluid movement due to density differences. Free convection is due to buoyancy differences, and the fluid will remain static when the temperature is uniform. Thermal convection is heat transfer through fluid motion. The Rayleigh-Bernard problem, describes convection in a fluid layer heated from below (See Figure 3.1).

3.1.1 The Rayleigh Number

The interaction between buoyancy forces and heat transfer for a fluid column heated from below has been studied, and this interaction is often characterized using the Rayleigh number. The Rayleigh number is defined as;

$$Ra = \frac{\alpha k g (\rho c_p)_f H \Delta T}{\nu \lambda} \tag{3.1}$$

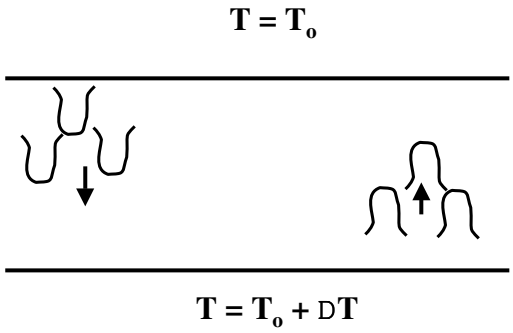

Figure 3.1: Convection in a fluid layer heated from below.

where α is the volumetric thermal expansion coefficient, g is acceleration due to gravity, ν is kinematic viscosity, k is permeability, λ is the effective thermal conductivity of fluid-filled medium, $(\rho c_p)_f$ is the product of the fluid density and heat capacity, H is the reservoir thickness and ΔT is the temperature difference across the system.

The Rayleigh number is a product of the Grashof (the ratio of viscous to buoyancy forces) and Prandtl (the ratio of momentum diffusivity to thermal diffusivity) dimensionless numbers. The onset of convection is defined by the critical Rayleigh number, Ra_c. The critical Rayleigh number has generally been given as $4\pi^2$ for single-component, single-phase fluid systems heated from below (Lapwood, 1948).

The use of the Rayleigh number has been extended to cover both vertical (Ra_V) and horizontal (Ra_H) ratios, as well as solutal ratios (Ra_S). The solutal Rayleigh number is a product of the Rayleigh number, the buoyancy ratio and the Lewis number.

$$Ra_S = Ra.N.Le \tag{3.2}$$

where

$$N = \frac{\alpha_S \Delta T}{\alpha_T \Delta C} \tag{3.3}$$

$$Le = \frac{\alpha_m}{D_m} \tag{3.4}$$

where ΔC is the concentration difference across the system, α_s is the concentration

expansion coefficient, α_T is the thermal expansion coefficient, α_m is the mass diffusivity and D_m is the mass diffusivity. In this study, the Rayleigh number was computed using average reservoir and fluid properties.

3.1.2 The Nusselt Number

The Nusselt number is a dimensionless number that measures the ratio of actual heat transferred by convection to the heat transferred due to conduction alone. The Nusselt number is 1 at values of the Rayleigh number less than the critical value when heat transfer is due to conduction alone, and increases with the movement of fluid as heat transfer by convection and fluid motion begins.

The Nusselt number is generally defined as;

$$Nu = \frac{hL}{k_f} = \frac{convective\ heat\ transfer}{conductive\ heat\ transfer} \tag{3.5}$$

where h is the convection heat transfer coefficient, k_f is the thermal conductivity of fluid and L is the characteristic length of the system.

3.2 Stability Analysis

Due to the complex nature of the equations that govern convection and diffusion in porous media, analytical solutions in terms of velocity and composition profiles in the reservoir as a function of position are impossible, except in very simple cases. Stability analysis may be used to determine the limit on certain parameters or variables at which convection occurs. For this, the continuity, energy and mass balance equations and an equation of state are solved. The following assumptions are made:

- Darcy's law is valid.
- Local thermal equilibrium exists between fluid and solid.
- Viscous dissipation results in negligible heating of the fluid.
- The effect of radiation is negligible.

- The fluid is incompressible and can be represented with the Boussinesq approximation. (The Boussinesq approximation states that density differences are negligible, with the exception of gravity force. This essentially means, with respect to this section, that changes of fluid density are ignored in all but the buoyancy terms of the governing equations.)

In stability analysis, the unknown to solve for is the critical Rayleigh number. For a reservoir with a single-component, single-phase fluid, subject to a vertical temperature gradient, as shown in Figure 3.2 the critical Rayleigh number is given as $Ra_c = 4\pi^2$. The addition of a solute with a vertical concentration gradient as shown in Figure 3.3 results in a critical Rayleigh number given as $Ra_c = (Ra + Ra_S) = 4\pi^2$. A number of authors (Lage and Nield, 1998, Manole et al., 1994, Qiao and Kaloni, 1997, Manole, 1995) have conducted studies on more complicated systems. Their publications should be consulted for a complete list of scenarios and their accompanying critical conditions.

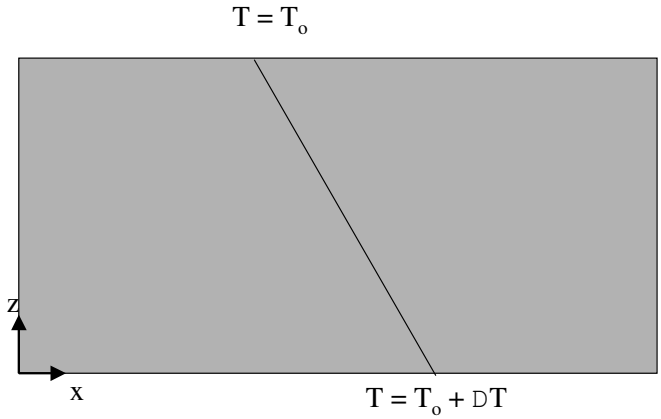

Figure 3.2: Porous medium with a vertical temperature gradient.

Appendix A shows in detail the procedure that may be followed to obtain values for the critical Rayleigh number when a reservoir is subject to a vertical temperature gradient and the fluid subject to a vertical concentration gradient.

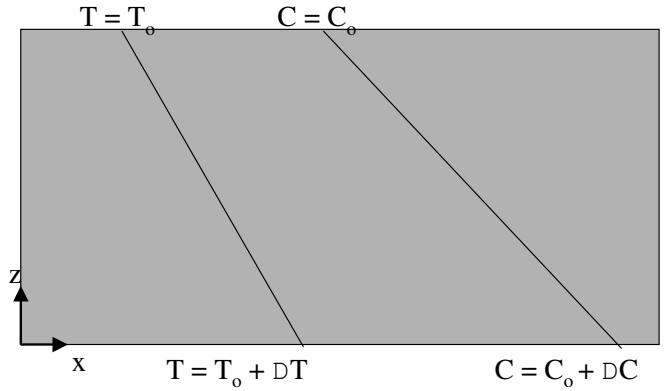

Figure 3.3: Porous medium with vertical temperature and solutal concentration gradients.

3.3 Gravity Segregation

In general, reservoirs are assumed to have uniform temperature fields. In a reservoir with a uniform temperature field, the pressure field is hydrostatic as shown in Figure 3.4. If gravity is a dominant force, the components of the fluid will be distributed in such a way as to maintain local thermodynamic equilibrium in the reservoir, assuming all other processes that might affect fluid distribution are absent. Figure 3.5 shows composition as a function of depth in a ternary system (methane, ethane and butane) in a reservoir with a uniform temperature field. The gradation in mole fraction follows the pressure gradient closely.

Reservoirs with areal and vertical compositional variations generally have existing temperature gradients, (for example, Figure 3.6 shows a temperature profile with both vertical and horizontal gradients), which influence greatly the distribution of fluid components. A reservoir with a uniform temperature field will have fluid components distributed in such a way to be in equilibrium under the prevailing gravitational force. Vertical temperature gradients alone may be insufficient to produce multicomponent convection and would result in a redistribution of the fluids under equilibrium conditions. This is due to the current Rayleigh number being less than the critical Rayleigh number and the absence of a perturbing force that would bring about instabilities

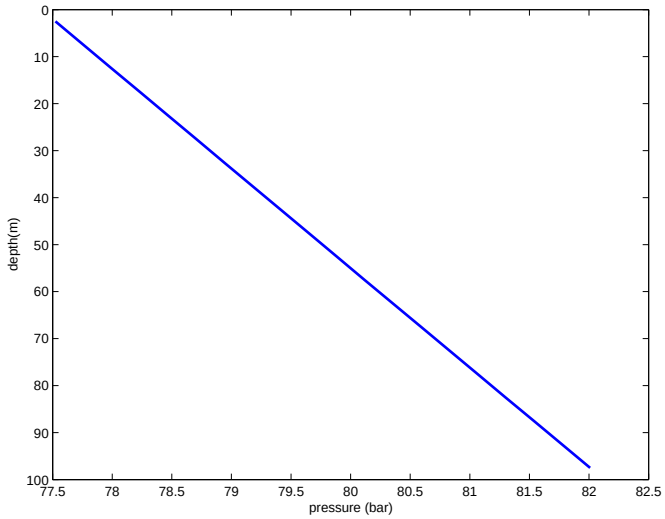

Figure 3.4: Pressure as a function of depth in a reservoir with a uniform temperature field.

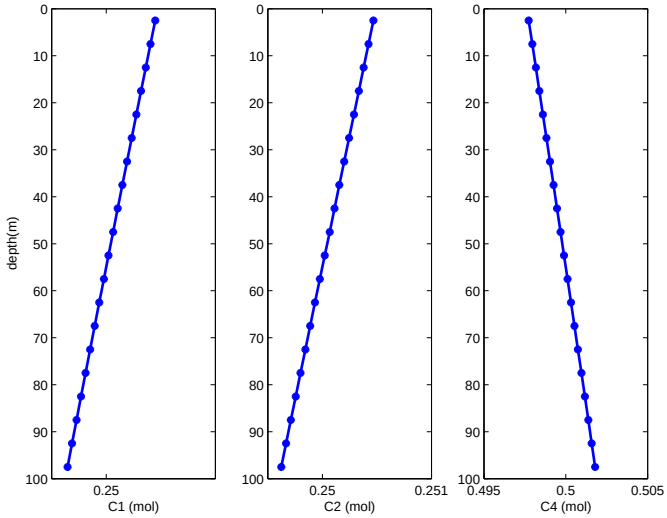

Figure 3.5: Composition as a function of depth in a reservoir with a uniform temperature field.

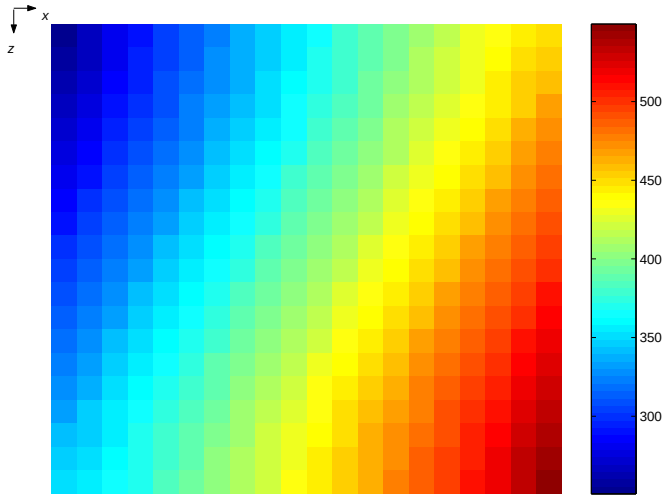

Figure 3.6: A temperature profile that could induce compositional variations. [Vertical and horizontal temperature gradients.]

which would lead to convection cells being formed. Faissat et al. (1994) observed that when the gradient is small enough and colinear with the gravity vector, no convection is observed. Horizontal temperature gradients induce horizontal density differences which induce fluid motion. Although a slow process, which occurs over geologic time, the understanding of convection is important in the understanding of the distribution of the chemical species in a reservoir. This variation of composition occurs because the tendency for convection to homogenize the fluid distribution in the reservoir is negated by the effect of gravity (Jacqmin, 1990). There are also diffusive effects that are dependent on pressure, temperature and molar gradients present in the reservoir, which also tend to homogenize the fluid distribution.

3.4 Diffusion

Diffusion is the transport of matter by molecular motion. Diffusion leads to an equalization of concentrations within a phase. Temperature affects the rate of diffusion because the kinetic energy of the molecules changes with a change in temperature. Diffusion that is dependent on concentration gradients is the most common type of

diffusion recorded in the literature. Diffusion of species depends on composition gradients (ordinary diffusion), on pressure gradients (pressure diffusion), on temperature gradients (thermal diffusion), and on external forces (forced diffusion). Osmotic diffusion takes place when a component diffuses due to a concentration gradient in another component and reverse diffusion occurs when a component diffuses in the opposite direction to its concentration gradient. In certain situations, diffusion may negate gravitational effects. This occurs because gravity wants to segregate the heavier and lighter components, while diffusion tends to make the mixture uniform. Hence, at equilibrium, the mixture will not be uniform.

Although the movement of molecules is Brownian, the net motion in molecular diffusion will be from a region of high concentration to one of lower concentration. The diffusion of component i in a solution of j is given as:

$$J_i = -D_{ij}\frac{dC_i}{d\mathbf{x}} \tag{3.6}$$

where J is the diffusion flux, C is the concentration, D is the diffusion coefficient or diffusivity and x is the distance. This is generally referred to as Fick's first law. This equation holds true in an isobaric binary mixture (Cunningham and Williams, 1980). In this study, for component i, the diffusion term is given as;

$$\mathbf{J}_i^m = -\rho^m\left(\sum_{j=1}^{n_c-1} D_{ij}^M\frac{\partial y_j}{\partial \mathbf{x}} + D_i^p\frac{\partial p}{\partial \mathbf{x}} + D_i^T\frac{\partial T}{\partial \mathbf{x}}\right) \tag{3.7}$$

where D_{ij}^M, D_i^p and D_i^T are the molecular, pressure and thermal diffusion coefficients (Ghorayeb and Firoozabadi, 2000a).

Diffusion coefficients are obtained either from experiments or from solving the constitutive equations on a phenomenological basis (using the Kinetic theory and/or the Chapman-Enskog theory and other laws (Ghorayeb and Firoozabadi, 2000b, Shapiro, 2003)). The diffusion coefficients are usually assumed to be constant, although they are functions of pressure, temperature and composition. Their dependence on pressure, temperature and composition will be discussed in Chapter 7.

Thermal diffusion occurs when a uniform mixture is subject to temperature gradients, and results in the mixture unmixing itself. Diffusion, or the flow of material, in

this case is not driven by the concentration gradient, but by the temperature gradient. Interdiffusion, which is the inverse effect of thermal diffusion, causes significant temperature differences. Thermal diffusion in liquids is referred to as the Soret effect (Ghorayeb and Firoozabadi, 2000b). Thermal diffusion also occurs in solids.

3.5 Numerical Solution

Numerical solutions are useful in calculating profiles of velocity, pressure, temperature, fluid composition, etc., especially when analytical solutions are not possible. In this study, a numerical solution to the set of partial differential equations that govern convection and diffusion in porous media was sought. A detailed description of the development of the numerical scheme may be found in Chapter 4

Chapter 4

Numerical Analysis

In this chapter, the numerical scheme used in this study is outlined. Documented are the governing equations, the discretization scheme, the handling of the boundary conditions and the convergence criteria.

4.1 Mass and Energy Balance Equations

The general mass and energy balance equations were used and are given in this section. The total mass balance and component mass balance equations are given as:

$$\frac{\partial}{\partial t}(\phi \sum_p \rho_p^m S_p) + \nabla \cdot (\sum_p \rho_p^m \mathbf{u}) + \sum_p q_p = 0 \tag{4.1}$$

$$\frac{\partial}{\partial t}(\phi \sum_p y_{cp} \rho_p^m S_p) + \nabla \cdot (\sum_p y_{cp} \rho_p^m \mathbf{u}) + \nabla \cdot \mathbf{J}_c^m + \sum_p q_{cp} = 0 \tag{4.2}$$

where t is time, ϕ is the porosity of the medium, ρ is the density, $\mathbf{u}$ is the velocity, S is saturation, q is production rate, y is the component mole fraction, J is the diffusion flux, the subscripts p and c refer to phase and component respectively and the superscript m refers to the molar quantity.

The momentum balance equation is substituted with Darcy's law:

$$\mathbf{u}_p = -\frac{k k_{rp}}{\mu}(\nabla p + \rho g) \tag{4.3}$$

where k is the reservoir permeability, k_r is the relative permeability, g is the gravitational acceleration, p is the pressure and μ is the viscosity.

The diffusion term for component i is expanded as:

$$\mathbf{J}_i^m = -\rho^m \left(\sum_{j=1}^{n_c-1} D_{ij}^M \frac{\partial y_j}{\partial \mathbf{x}} + D_i^p \frac{\partial p}{\partial \mathbf{x}} + D_i^T \frac{\partial T}{\partial \mathbf{x}}\right) \tag{4.4}$$

taking into account molecular diffusion, pressure diffusion and thermal diffusion associated with the movement of fluid molecules due to gradients in concentration, pressure and temperature. The energy balance equation is given as:

$$\frac{\partial}{\partial t}((1-\phi)\rho_{rr}^m U_{rr} + \phi \sum_p \rho_p^m U_p S_p) + \nabla \cdot (\sum_p \rho_p^m H_p \mathbf{u} - K_{rrT} \nabla T) + q_T = 0 \tag{4.5}$$

where U is the internal energy, H is enthalpy, K is the conductivity and the rock properties are defined with a subscript rr.

The boundary conditions are no-flow boundary conditions for the pressure equation and fixed temperature boundaries for the energy equation:

$$\mathbf{u} = 0 \tag{4.6}$$

$$T = constant \tag{4.7}$$

Therefore, we have $n_c + 2$ equations, namely:

1. a total mass balance equation
2. n_c component balance equations
3. an energy balance equation

that must be solved for the $n_c + 2$ unknowns, namely:

1. pressure
2. n_c component mole fractions
3. temperature

Darcy's law is substituted into Equations 4.1, 4.2 and 4.5 to obtain the following equations in terms of pressure. Production of fluid from the reservoir is set to zero. The total mass balance equation is:

$$\frac{\partial}{\partial t}(\phi \sum_p \rho_p^m S_p) = \nabla \cdot (\sum_p \rho_p^m \frac{\mathbf{k} k_{rp}}{\mu_p} \cdot \nabla \Phi) \tag{4.8}$$

The component mass balance equation is:

$$\frac{\partial}{\partial t}(\phi \sum_p y_{cp} \rho_p^m S_p) = \nabla \cdot (\sum_p y_{cp} \rho_p^m \frac{\mathbf{k} k_{rp}}{\mu_p} \cdot \nabla \Phi) + \nabla \cdot \mathbf{J}_c^m \tag{4.9}$$

The energy balance equation:

$$\frac{\partial}{\partial t}((1-\phi)\rho_{rr}^m U_{rr} + \phi \sum_p \rho_p^m U_p S_p) + \nabla \cdot (\sum_p \rho_p^m H_p \frac{\mathbf{k} k_{rp}}{\mu_p} \cdot \nabla \Phi) + \nabla \cdot (K_T \nabla T) + q_T = 0 \tag{4.10}$$

Due to the dependence between component mole fractions

$$\sum_{i=1}^{n_c} y_i = 1 \tag{4.11}$$

and phase saturations

$$\sum_{i=1}^{n_p} S_p = 1 \tag{4.12}$$

the set of variables can be reduced to $n_c + 1$ primary variables, namely:

1. pressure
2. $n_c - 1$ component mole fractions
3. temperature

and the corresponding equations:

1. the total mass balance equation
2. $n_c - 1$ component balance equations
3. the energy balance equation

4.2 Numerical Scheme

The set of nonlinear equations must be formulated in a way to allow them to be coded within a program that would be able to solve the system of equations for the primary variables. In order to do this the equations are discretized.

4.2.1 Discretization of Equations

The discretization is carried out with respect to the primary variables; pressure, temperature and composition. The following equations were obtained for each grid block using a central finite-difference scheme in space on a Cartesian grid and a first-order finite-difference approximation for the derivative in the accumulations term, in time.

The total mass balance equation for phase p is given as:

$$\sum_{l}\sum_{p}\Gamma_p\nabla\Phi - \frac{V}{\Delta t}\Delta_t(\phi\sum_{p}\rho_p^m S_p) = 0 \tag{4.13}$$

$$\begin{aligned}
&\Gamma_{p,i-\frac{1}{2}}[(p_{p,i-1}-p_{p,i}) - \gamma_{p,i-\frac{1}{2}}(z_{i-1}-z_i)] + \\
&\Gamma_{p,i+\frac{1}{2}}[(p_{p,i+1}-p_{p,i}) - \gamma_{p,i+\frac{1}{2}}(z_{i+1}-z_i)] + \\
&\Gamma_{p,j-\frac{1}{2}}[(p_{p,j-1}-p_{p,j}) - \gamma_{p,j-\frac{1}{2}}(z_{j-1}-z_j)] + \\
&\Gamma_{p,j+\frac{1}{2}}[(p_{p,j+1}-p_{p,j}) - \gamma_{p,j+\frac{1}{2}}(z_{j+1}-z_j)] + \\
&\Gamma_{p,k-\frac{1}{2}}[(p_{p,k-1}-p_{p,k}) - \gamma_{p,k-\frac{1}{2}}(z_{k-1}-z_k)] + \\
&\Gamma_{p,k+\frac{1}{2}}[(p_{p,k+1}-p_{p,k}) - \gamma_{p,k+\frac{1}{2}}(z_{k+1}-z_k)] = \\
&\qquad \frac{V_{i,j}}{\Delta t}[(\phi\rho_p^m S_p)^{n+1} - (\phi\rho_p^m S_p)^n]
\end{aligned} \tag{4.14}$$

where

$$\begin{aligned}
\Gamma_{p,l\pm\frac{1}{2}} &= \alpha[\frac{k_l k_{rp}\rho_p^m A}{\Delta l \mu_p}]|_{l\pm\frac{1}{2}} cos^2\theta \\
\gamma_{p,l\pm\frac{1}{2}} &= g[\rho_p^m]|_{l\pm\frac{1}{2}}
\end{aligned} \tag{4.15}$$

where θ is the angle the reservoir makes with the horizontal, α is a conversion factor, k is the l-direction weighted harmonic average permeability, A is the cross-sectional area, μ_p is the phase viscosity and , k_{rp} is the relative permeability in phase p, g is the acceleration due to gravity and ρ_p^m is the phase molar density. The transmissibility term, Γ includes a flow term which is computed based on the upstream values for viscosity, density, saturation and relative permeability (referred to as upwinding). This applies to all the primary equations, namely; total mass balance, component mass balance and the energy balance equations.

The component balance equation for component c in phase p is given as:

$$\sum_l \sum_p \Gamma_p y_{cp} \nabla\Phi - \sum_l \sum_p \tau^D \rho_p^m (\sum_{j-1}^{n_c-1} D_{ij}^M \nabla y_j + D_i^P \nabla p + D_i^T \nabla T) - \frac{V}{\Delta t} \Delta_t (\phi \sum_p y_{cp} \rho_p^m S_p) = 0$$

$$\begin{aligned}
&\Gamma_{cp,i-\frac{1}{2}}[(p_{p,i-1} - p_{p,i}) - \gamma_{p,i-\frac{1}{2}}(z_{i-1} - z_i)] - \\
&\Upsilon_{cp,i-\frac{1}{2}}[D_{cc'}^M (y_{i-1} - y_i) + D_c^p (p_{i-1} - p_i) + D_c^T (T_{i-1} - T_i)] + \\
&\Gamma_{cp,i+\frac{1}{2}}[(p_{p,i+1} - p_{p,i}) - \gamma_{p,i+\frac{1}{2}}(z_{i+1} - z_i)] - \\
&\Upsilon_{cp,i+\frac{1}{2}}[D_{cc'}^M (y_{i+1} - y_i) + D_c^p (p_{i+1} - p_i) + D_c^T (T_{i+1} - T_i)] + \\
&\Gamma_{cp,j-\frac{1}{2}}[(p_{p,j-1} - p_{p,j}) - \gamma_{p,j-\frac{1}{2}}(z_{j-1} - z_j)] - \\
&\Upsilon_{cp,j-\frac{1}{2}}[D_{cc'}^M (y_{j-1} - y_j) + D_c^p (p_{j-1} - p_j) + D_c^T (T_{j-1} - T_j)] + \\
&\Gamma_{cp,j+\frac{1}{2}}[(p_{p,j+1} - p_{p,j}) - \gamma_{p,j+\frac{1}{2}}(z_{j+1} - z_j)] - \\
&\Upsilon_{cp,j+\frac{1}{2}}[D_{cc'}^M (y_{j+1} - y_j) + D_c^p (p_{j+1} - p_j) + D_c^T (T_{j+1} - T_j)] + \\
&\Gamma_{cp,k-\frac{1}{2}}[(p_{p,k-1} - p_{p,k}) - \gamma_{p,k-\frac{1}{2}}(z_{k-1} - z_k)] - \\
&\Upsilon_{cp,k-\frac{1}{2}}[D_{cc'}^M (y_{k-1} - y_k) + D_c^p (p_{k-1} - p_k) + D_c^T (T_{k-1} - T_k)] + \\
&\Gamma_{cp,k+\frac{1}{2}}[(p_{p,k+1} - p_{p,k}) - \gamma_{p,k+\frac{1}{2}}(z_{k+1} - z_k)] - \\
&\Upsilon_{cp,k+\frac{1}{2}}[D_{cc'}^M (y_{k+1} - y_k) + D_c^p (p_{k+1} - p_k) + D_c^T (T_{k+1} - T_k)] = \\
&\frac{V_{i,j}}{\Delta t}[(\phi \rho_p^m S_p y_{cp})^{n+1} - (\phi \rho_p^m S_p y_{cp})^n]
\end{aligned} \tag{4.16}$$

where

$$\Gamma_{cp,l\pm\frac{1}{2}} = \alpha[\frac{k_l k_{rp} y_{cp} \rho_p^m A}{\Delta l \mu_p}]|_{l\pm\frac{1}{2}} cos^2\theta$$
$$\Upsilon_{cp,l\pm\frac{1}{2}} = \frac{\phi\rho_p^M}{A}|_{l\pm\frac{1}{2}}$$

The energy balance equation for phase p becomes:

$$\sum_l \sum_p \Gamma_p H_p^m \nabla\Phi - \sum_l \tau^K K_c \nabla T + q - \frac{V}{\Delta t}[\phi \sum_p \rho_p^m U_p S_p + (1-\phi) U_{rr} \Delta T^o] \quad (4.17)$$

$$\begin{aligned}
&\Gamma_{Tp,i-\frac{1}{2}}[(p_{p,i-1} - p_{p,i}) - \gamma_{p,i-\frac{1}{2}}(z_{i-1} - z_i)] - \tau_{i-\frac{1}{2}}(T_{i-1} - T_i) + \\
&\Gamma_{Tp,i+\frac{1}{2}}[(p_{p,i+1} - p_{p,i}) - \gamma_{p,i+\frac{1}{2}}(z_{i+1} - z_i)] - \tau_{i+\frac{1}{2}}(T_{i+1} - T_i) + \\
&\Gamma_{Tp,j-\frac{1}{2}}[(p_{p,j-1} - p_{p,j}) - \gamma_{p,j-\frac{1}{2}}(z_{j-1} - z_j)] - \tau_{j-\frac{1}{2}}(T_{j-1} - T_i) + \\
&\Gamma_{Tp,j+\frac{1}{2}}[(p_{p,j+1} - p_{p,j}) - \gamma_{p,j+\frac{1}{2}}(z_{j+1} - z_j)] - \tau_{j+\frac{1}{2}}(T_{j+1} - T_i) + \\
&\Gamma_{Tp,k-\frac{1}{2}}[(p_{p,k-1} - p_{p,k}) - \gamma_{p,k-\frac{1}{2}}(z_{k-1} - z_k)] - \tau_{k-\frac{1}{2}}(T_{k-1} - T_i) + \\
&\Gamma_{Tp,k+\frac{1}{2}}[(p_{p,k+1} - p_{p,k}) - \gamma_{p,k+\frac{1}{2}}(z_{k+1} - z_k)] - \tau_{k+\frac{1}{2}}(T_{k+1} - T_i) = \\
&\frac{V_{i,j}}{\Delta t}[((1-\phi)\rho_{rr}^m U_{rr} + \phi\rho_p^m S_p U_p)^{n+1} - ((1-\phi)\rho_{rr}^m U_{rr} + \phi\rho_p^m S_p U_p)^n]
\end{aligned} \quad (4.18)$$

where

$$\Gamma_{Tp,l\pm\frac{1}{2}} = \alpha[\frac{k_l k_{rp} \rho_p^m H_p^m A}{\Delta l \mu_p}]|_{l\pm\frac{1}{2}} cos^2\theta$$
$$\tau_{p,l\pm\frac{1}{2}} = \frac{AK_c}{L}|_{l\pm\frac{1}{2}}$$

Dependencies

The dependencies to be considered are as follows (Coats, 1980):

$$\phi \rightarrow f(p)$$
$$\rho, \mu, \gamma \rightarrow f(p, T, x)$$
$$M_f \rightarrow f(T)$$
$$H, U \rightarrow f(p, T)$$

The dependence of porosity on pressure is given as follows:

$$\phi = \phi_{ref}[1 + c_r(p - p_{ref})] \tag{4.19}$$

4.2.2 Solution of Nonlinear Equations

An implicit scheme was used where all the flow terms on the left hand side are evaluated at the new time step. To solve Equation 4.20 obtained from the discretization process, a number of numerical tools were used, namely GMRES and Sparselib.

$$J\delta = -R \tag{4.20}$$

where

$$\delta = p^{n+1} - p^n \tag{4.21}$$

p is the vector of unknowns (primary variable), J is the Jacobian matrix, comprising of derivatives of the individual terms with respect to the primary variables, R is the residual vector and the superscripts n and $n + 1$ refer to the timestep.

Time Step Control

In order to obtain sufficient accuracy, while maintaining optimal processing time, the value of incremental timestep, ΔT must be chosen carefully. The initial time step is set to a hundredth of a day and subsequent time steps are computed based on Equation 4.22 until the maximum time step is reached at a thousand days.

Table 4.1: Desired change in primary variables

Variable	**Desired change**
Pressure	5 bars
Composition	0.05 moles
Temperature	5.0 K

Table 4.2: Convergence criteria for primary variables

Variable	**Tolerance**
Pressure	5 bars
Composition	0.005 moles
Temperature	0.05 K

$$\Delta t^{n+1} = \Delta t^{n}[\frac{(1+\omega)\eta_v}{\delta_v + \omega\eta_v}] \mid_{minimum\ over\ all\ unknowns} \tag{4.22}$$

where ω is the weighting factor ($0 < \omega < 1$), δ is the observed change in the variable and η is the desired change in the variable (Table 4.1).

Convergence Tolerances

In order to determine when to stop the Newton iterations, convergence criteria for the primary variables were set as listed in Table 4.2

The maximum number of iterations within each loop is thirty, after which if convergence has not been reached, the timestep increment is divided by a factor of 2 and the loop begun again.

Determination of Steady-state Solution

In order to obtain the steady-state profiles for the primary variables, certain criteria were defined, which when met lead to the termination of the program. Therefore, based on Table 4.3, when the largest change in pressure over all the gridblocks is less than the tolerance prescribed, the simulation is stopped. This is used in conjunction with changes in composition and temperature as well.

Table 4.3: Steady-state criteria for primary variables

Variable	**Tolerance**
Pressure	1 bar
Composition	0.001 moles
Temperature	0.1 K

4.2.3 Initialization

Component mole fractions - The reservoirs used in the simulations are either two-dimensional cross-sections (i.e. x-z) or three-dimensional reservoirs, hence the effect of gravity should be taken into account. The component mole fractions may either be initialized uniformly across the reservoir or according to Gibb's sedimentation equation (Kovseck, 2001, Chapter 9).

For component i,

$$f_i(T,p) = f_i(T_{ref}, p_{ref}) + M_i g(h - h_{ref}) \tag{4.23}$$

where f is fugacity.

Pressure - The pressure field is initialized based on the depth of the gridblock centers with respect to the datum depth and the pressure at the datum depth.

Temperature - The temperature field is initialized as purely conductive. The vertical and horizontal temperature gradients are defined, taking into consideration the boundary values, such that the Nusselt number across the reservoir is one.

The primary variables may also be initialized as being uniform across the reservoir, although runs with this initialization method take a longer time to stabilize.

4.3 Fluid Properties

The fluid properties are calculated based on reservoir pressure and temperature as well as fluid composition. Mixture density and viscosity are computed using the

methodology described by Alani (1960) and Lohrenz et al. (1964). The vapor-liquid equilibrium routine which includes a flash routine is extremely important as most of the fluid properties, particularly density and fluid composition at the prevailing pressure and temperature are computed within this routine.

4.3.1 Vapor-Liquid Equilibrium

The vapor-liquid equilibrium calculations are based on a cubic equation of state.

$$Z^3 - (1 + B - uB)Z^2 + (A + wB^2 - uB - uB^2)Z - AB - wB^2 - wB^3 = 0 \quad (4.24)$$

where

$$A = a_m \frac{p^2}{R^2T^2} \quad (4.25)$$

$$B = b_m \frac{p}{RT} \quad (4.26)$$

and

$$a_m = \sum_i \sum_j x_i x_j (a_i a_j)^{\frac{1}{2}} (1 - \bar{k}_{ij}) \quad (4.27)$$

$$b_m = \sum_i x_i b_i \quad (4.28)$$

This equation is solved for the compressiblity, Z, of the fluid system.

The Peng-Robinson equation defines the constants u and w and variables a_i and b_i respectively as:

$$u = 2 \quad (4.29)$$

$$w = -1 \quad (4.30)$$

$$b = 0.0778 \frac{RT_c}{p_c} \quad (4.31)$$

$$a = 0.45724 \frac{R^2 {T_c}^2}{p_c} [1 + fw(1 - {T_r}^{\frac{1}{2}})]^2 \quad (4.32)$$

$$fw = 0.37464 + 1.5422\omega - 0.26992\omega^2 \quad (4.33)$$

The phase molar densities are computed based on molar volume and composition.

4.4 Metrics

The nature of fluid flow in a nonproducing reservoir under convection and diffusion is very slow and the changes in composition, from one timestep to the next, are less than ten percent (10%) in most cases. In order to be able to compare the results of different reservoir and fluid configurations in a concise manner, certain metrics were used throughout this study, namely;

The Rayleigh number - ratio of buoyancy forces to heat transfer.

$$Ra = \frac{\alpha k g (\rho c_p)_f H \Delta T}{\nu \lambda}$$

The Rayleigh number is computed based on the average values of properties such as permeability, fluid viscosity and density, as well as heat capacity. The temperature difference is the difference in temperature across the reservoir, i.e. from top to bottom.

The Nusselt number - ratio of convective to conductive heat transfer.

$$Nu = \frac{hL}{k_f}$$

The Nusselt number was computed based on the thermal gradients across the reservoirs' lower and upper boundaries and the thermal gradient across the reservoir. Therefore, the Nusselt number is defined as;

$$Nu = \frac{\frac{dT}{dx}\big|_{\text{horizontal boundaries}}}{\frac{dT}{dx}\big|_{\text{reservoir}}} \tag{4.34}$$

The thermal conductivity is assumed constant in liquids and a function of the gas saturation in multicomponent mixtures (Coats, 1980).

$$\lambda = \lambda_i (1 - \omega S_g) \tag{4.35}$$

where ω should be in the range of 0 to 0.8

The separation factor - measures the difference in fluid composition of any two components from the top to the bottom of the reservoir.

$$SF = \frac{(x_2/x_1)_{bottom}}{(x_2/x_1)_{top}} \tag{4.36}$$

where x_1 is mole fraction of component 1 and x_2 is mole fraction of component 2.

The density factor - measures the average density gradient in the reservoir.

$$DF = \frac{abs(\overline{\rho}_{top} - \overline{\rho}_{bottom})}{H} \tag{4.37}$$

where ρ is fluid density and H is the reservoir thickness.

These four metrics used together enable the quick analysis of reservoirs of any size, composition and temperature profile. Together with the velocity and composition profiles, the effect of any variable on compositional gradient can be analyzed quickly.

4.5 Program

The discretized equations listed in Section 4.2.1 form the basis for the program.

4.5.1 Parameter Space

The program is coded for multiphase flow in three dimensions, dipping reservoir, homogeneous or heterogenous permeability field and multicomponent fluids. See Appendices C and D for more details.
In this study, only single-phase oil fluids were analyzed, with two or three components.

Chapter 5

Effect of Convection and Diffusion on Composition

This chapter looks at the effect of different reservoir configurations and processes on the fluid compositions in general.

5.1 The Critical Rayleigh Number

From the literature, certain configurations of reservoir and fluid properties have exact known values at which convection begins. The Rayleigh number at which this occurs is referred to as the critical Rayleigh number. At this point the Nusselt number deviates from 1(its value when the temperature field is purely conductive), it increases to account for the increase in heat transfer due to the convection of fluid in the reservoir. For incompressible single-component fluids heated from below, the critical Rayleigh number is known to be exactly $4\pi^2$.

In this section, the fluid discussed is a single-phase, two-component fluid used to represent a single-phase, single-component fluid. The fluid density is computed using an equation of state for density and the fluid viscosity is assumed to vary as a function of temperature only. Two components were used for ease in computing because the program was designed specifically for multicomponent mixtures. The reservoir and fluid properties used to establish critical Rayleigh numbers are given in Table 5.1.

Figure 5.1 shows the temperature profile in the reservoir. The average temperature difference in the reservoir is 13K.

Table 5.1: Reservoir and fluid properties for a single-phase fluid.

Reservoir properties	
Dimensions	1000m x 100m x 450m
Grid	20x1x20
Porosity	0.25
Thermal conductivity	120 kJ/kgK
Rock heat capacity	95 kJ/kg
Temperature gradient	0.0065 K/m
Fluid properties	
Average density	950 kg/m^3
Specific heat capacity	4.5 kJ/kgK
Coefficient of thermal expansion	2E-04 K^{-1}
Oil viscosity	standard values of viscosity of liquid water as a function of temperature

There are two dominant configurations that are possible for fluids under thermal gradients, namely the diffusion-dominated configuration and the convection-dominated configuration. The configuration in a reservoir with a Rayleigh number less than the critical Rayleigh number will most often be diffusion-dominated. This is shown in Figure 5.2. When the Rayleigh number is greater that the critical value, the configuration is more likely to be convection-dominated as shown in Figure 5.3

Tilted reservoirs, with horizontal and vertical hydrostatic pressure gradients, do not need additional forces or perturbations for convection to occur. Convection of fluids occurs readily in such reservoirs, as shown in Figure 5.4.

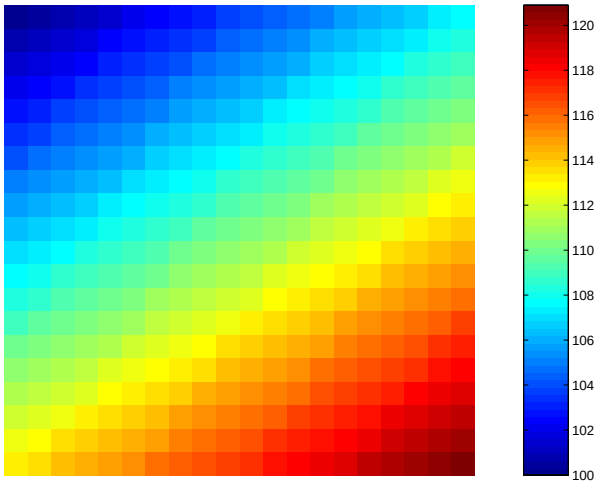

Figure 5.1: Temperature field with horizontal and vertical gradients. [T (K)]

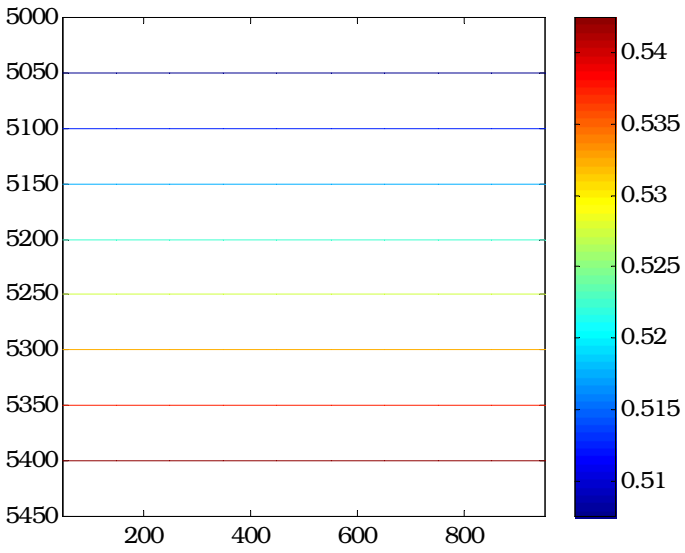

Figure 5.2: Concentration profile in a diffusion-dominated reservoir. [mole fraction]

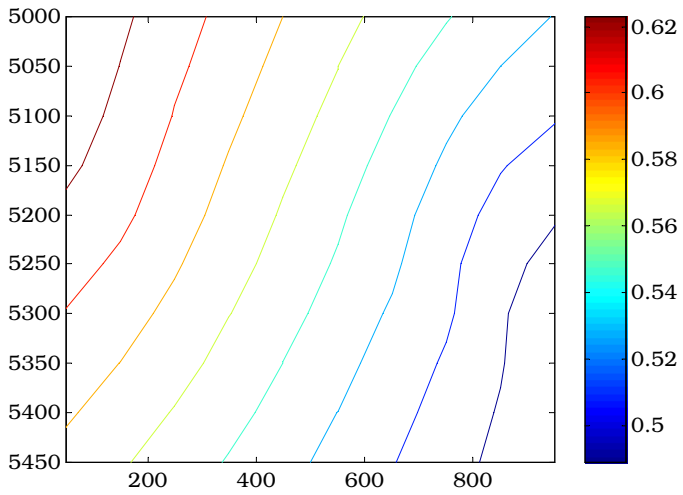

Figure 5.3: Concentration profile in a convection-dominated reservoir. [mole fraction]

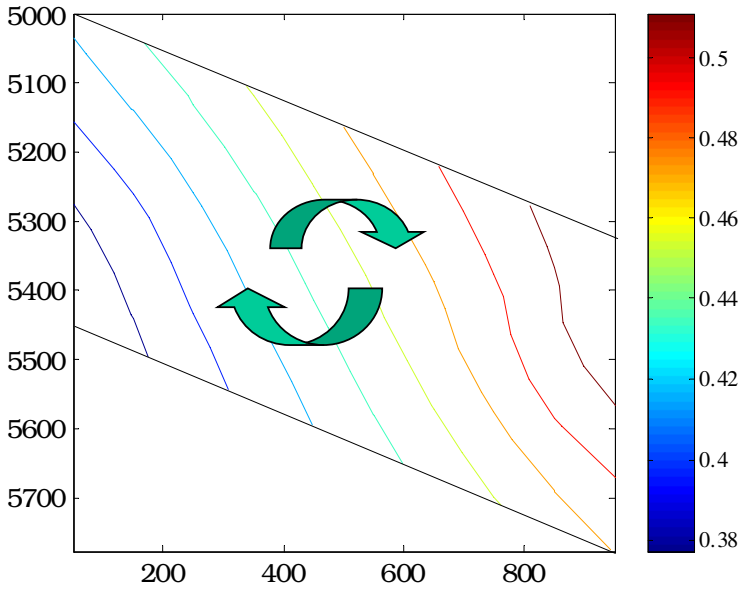

Figure 5.4: Concentration profile in a tilted reservoir. [mole fraction]

5.2 Convection and Diffusion in a Reservoir with a Uniform Temperature Field

The assumption that reservoirs have uniform temperature fields is one that is often made in the process of reservoir characterization. In order to gain an understanding of the way components distribute themselves in the reservoir, the following simulation was run with a fixed, uniform temperature field. The reservoir and fluid properties are listed in Table 5.2.

Table 5.2: Reservoir properties for a reservoir with a uniform temperature field.

Dimensions	1000m x 50m x 100m
Permeability	100md
Porosity	0.25
Reservoir temperature	302.3K
Datum reservoir pressure	80 bars
Grid	20 x 1 x 20
Fluid components	C_1, C_2 and C_4
Datum fluid composition	0.25, 0.25 and 0.5

Figure 5.5 shows the concentration profile in the reservoir. The components are distributed in such a way as to reflect the influence of gravity and will remain so until some external force leads to a perturbation within the system. This would be the expected state of fluids in a static reservoir. Although there are no convection cells, diffusion is expected to occur on a small-scale, due to the gradients in both pressure and concentration. Figure 5.6 shows the velocity profile in this reservoir. The net motion appears to be downwards at the initial states of the reservoir when the fluid distributed itself according to the gravitational effect. Once the configuration is stable, the net velocity in the reservoir is zero.

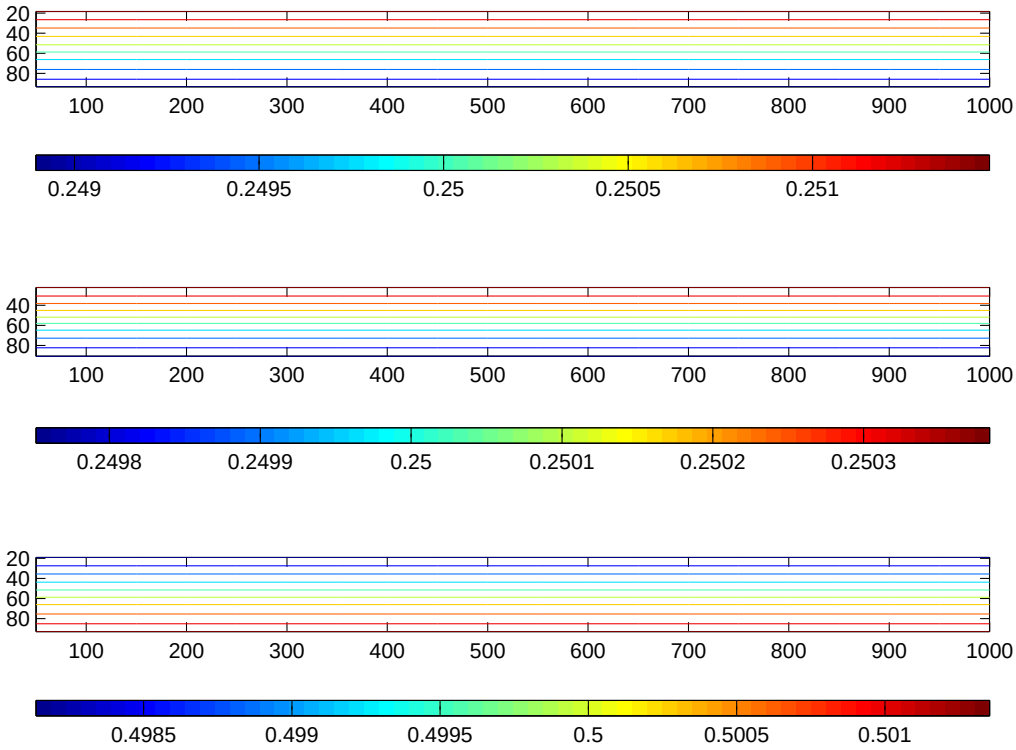

Figure 5.5: Compositional variation in a reservoir with a uniform temperature field. [C_1, C_2 and C_4 mole fractions]

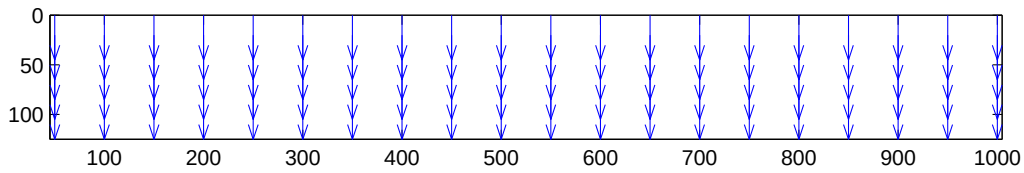

Figure 5.6: Velocity profile in a reservoir with a uniform temperature field.

5.3 Convection and Diffusion in a Reservoir with Vertical and Horizontal Temperature Gradients

The reservoir and fluid properties used in this run are listed in Table 5.3.

Table 5.3: Reservoir properties for a reservoir with horizontal and vertical temperature gradients.

Dimensions	1000m x 50m x 100m
Permeability	100md
Porosity	0.25
Grid	20 x 1 x 20
Datum temperature	300K
Horizontal temperature gradient	0.02K/m
Vertical temperature gradient	0.2K/m
Datum reservoir pressure	80 bars
Fluid components	C_1, C_2 and C_4
Datum fluid composition	0.25, 0.25 and 0.5

This reservoir has both vertical and horizontal temperature gradients as shown in Figure 5.7. The temperature profile was held constant over the all simulations (energy balance excluded). Over the range of temperature and pressure for this reservoir, the fluid remains a single-phase mixture, as shown in the phase diagram, Figure 5.8.

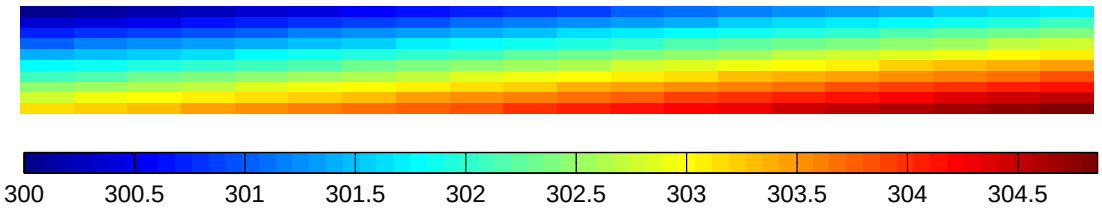

Figure 5.7: Reservoir temperature profile.
[The reservoir has both vertical and horizontal temperature gradients.]

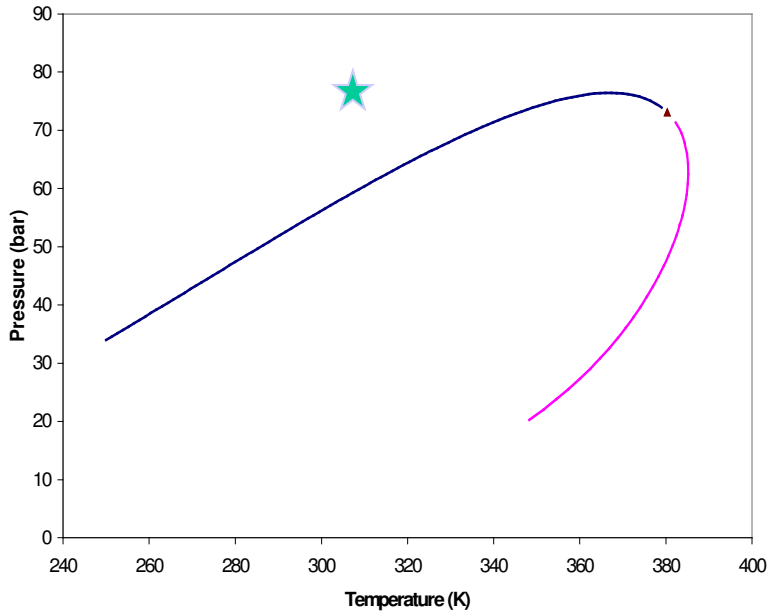

Figure 5.8: Phase diagram for reservoir mixture at reference composition.

Figure 5.10 shows the concentration profiles obtained. The concentration contours show that there is compositional variation in the reservoir. They also imply that there is fluid movement over time in the reservoir, particularly looking at the contours for ethane, C_2. To show that there is indeed movement of the fluid, the velocity profile is plotted in Figure 5.9. Fluid moves in a circular convecting motion, with fluid rising from the lower right (the hottest part of the reservoir).

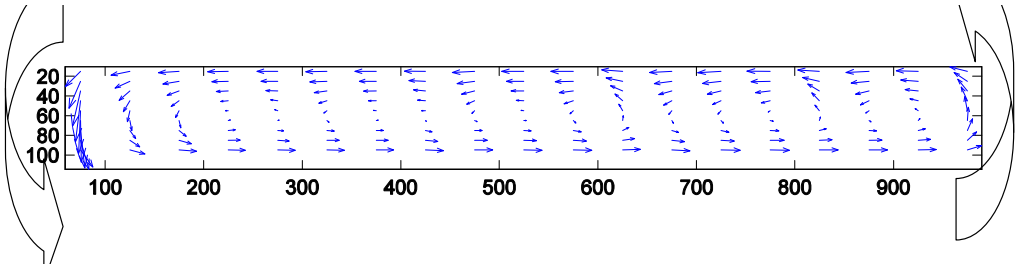

Figure 5.9: Velocity profile in a reservoir with horizontal and vertical temperature gradients.

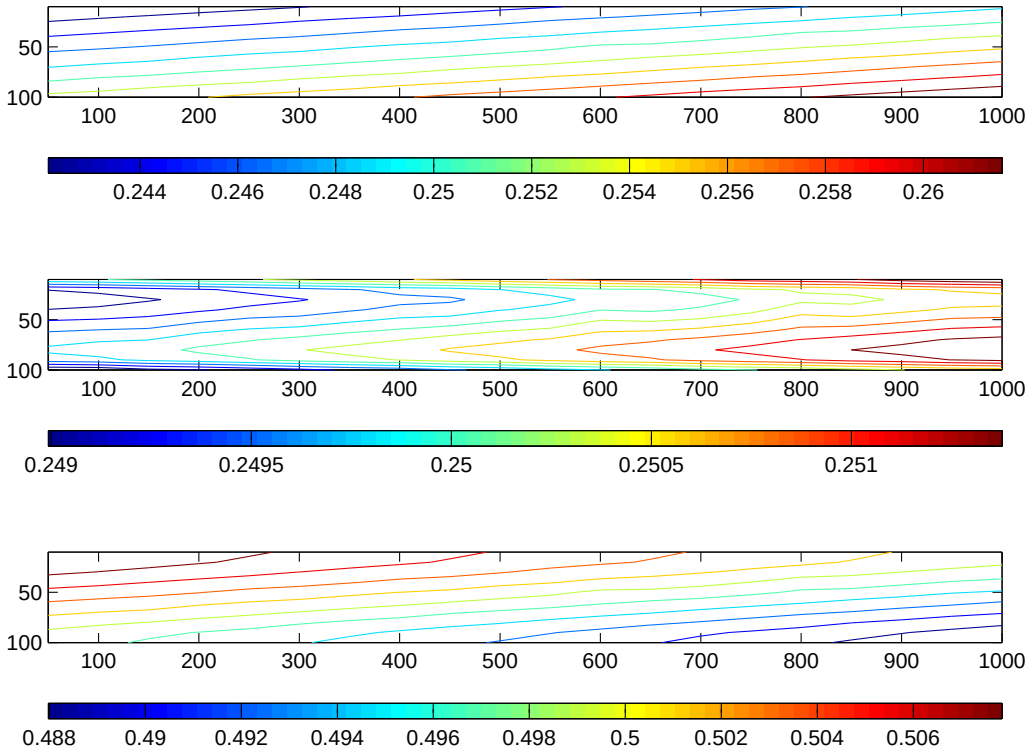

Figure 5.10: Compositional variation in a reservoir with vertical and horizontal temperature gradients.

[C_1, C_2 and C_4 mole fractions]

5.3.1 Effect of the Diffusion Terms

The diffusion term used in the program comprises three parts, an ordinary diffusion term, a pressure diffusion term and a thermal diffusion term. In order to study the effects of these terms separately, simulation runs were made with the same reservoir configuration and fluid properties. Sensitivity to diffusion terms was the goal in these runs.

Effect of Molecular Diffusion

Pressure and thermal diffusion coefficients were set to zero in this case. Figure 5.11 shows the concentration profiles of C_1, C_2 and C_4. Hence, the results in Figure 5.11 show only the effect of ordinary diffusion under fixed temperature gradients.

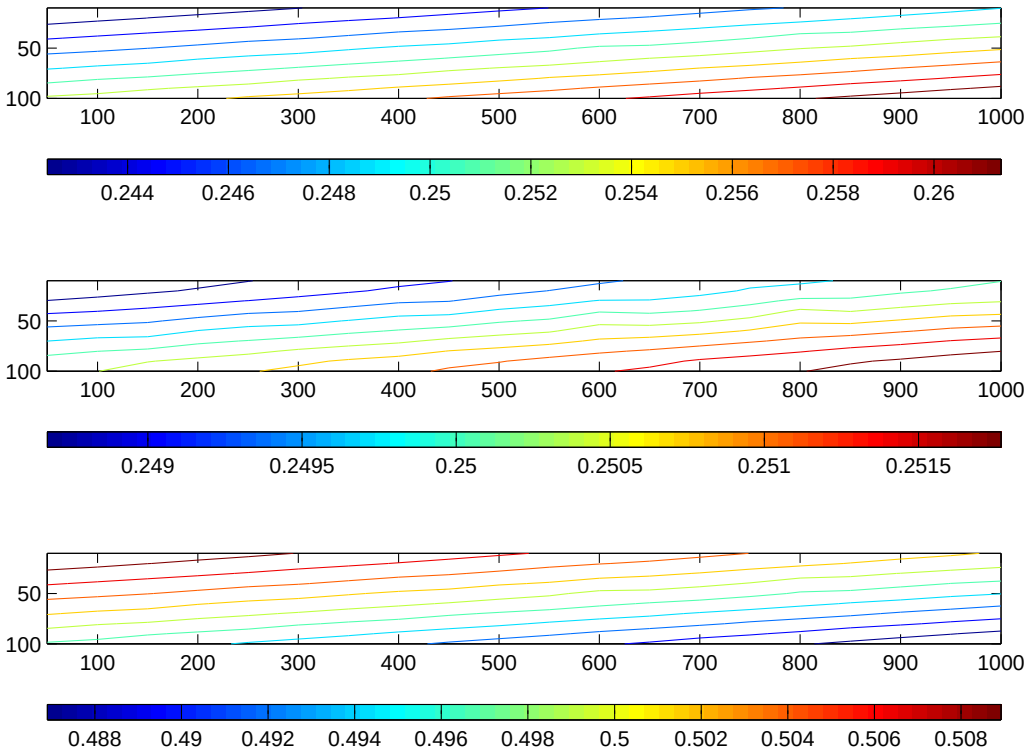

Figure 5.11: Compositional variation of only molecular diffusion.
[C_1, C_2 and C_4 mole fractions]

It is noted here that the profiles are consistent with the temperature field and the influence of gravity.

Effect of Pressure Diffusion

In this case, the pressure diffusion terms was included in addition to the molecular diffusion. The thermal diffusion coefficients were set to zero. Figure 5.12 shows the concentration profiles obtained.

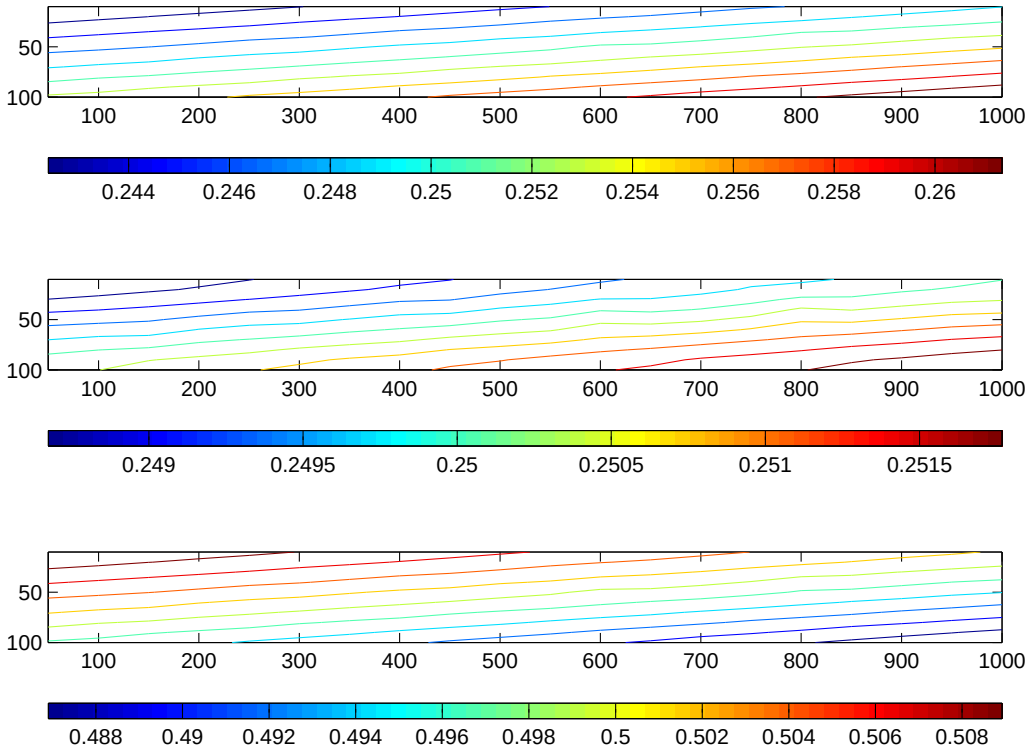

Figure 5.12: Compositional variation of molecular and pressure diffusion. [C_1, C_2 and C_4 mole fractions]

The concentration profiles in this case imply that the addition of the pressure diffusion term does not change the compositional variation in the reservoir. It may be possible to neglect the pressure diffusion term in the future without any loss in accuracy. This will be tested on other reservoir fluids.

Effect of Thermal Diffusion

In this case, the thermal diffusion coefficients were included, in addition to the molecular diffusion coefficients. The pressure diffusion term was neglected. Figure 5.13 shows the concentration profiles obtained.

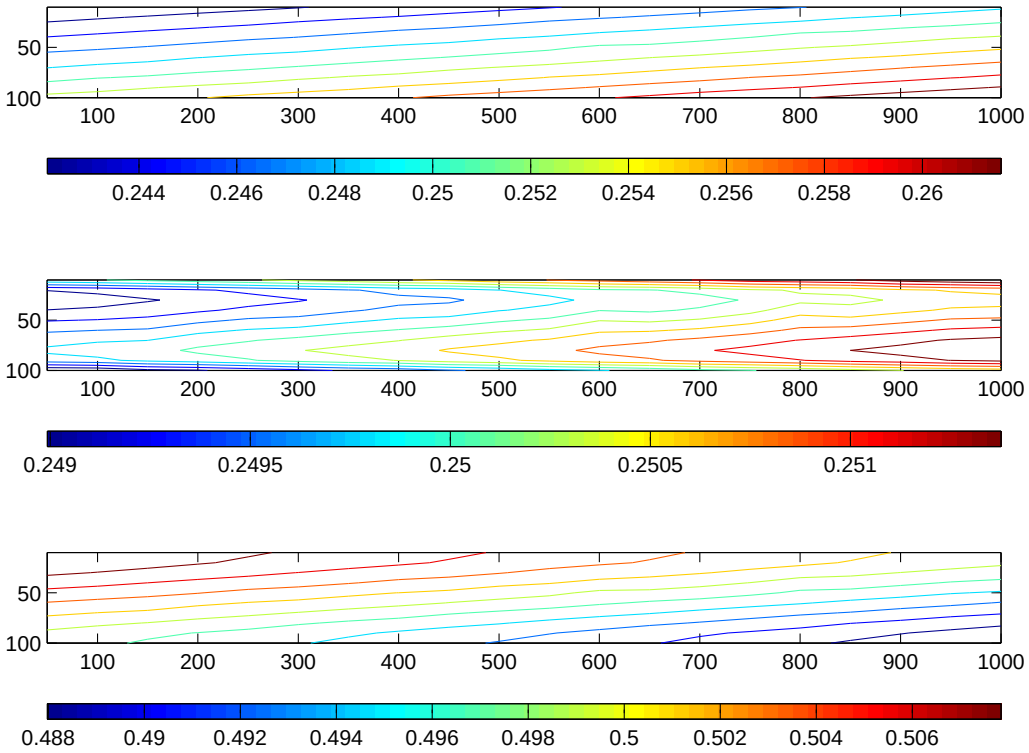

Figure 5.13: Compositional variation of molecular and thermal diffusion. [C_1, C_2 and C_4 mole fractions]

It is noted here that the figure shows profiles similar to those of Figure 5.10. This implies that the thermal diffusion term is the dominant diffusion term under the conditions studied. It also implies that the temperature field should not be fixed, but allowed to changed dynamically as the fluid moves in the reservoir due to convection and diffusion.

This conclusion may be confirmed by looking at the ratio of these terms. The

ratio of the pressure diffusion term to that of the thermal diffusion term is given by:

$$\frac{\tau^D \rho_p^m D_i^p \Delta p}{\tau^D \rho_p^m D_i^T \Delta T} \tag{5.1}$$

which may be approximated as being of the order of:

$$\frac{\frac{D_i^p}{L}}{\frac{D_i^T}{L}} = \frac{D_i^p}{D_i^T} \approx 0.001 \tag{5.2}$$

5.4 Summary

Based on the results shown in this section, some preliminary conclusions may be noted.

1. Convection could be the dominant process under conditions where the Rayleigh number is larger that the critical value or the reservoir is tilted.

2. In reservoirs with horizontal and vertical temperature gradients, the pressure diffusion term may be neglected.

3. Thermal diffusion appears to be the most dominant diffusion term. The temperature gradients is the main driving force for the movement of the fluids in such reservoirs.

Chapter 6

Inclusion of a Dynamic Temperature Field

In general, the temperature field of a reservoir is usually assumed to be uniform and fixed. This assumption reduces the complexity of the problem and in most situations is a valid assumption to make given the negligible change in temperature over time in many reservoirs. However, it has been shown in the literature that for a fluid layer heated from below the isotherms may change over time. This implies that the temperature at various locations in the reservoir changes over time, as heat is transferred from the underburden to the reservoir, from the reservoir to the overburden and from point to point within the reservoir.

In this study, this change in temperature has been taken into account by adding an energy balance equation (which takes into account heat transfer by convection and conduction and neglects heat transfer by radiation) to the set of nonlinear equations to be solved.

To investigate the effect of heat transfer on compositional variation in an oil reservoir, three example reservoirs were defined (see Table 6.1). For each reservoir, two runs were made and compared, one with a fixed temperature gradient, T_o and the other with a dynamic temperature gradient, with the initial value for the temperature field being T_o. The results were then compared based on the reservoir metrics and the composition profiles.

Table 6.1: Key of cases for the inclusion of an energy balance.

Reservoir	Fluid description	Reservoir and fluid properties
A	Single-component fluid	Table 6.2
B	Binary fluid	Table 6.3
C	Ternary fluid	Table 6.4

6.1 Single-Component Fluid

In this section, the reservoir fluid is a single-component fluid.

Table 6.2: Reservoir and fluid properties for Reservoir A

Dimensions	2000m x 100m x 2000m
Porosity	0.25
Permeability	200md
Datum reservoir pressure	55bars
Datum reservoir temperature	373K
Temperature gradients	0.01K/m and 0.003K/m

Figure 6.1 shows the temperature field for Reservoir A, fixed throughout for run 1 and set as the initial condition for run 2. Figure 6.2 shows the four metrics, the Nusselt number, the separation factor, the Rayleigh number and the density factor, for Reservoir A with a fixed temperature field. These metrics are constant over time, for example, the Nusselt number remains 1 because the temperature field is fixed and therefore no heat is transferred due to convection of the fluid within the system. This profile implies a purely conductive temperature field. The Rayleigh number remains constant as well because the temperature gradient and the average fluid properties are constant. The density factor remains constant over time as well, after the initial drop from the value based on the initialized reservoir and fluid properties. The separation factor is one in this case only because the fluid is a single-component fluid and composition is neglected in the analysis.

The reservoir pressure is shown in Figure 6.3. For this reservoir and fluid configurations, the isotherms in the reservoir remain constant over time and are fixed at each gridblock within the reservoir, as is expected and are shown in Figure 6.4.

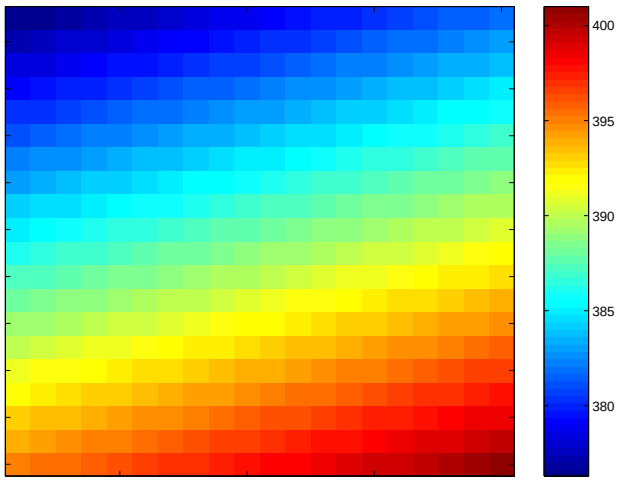

Figure 6.1: Temperature field for Reservoir A.

In the second scenario of Reservoir A, the temperature field is dynamic and the energy balance is included as a primary equation and gridblock temperatures become simulation variables. The metrics are quite different from those in the first scenario. Figure 6.5 shows the metrics for Reservoir A with a dynamic temperature field. The figure shows that the values of the Nusselt and Rayleigh numbers increase steadily as the movement of fluid within the reservoir becomes more vigorous. This is because heat transfer is allowed to take place across the reservoir due to both the convection of fluid and conduction of heat from point to point. This implies that the heat transfer across the reservoir increases as the mode of heat transfer goes from purely conductive to both conductive and convective (heat transfer by radiation is assumed to be negligible). The Nusselt number and Rayleigh number are shown in Figure 6.5 to increase over time and then slowly taper off as the configuration in the reservoir becomes more stable. The Nusselt number reaches a plateau as the amount of heat within the system reaches a constant value.

Figures 6.6 and 6.7 show the pressure and velocity profiles corresponding to a dynamic temperature field. Figure 6.7 also shows the isotherms in the reservoir. It is

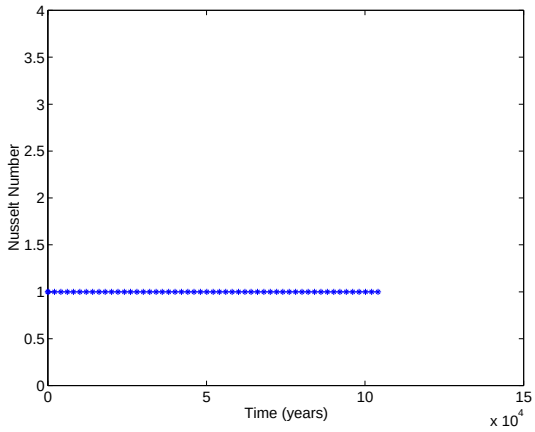

(a) Nusselt Number

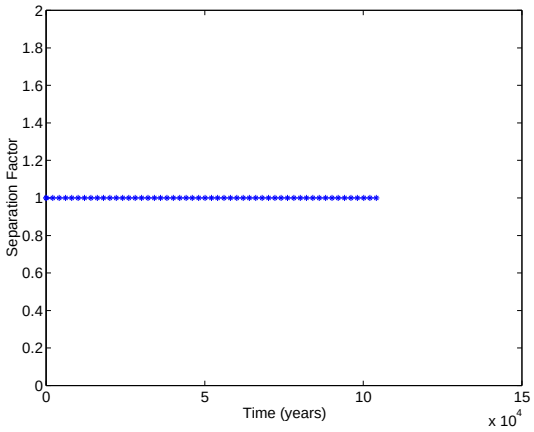

(b) Separation Factor

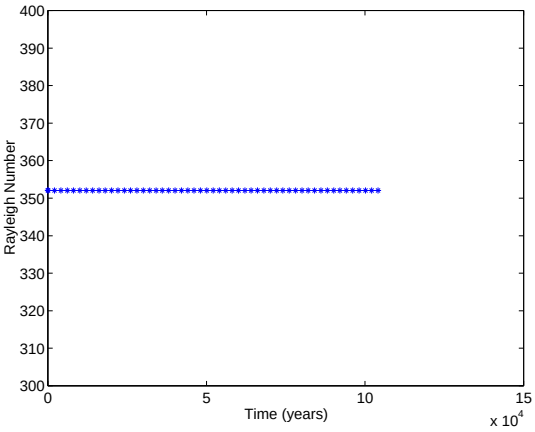

(c) Rayleigh Number

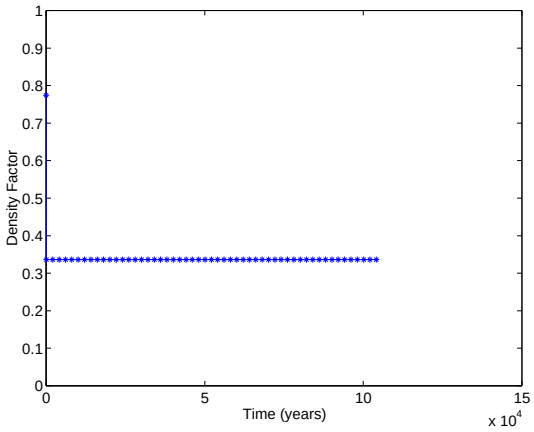

(d) Density Factor

Figure 6.2: Metrics for Reservoir A with a fixed temperature field.

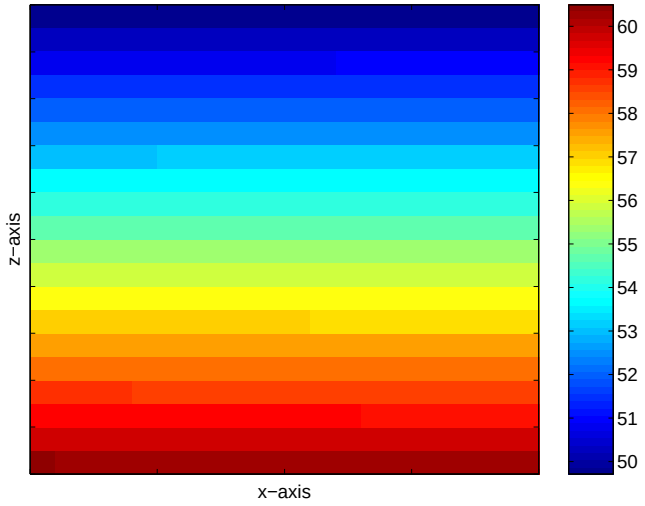

Figure 6.3: Pressure profile for Reservoir A with a fixed temperature field.

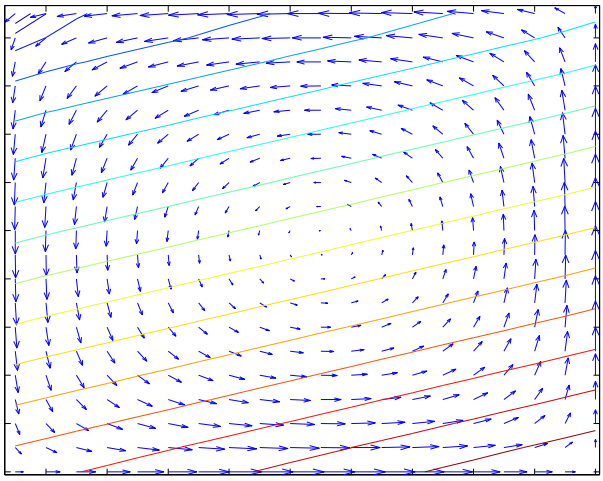

Figure 6.4: Velocity profile and isotherms for Reservoir A with a fixed temperature field.

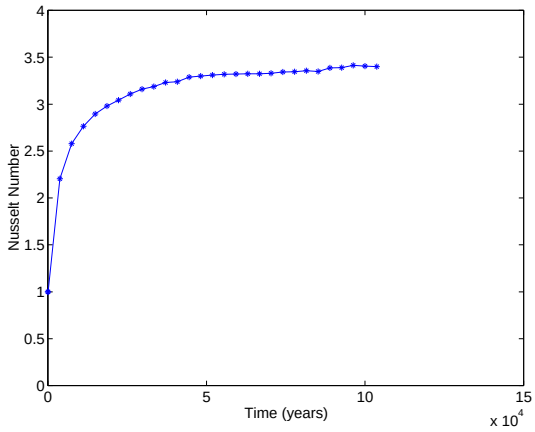

(a) Nusselt Number

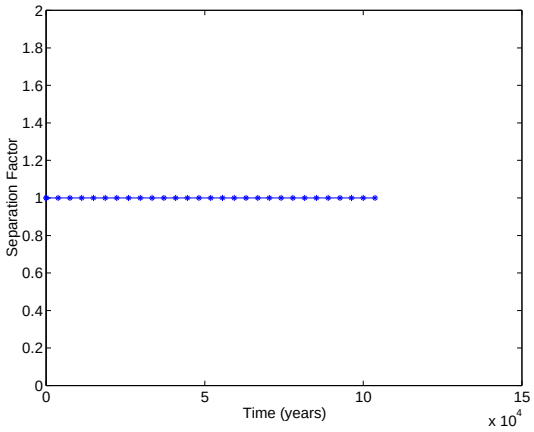

(b) Separation Factor

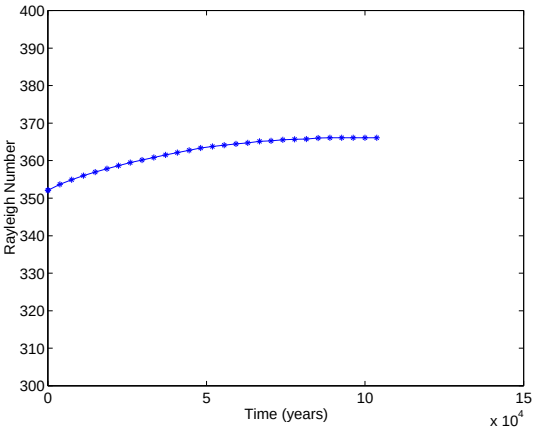

(c) Rayleigh Number

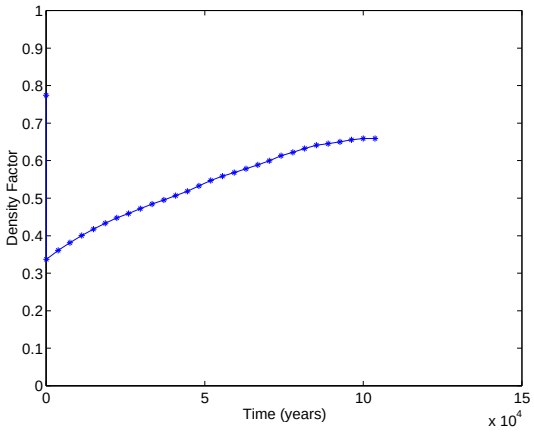

(d) Density Factor

Figure 6.5: Metrics for Reservoir A with a dynamic temperature field.

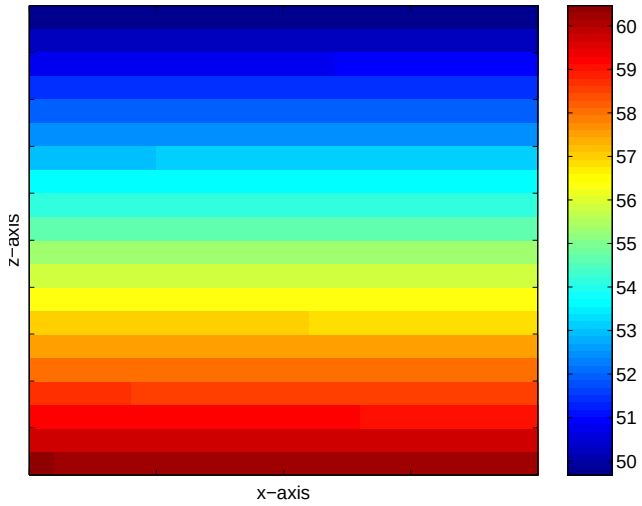

Figure 6.6: Pressure profile for Reservoir A with a dynamic temperature field.

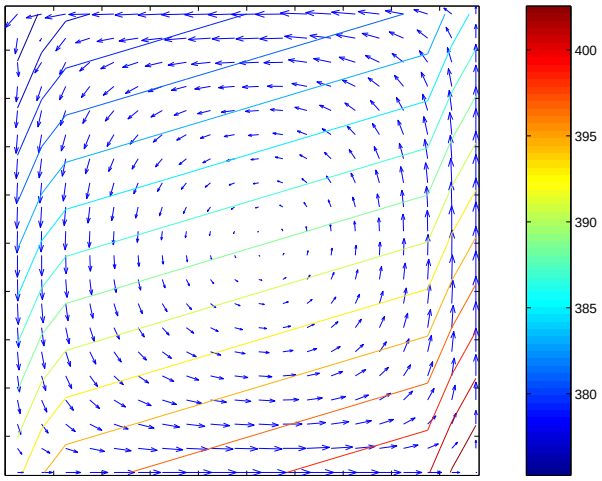

Figure 6.7: Velocity profile and isotherms for Reservoir A with a dynamic temperature field.

observed that for a fixed temperature field, although the fluid is in motion, the thermal gradient in the reservoir is uniform. In the case of a dynamic temperature field, the thermal gradients though initially uniform across the reservoir become steeper towards the top and bottom of the reservoir. This implies that heat transfer due to convection is increasing and hence becomes more significant.

6.2 Multicomponent Fluid

In reservoirs with multicomponent mixtures, the compositions are additional unknowns and the separation factor becomes an important metric in analyzing the results. It has been observed that under stable conditions, the composition profiles either remain in the initial state, or align themselves according to gravitational field (gravity segregation) based on the fluid potential and temperature.

Table 6.3: Reservoir and fluid properties for Reservoir B

Dimensions	1000m x 100m x 100m
Porosity	0.25
Fluid composition	C_3 and C_8
Permeability	100md
Datum pressure	55bars
Temperature gradients	0.01K/m and 0.005K/m
Rock heat capacity	1800KJ/kgK
Rock conductivity	280KJ/kg

Tables 6.3 and 6.4 list the reservoir and fluid properties used for Reservoirs B and C. Reservoir B is a reservoir with a binary fluid mixture of propane and octane and Reservoir C contains a ternary fluid mixture of methane, ethane and butane.

The temperature field of Reservoir B is shown in Figure 6.8. Figure 6.9 shows the metrics for Reservoir B with a fixed temperature field. It has been established that for cases where the temperature field is assumed to be constant over time, the Nusselt number remains constant. The Rayleigh number is also assumed to be constant as the change in the Rayleigh number with respect to its initial value is less than 0.001%. This is not so for the separation and density factors. The separation factor changes

Table 6.4: Reservoir and fluid properties for Reservoir C

Dimensions	1000m x 100m x 1000m
Porosity	0.25
Fluid composition	C_1, C_2 and C_4
Permeability	100md
Datum pressure	80bars
Temperature gradients	0.01K/m and 0.003K/m
Rock heat capacity	1800KJ/kgK
Rock conductivity	280KJ/kg

as fluid moves within the reservoir and the composition changes and by extension, the density within the reservoir changes as well from point to point. The changes in these two metrics are therefore significant. The pressure and velocity profiles and the isotherms in the reservoir are as expected and are shown in Figure 6.10. The composition profile in the reservoir is shown in Figure 6.11. Figure 6.12 shows the metrics for Reservoir B with a dynamic temperature field. Figure 6.14(a) shows the pressure profile, while Figure 6.13 shows the composition profile. The average difference in composition in the reservoir is $3x10^{-3}$ moles which is approximately 1.2% of the initial reservoir composition. Figure 6.15 shows a comparison of the average x- and z-directional velocities in the reservoir. Overall, it appears that the inclusion of a dynamic temperature field results in a reduction in the fluid velocity and an increase in the degree of compositional variation within the reservoir.

The same analysis was carried out with Reservoir C. Figures 6.16 and 6.18 show the metrics for Reservoir C with fixed and dynamic temperature fields respectively. In this case, the change in the Nusselt and Rayleigh numbers is small, when compared to the changes observed for Reservoir B as shown in Figure 6.12. The separation factor in this case shown in Figure 6.18b fluctuates until a stable configuration is established in the reservoir. This fluctuation did not occur in Reservoir B whose fluid is comprised of two components only. Figure 6.21 shows that for multicomponent mixtures, the segregation of fluid components according to the pressure and temperature in the reservoir, overshadow the change in the temperature field to reflect high heat transfer due to convection. This conclusion can be drawn because the changes in the isotherms

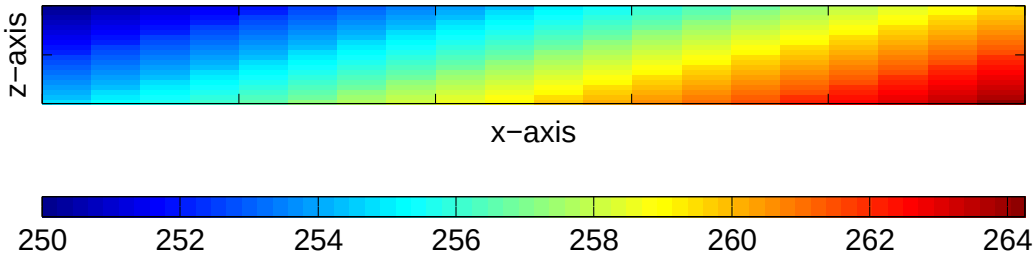

Figure 6.8: Temperature field for Reservoir B.

within the reservoir are subtle. It would appear that the fluid motion would rather align the components in such a way as to maintain the pressure and temperature in the reservoir, rather than transfer heat more vigorously from one point to the other. Another explanation could be that a multicomponent fluid is better equipped to move heat and mass from one location in the reservoir to another due to the ability to vaporize and condense heavier or lighter components to accommodate changes in temperature and pressures.

Figure 6.20 shows the pressure profile in Reservoir C. It is noted that the change in temperature is of the order of 0.05, less than a 1% change in the reservoir temperature gradient. This is in part due to the fact that the temperature at the upper and lower boundaries is fixed.

In general, it has been shown that with the inclusion of a dynamic temperature field, the profiles of pressure, temperature and composition change, compared to a fixed temperature field. It was observed that for large Rayleigh numbers, the change in the Nusselt number is small, for example, Figure 6.16 whereas for small Rayleigh numbers, the change in the Nusselt number is large, for example, Figure 6.18. The increase in the Nusselt number is small for Reservoir C primarily because the thermal gradients across the reservoir are small and the fluid is a multicomponent fluid.

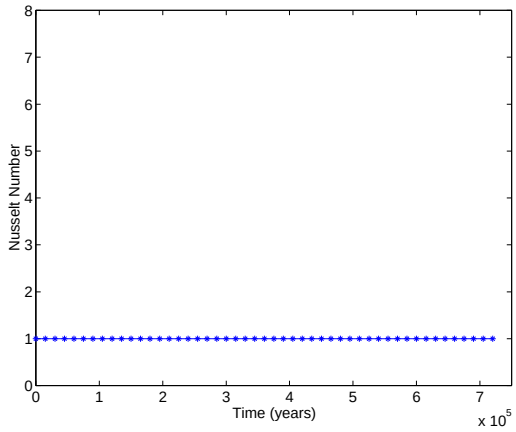

(a) Nusselt Number

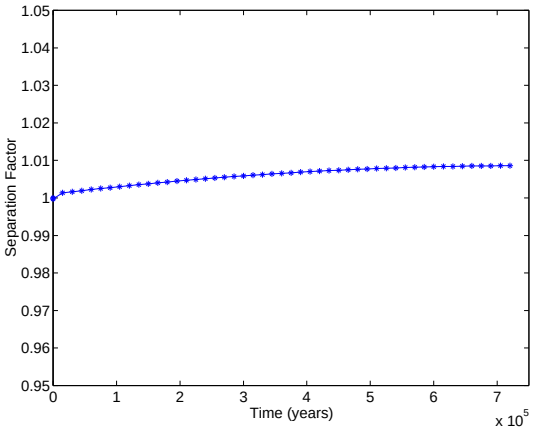

(b) Separation Factor

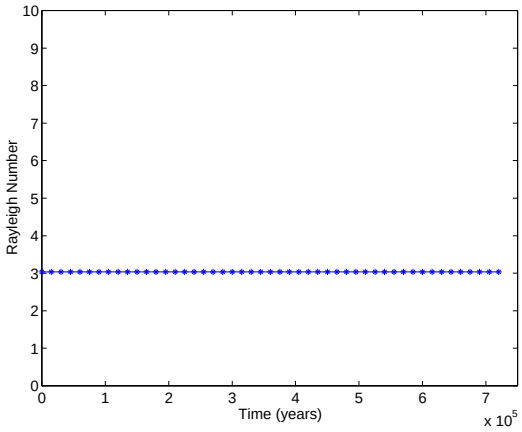

(c) Rayleigh Number

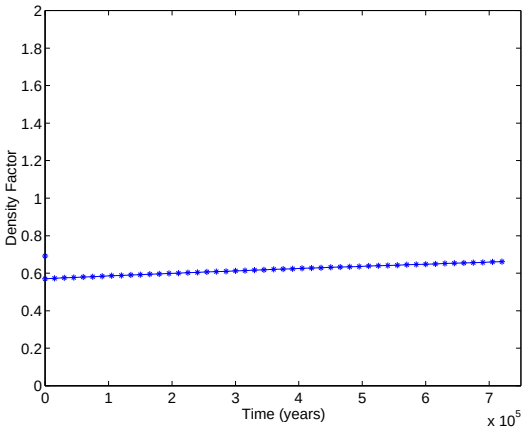

(d) Density Factor

Figure 6.9: Metrics for Reservoir B with a fixed temperature field.

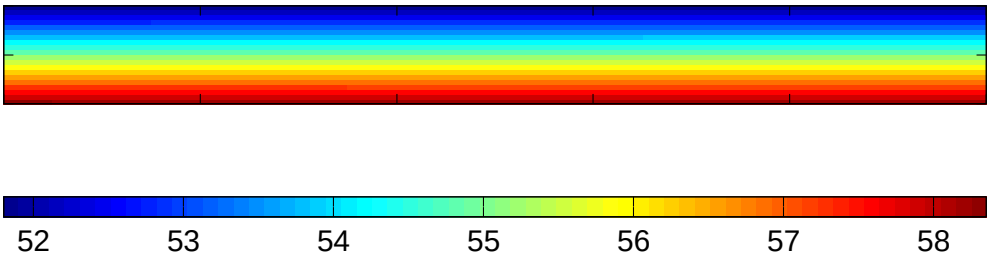

(a) Pressure profile

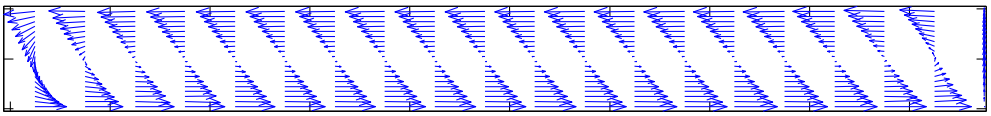

(b) Velocity profile

Figure 6.10: Pressure and velocity profiles for Reservoir B with a fixed temperature field.

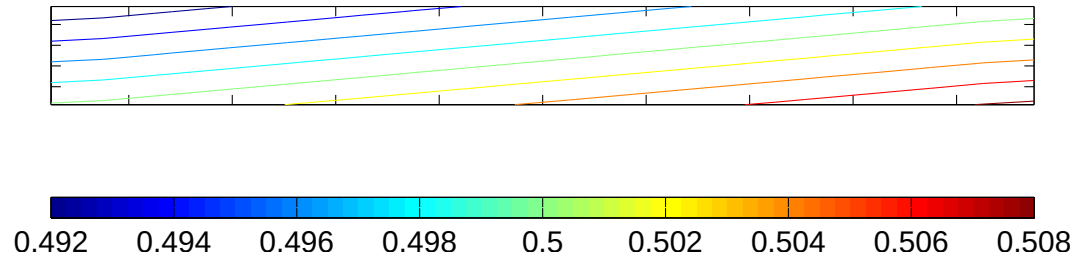

(a) C_3

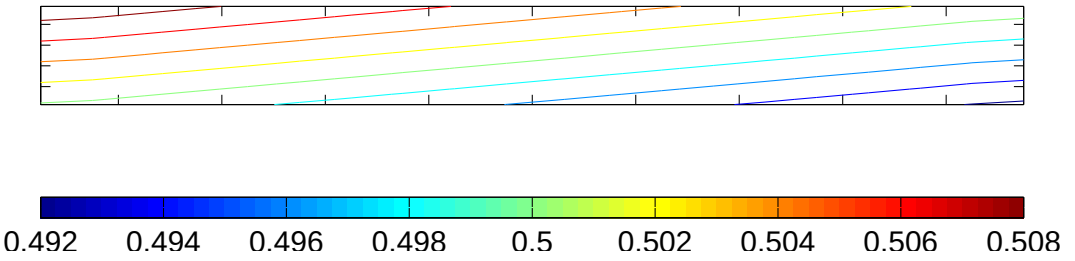

(b) C_8

Figure 6.11: Composition profile for Reservoir B with a fixed temperature field.

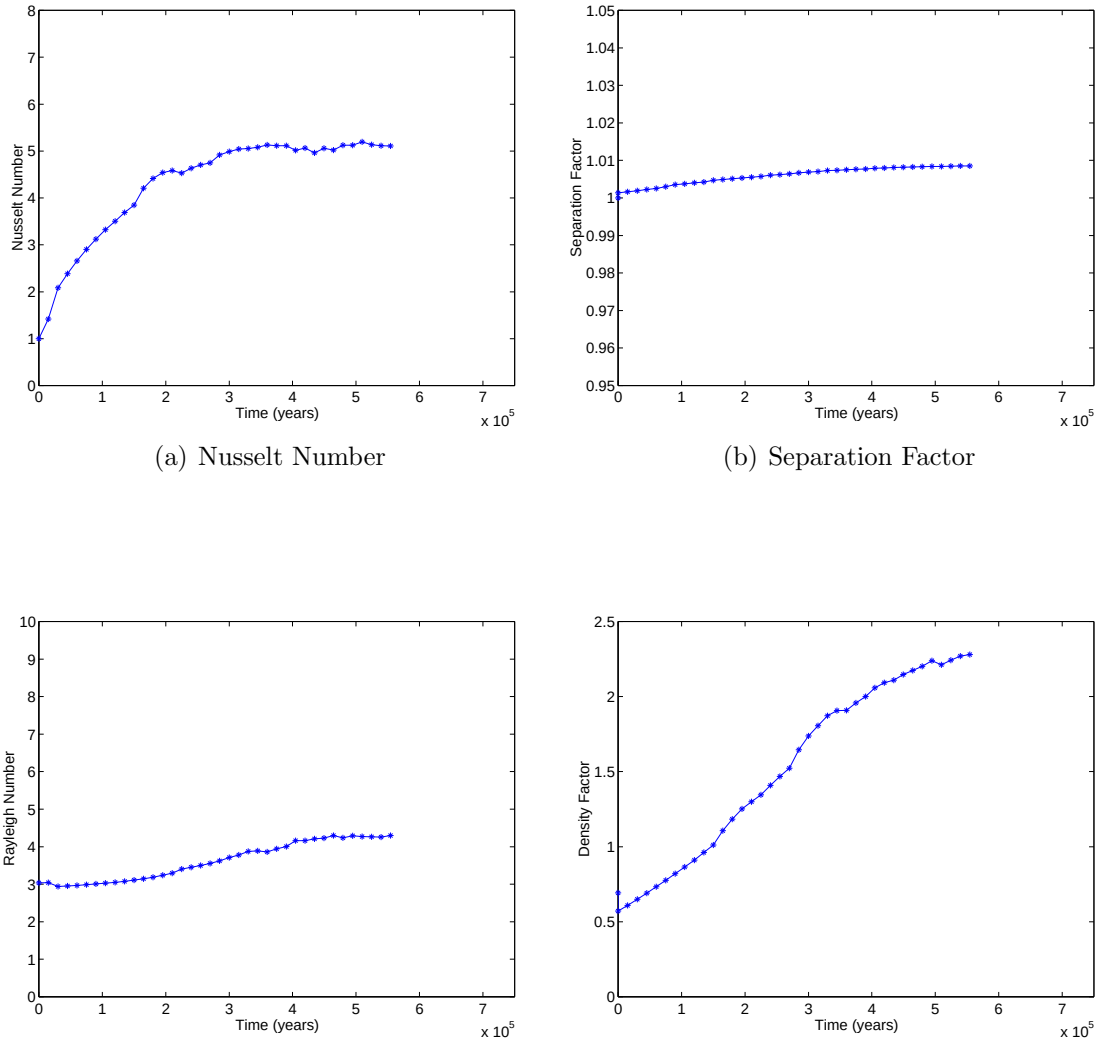

(a) Nusselt Number

(b) Separation Factor

(c) Rayleigh Number

(d) Density Factor

Figure 6.12: Metrics for Reservoir B with a dynamic temperature field.

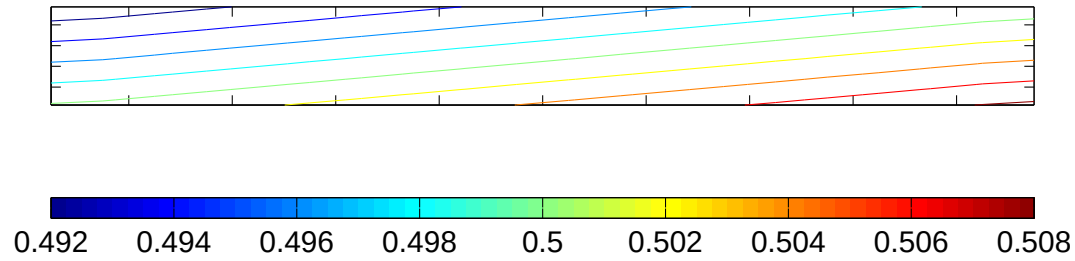

(a) C_3

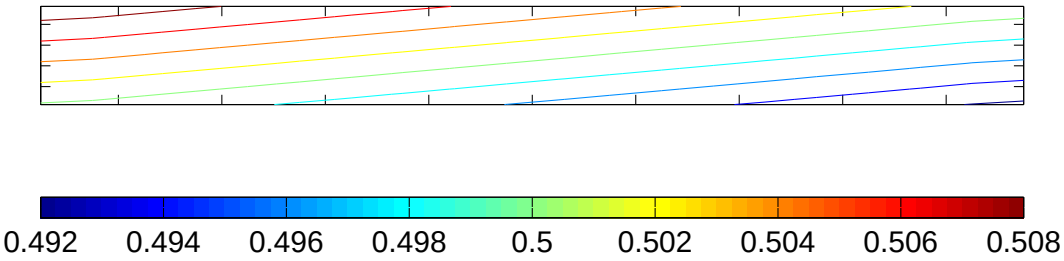

(b) C_8

Figure 6.13: Composition profile for Reservoir B with a dynamic temperature field.

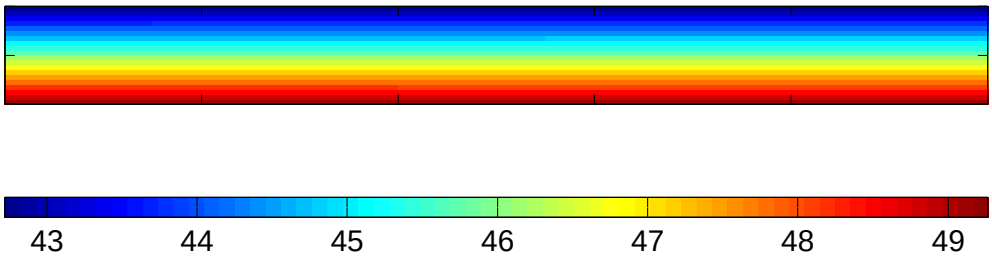

(a) Pressure profile

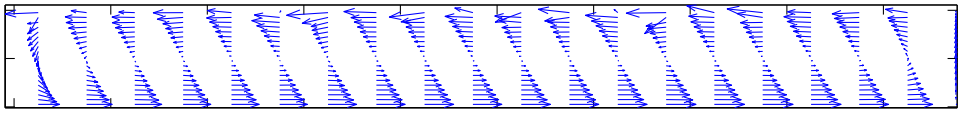

(b) Velocity profile

Figure 6.14: Pressure and velocity profile for Reservoir B with a dynamic temperature field.

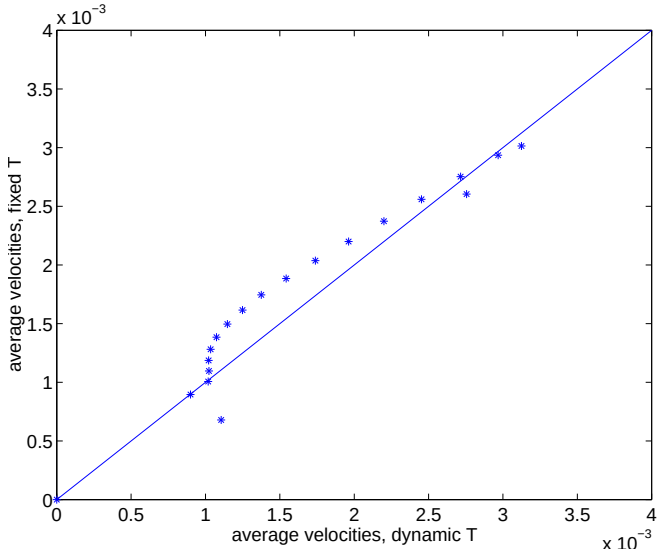

(a) x-velocity

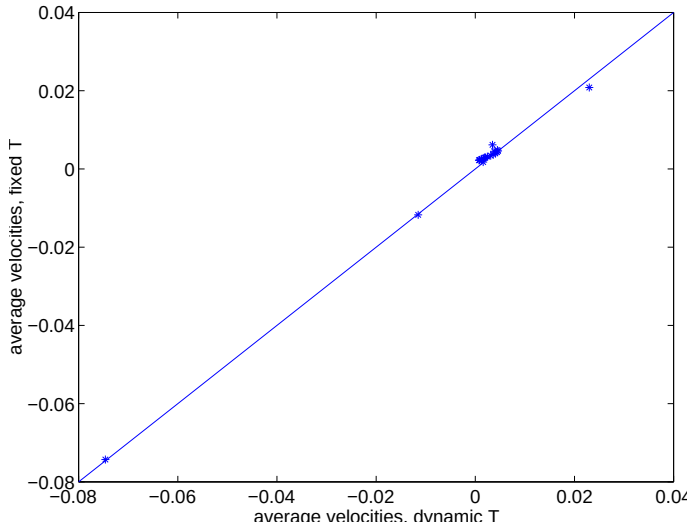

(b) z-velocity

Figure 6.15: Comparison of average velocities for Reservoir B with fixed and dynamic temperature fields.

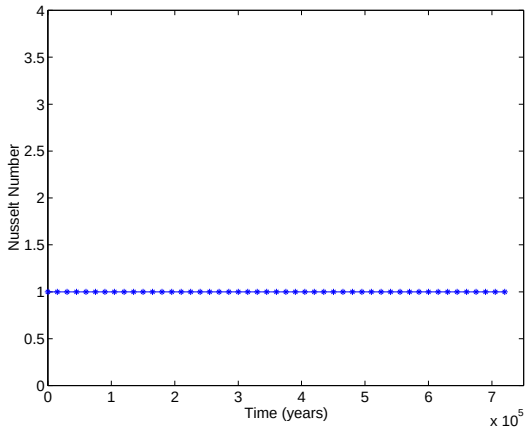

(a) Nusselt Number

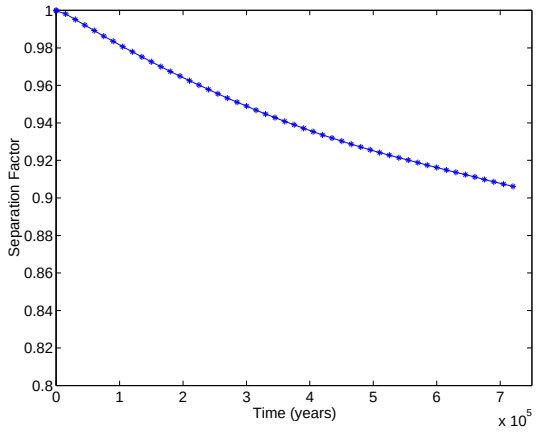

(b) Separation Factor

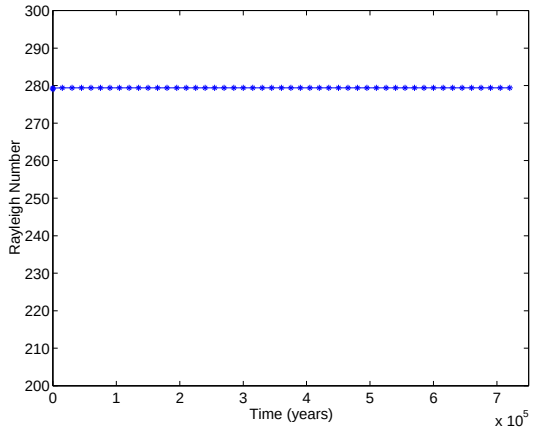

(c) Rayleigh Number

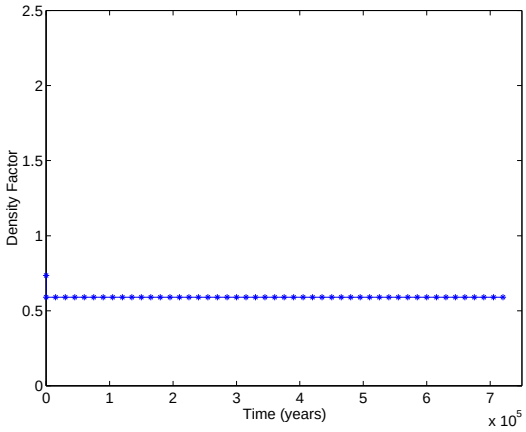

(d) Density Factor

Figure 6.16: Metrics for Reservoir C with a fixed temperature field.

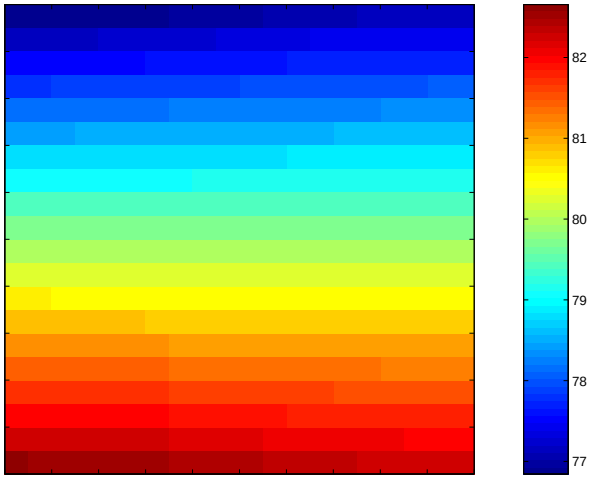

Figure 6.17: Pressure profile for Reservoir C with a fixed temperature field.

,

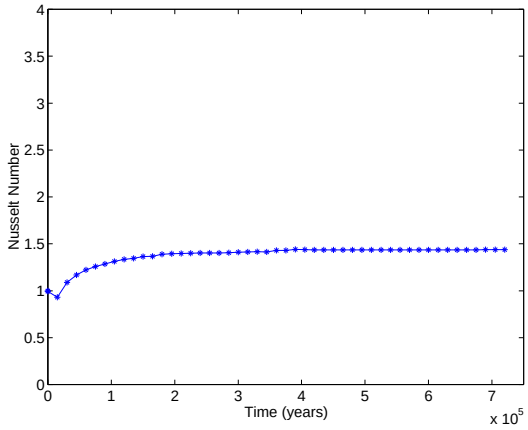

(a) Nusselt Number

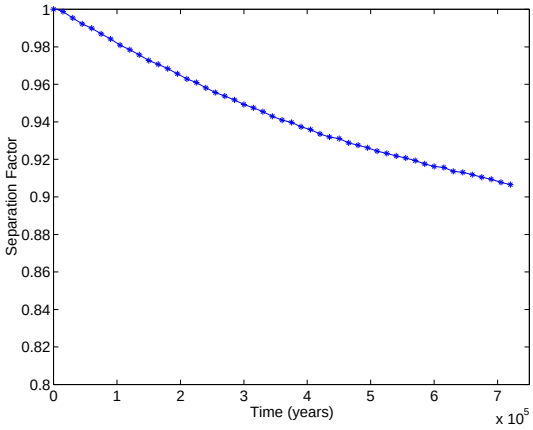

(b) Separation Factor

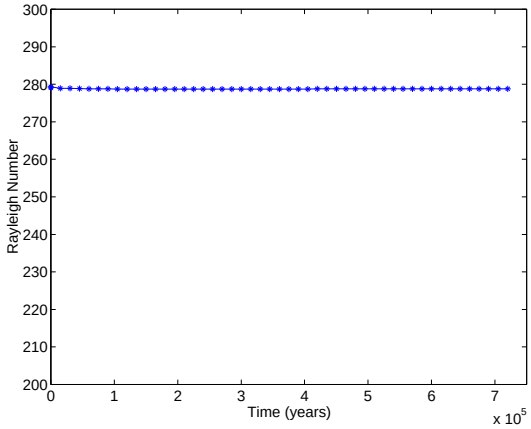

(c) Rayleigh Number

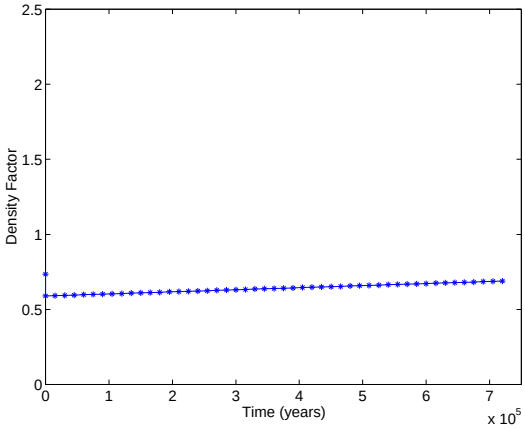

(d) Density Factor

Figure 6.18: Metrics for Reservoir C with a dynamic temperature field.

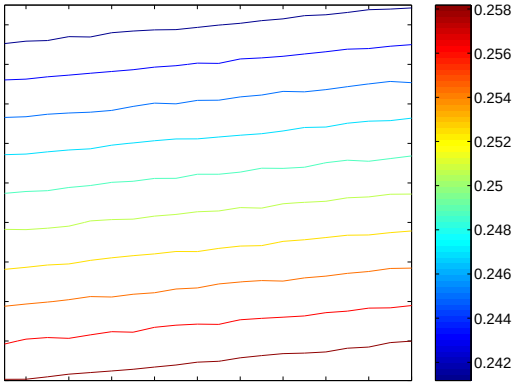

(a) C_1 profile

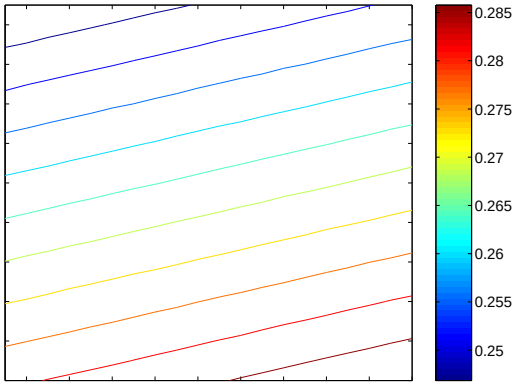

(b) C_2 profile

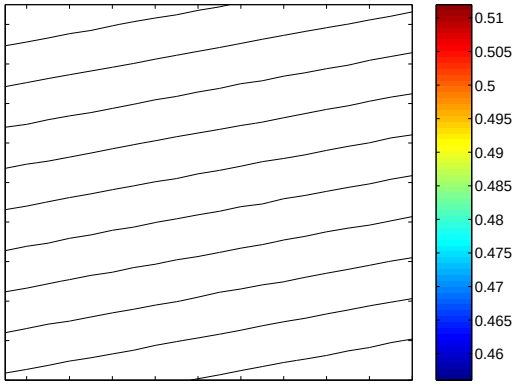

(c) C_4 profile

Figure 6.19: Composition profiles for Reservoir C with a dynamic temperature field.

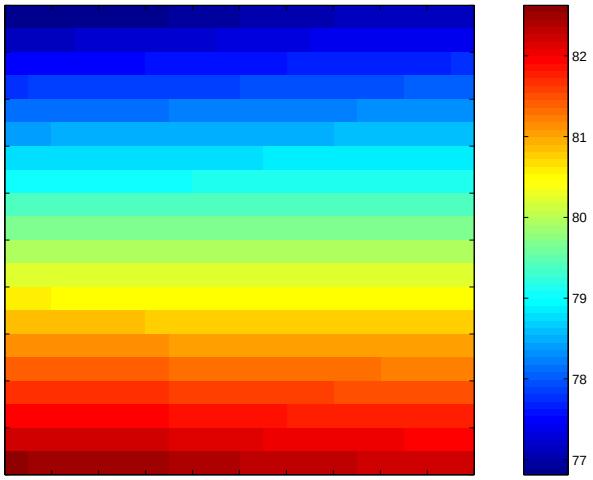

Figure 6.20: Pressure profile for Reservoir C with a dynamic temperature field.

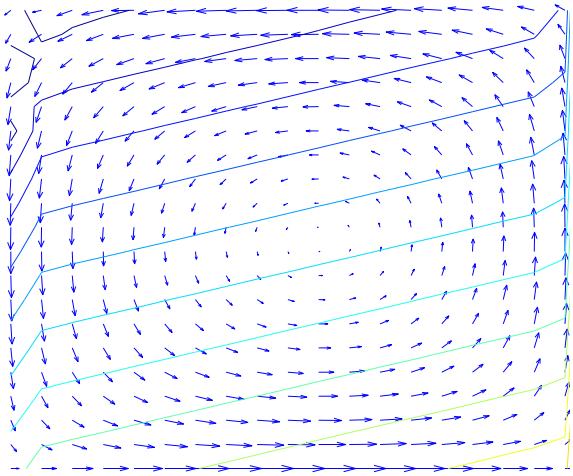

Figure 6.21: Velocity profile and isotherms for Reservoir C with a dynamic temperature field.

6.2.1 Test Case

Although a case study of a field example was not readily available, an analysis of an example from the literature is presented here to provide a framework for the conclusions that are drawn in this study. The reservoir and fluid data is taken from Ghorayeb and Firoozabadi (2000a) and repeated here as Reservoir D.

Table 6.5: Reservoir and fluid properties for Reservoir D

Reservoir dimenstions	10km x 1.5km
Porosity	0.20
Fluid composition	CO_2, C_1, C_2, C_3-C_4, C_5-C_6, C_{7+}
Permeability	10md
Datum pressure	4.66 x 10^7Pa
Datum temperature	422K
Temperature gradients	0.0275 and 0.0015K/m
Fluid viscosity	0.075cp

The first runs was done using a reservoir with a fixed temperature field, while the second was done including a dynamic temperature field. Figures 6.22 and 6.23 show the composition profiles for Reservoir D with a fixed temperature field. These profiles are in agreement with those shown in the literature (Ghorayeb and Firoozabadi, 2000a). Figures 6.24 and 6.25 show the composition profiles for Reservoir D when the energy balance is included, thus allowing for a dynamic temperature field. The separation factor (C_1/C_{7+}), changes from value of 4.43 for a fixed temperature field to 1.84 for a dynamic temperature field. This highlights the importance of the addition of a dynamic temperature field.

Table 6.6 shows the variation in the composition of the reservoir fluid in the two scenarios, the run with a dynamic temperature field and the run with a fixed temperature field. Essentially, from Table 6.6 and Figures 6.24 and 6.25, it is observed that effect of the inclusion of a dynamic temperature field depends on the fluid components. Although there is a change in the compositional variation across the entire reservoir in every component, the components with the most pronounced change are the ones with the larger mole fractions, in this example methane and the heptane

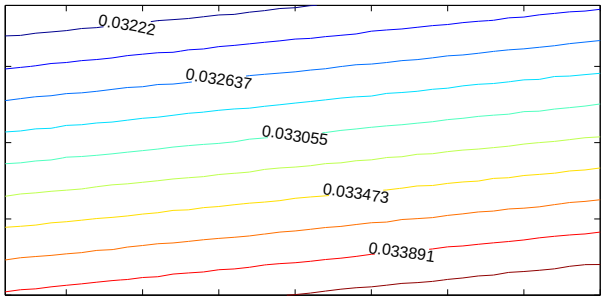

(a) CO_2 profile

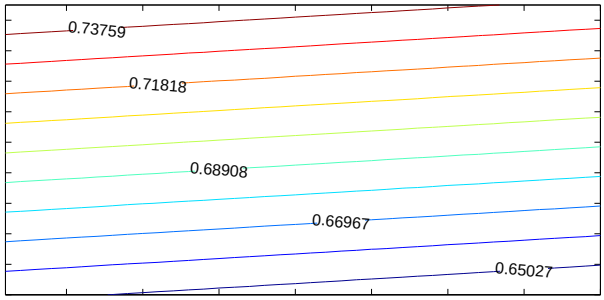

(b) C_1 profile

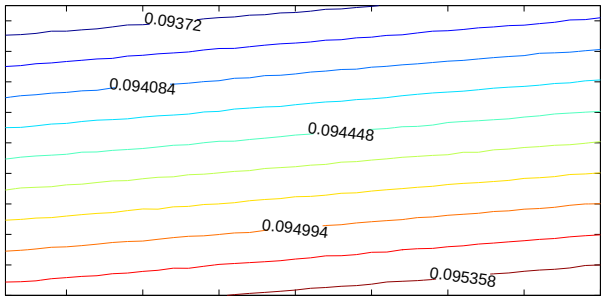

(c) C_2 profile

Figure 6.22: Composition profiles for Reservoir D with a fixed temperature field. [CO_2, C_1 and C_2]

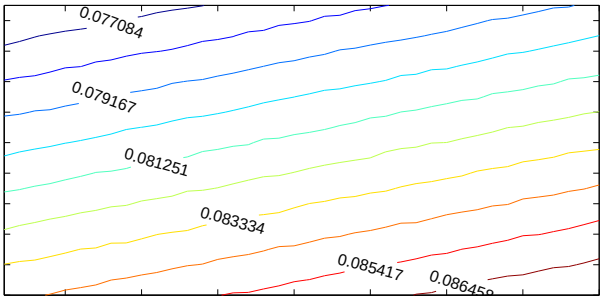

(a) C_3-C_4 profile

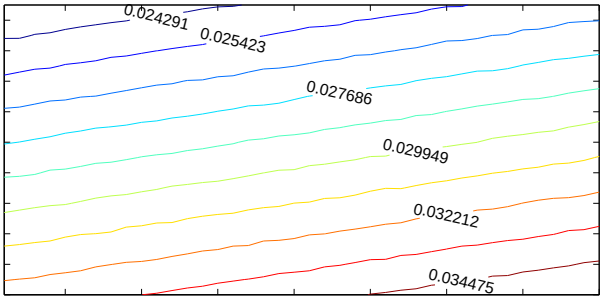

(b) C_5-C_6 profile

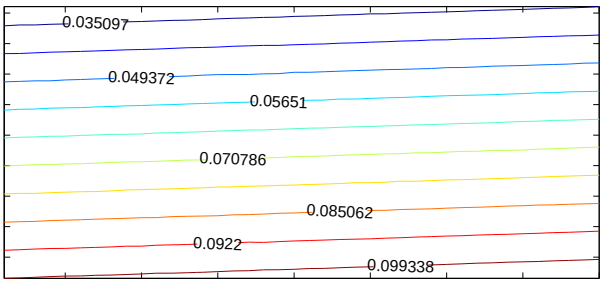

(c) C_{7+} profile

Figure 6.23: Composition profiles for Reservoir D with a fixed temperature field. [C_3-C_4, C_5-C_6 and C_{7+}]

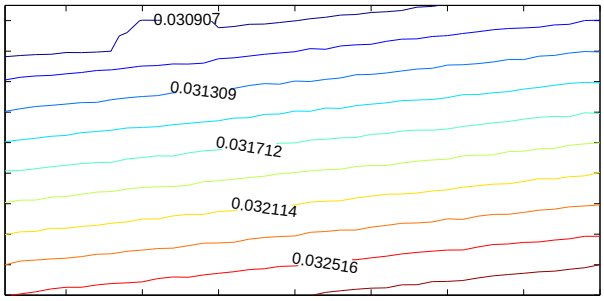

(a) CO_2 profile

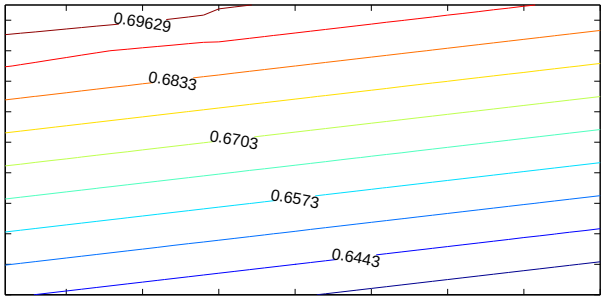

(b) C_1 profile

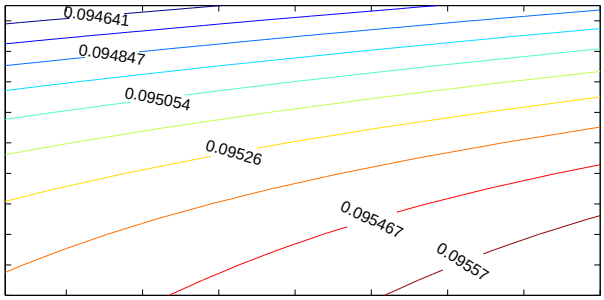

(c) C_2 profile

Figure 6.24: Composition profiles for Reservoir D with a dynamic temperature field. [CO_2, C_1 and C_2]

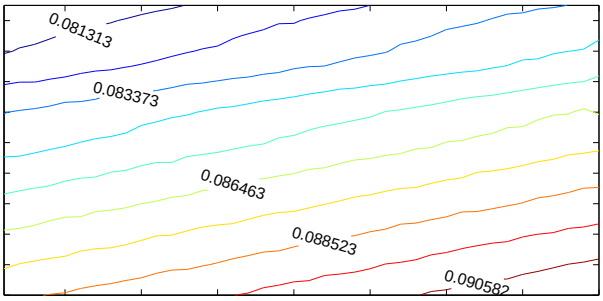

(a) C_3-C_4 profile

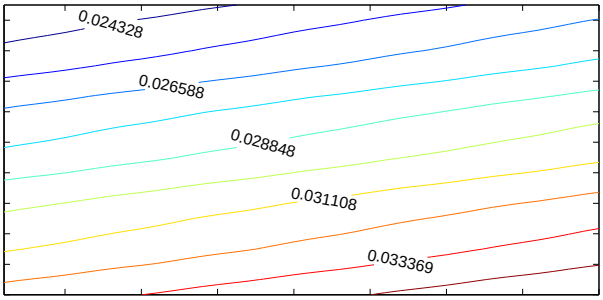

(b) C_5-C_6 profile

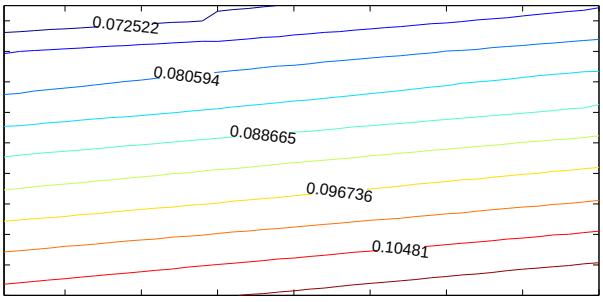

(c) C_{7+} profile

Figure 6.25: Composition profiles for Reservoir D with a dynamic temperature field. [C_3-C_4, C_5-C_6 and C_{7+}]

Table 6.6: Comparison of variation in component mole fractions

Component	Dynamic temperature field	Fixed temperature field
CO_2	0.0022	0.0022
C_1	0.0714	0.1066
C_2	0.0011	0.0019
C_3-C_4	0.0113	0.0115
C_5-C_6	0.0124	0.0124
C_{7+}	0.0443	0.0784

plus fractions.

Chapter 7

Three-dimensional Reservoirs

In earlier chapters, compositional variation has been studied in reservoirs in two dimensions, usually in the x-z orientation. Here, the effect of a third dimension on the computation of composition, pressure and velocity profiles is sought. In order to do this, two scenarios are compared for the same reservoir, including heat transfer effects, a two-dimensional grid and a three-dimensional grid. The y-averaged reservoir and fluid properties are then computed for the three-dimensional grid and compared to the global values of these properties for the two-dimensional grid. Based on such a comparison, the effect of a third dimension on the computation will be captured.

In general, two-dimensional representations of reservoirs average out the heterogeneity in one of the dimensions. Three-dimensional analysis of any problem in Reservoir Engineering is desirable because the connectivity within a reservoir is better represented in three dimensions. Therefore the flow of fluid within a reservoir may be quite different when the reservoir is represented in three dimensions as opposed to two dimensions, for example, by changing from a roll motion to a toroidal motion (which cannot be represented in two dimensions).

Tables 6.3 and 6.4 listed in Chapter **??** show the reservoir and fluid properties for Reservoir B and C. Figure 7.1 shows the metrics for the two-dimensional grid, while Figure 7.3 shows the y-averaged metrics for the three-dimensional grid. The composition and velocity profiles for the two- and three-dimensional grids are shown in Figures 7.2 and 7.5 respectively.

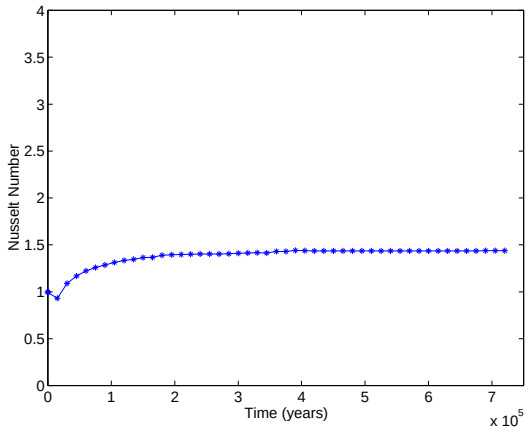

(a) Nusselt Number

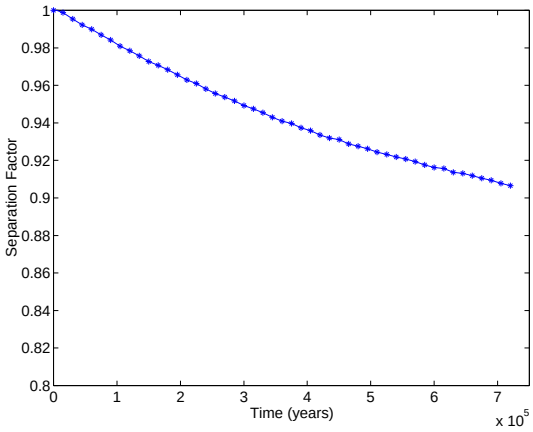

(b) Separation Factor

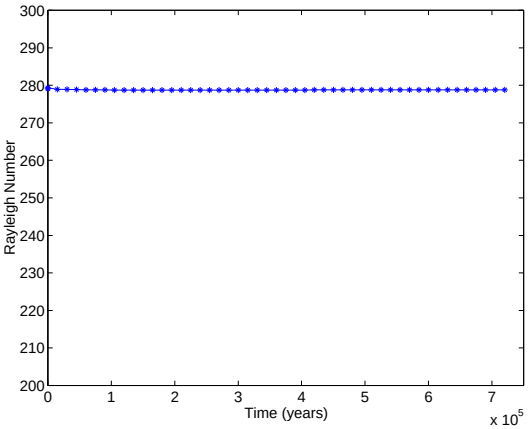

(c) Rayleigh Number

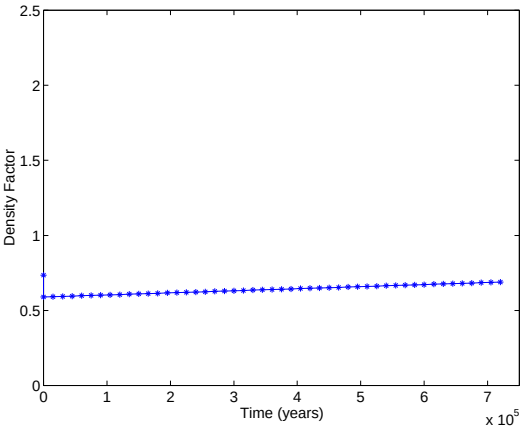

(d) Density Factor

Figure 7.1: Metrics for Reservoir C on a two-dimensional grid.

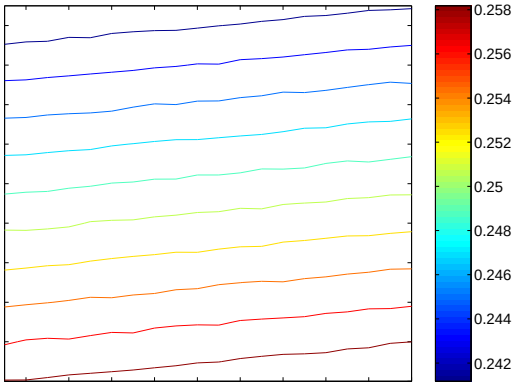

(a) C_1

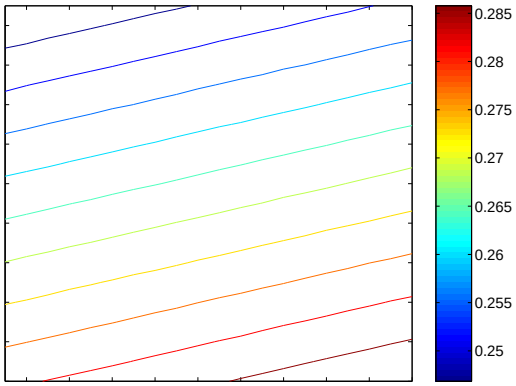

(b) C_2

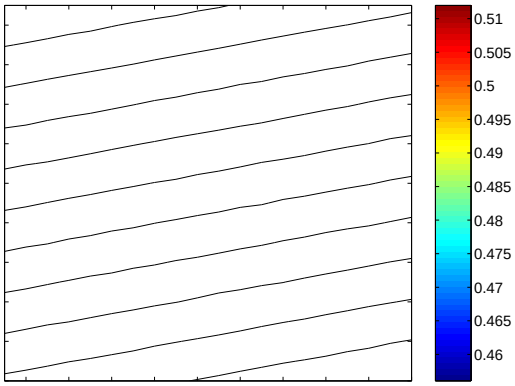

(c) C_4 profile

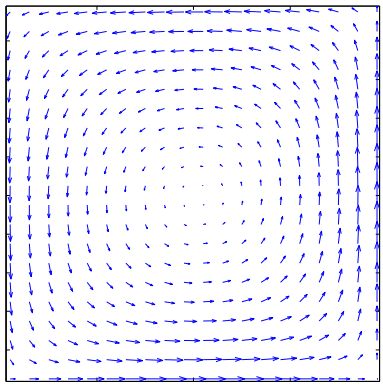

(d) Velocity profile

Figure 7.2: Composition and velocity profiles for Reservoir C on a two-dimensional grid.

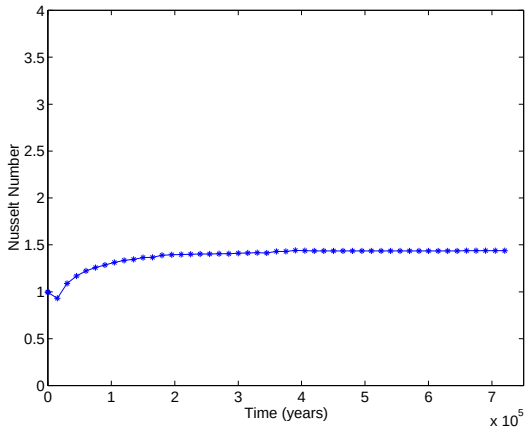

(a) Nusselt Number

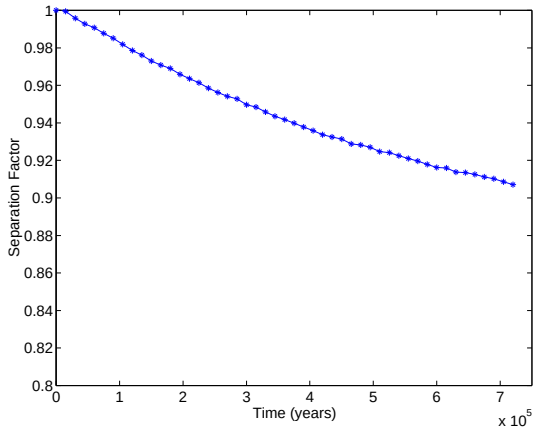

(b) Separation Factor

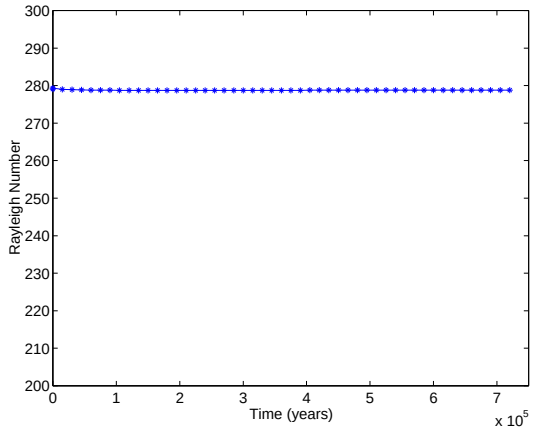

(c) Rayleigh Number

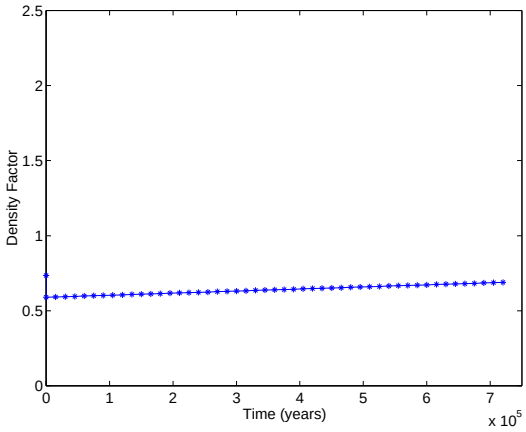

(d) Density Factor

Figure 7.3: y-averaged metrics for Reservoir C on a three-dimensional grid.

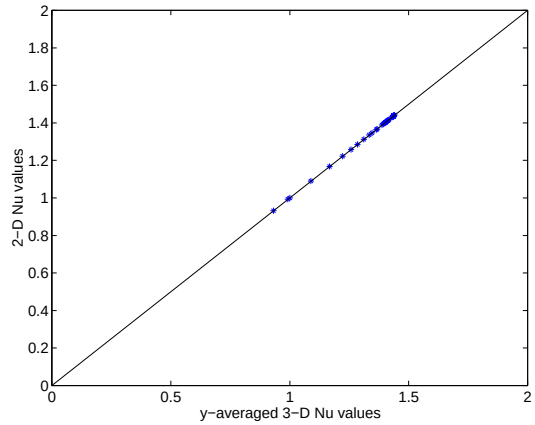

(a) Nusselt Number

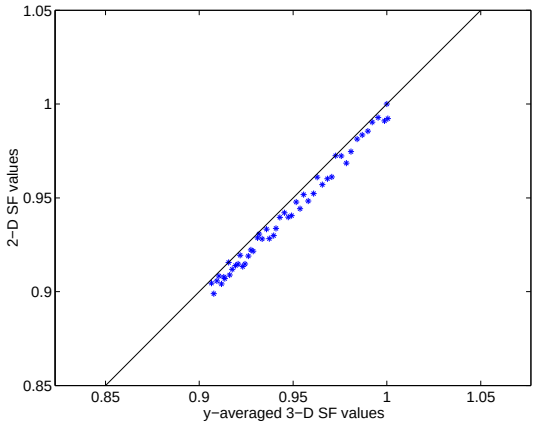

(b) Separation Factor

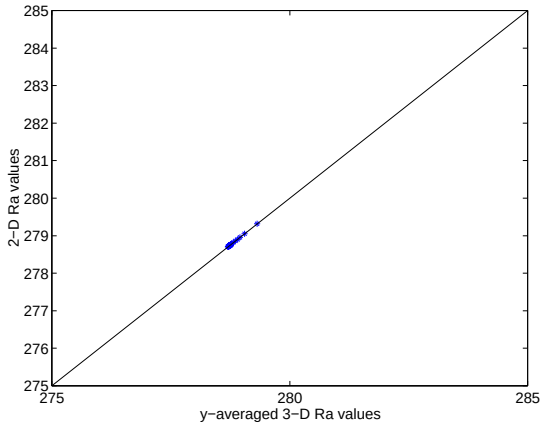

(c) Rayleigh Number

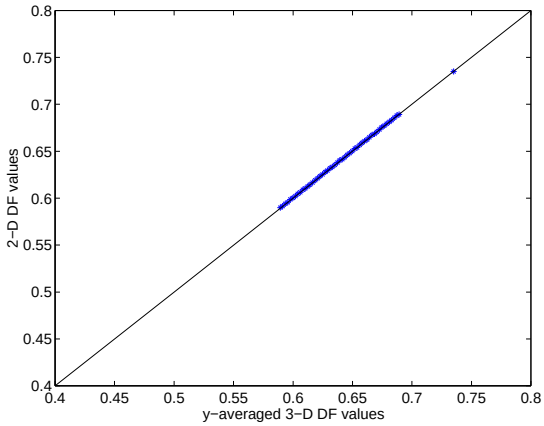

(d) Density Factor

Figure 7.4: Comparison of two- and three-dimensional metrics for Reservoir C.

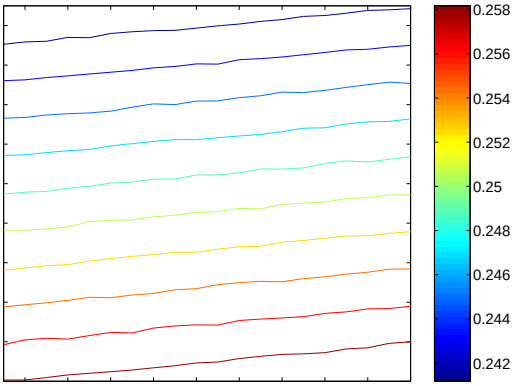

(a) C_1 profile

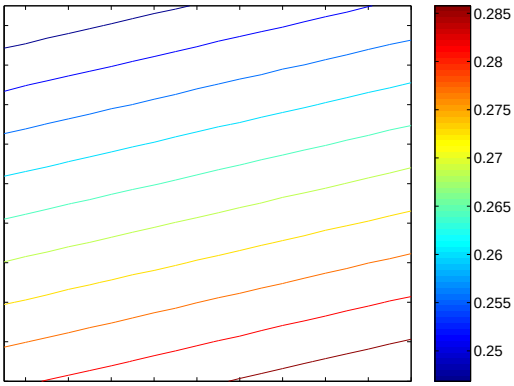

(b) C_2 profile

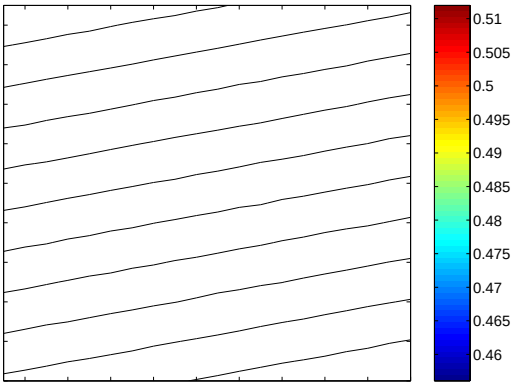

(c) C_4 profile

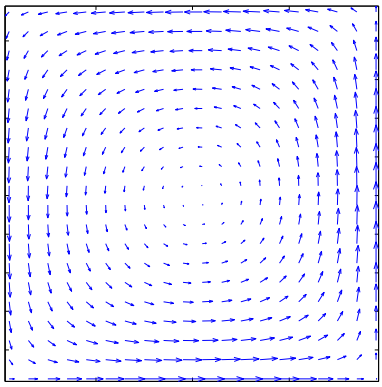

(d) Velocity profile

Figure 7.5: y-averaged composition and velocity profiles for Reservoir C on a three-dimensional grid.

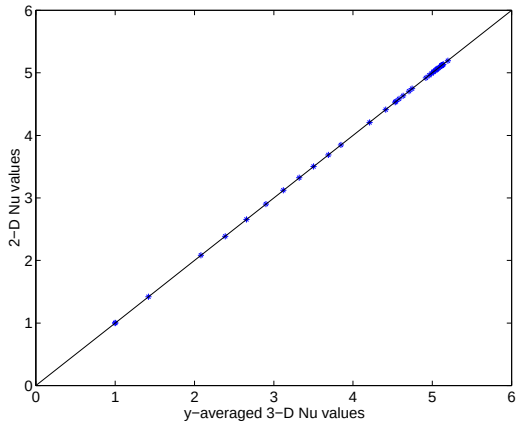

(a) Nusselt Number

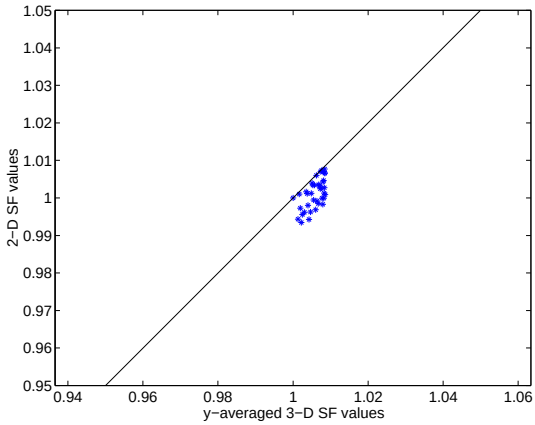

(b) Separation Factor

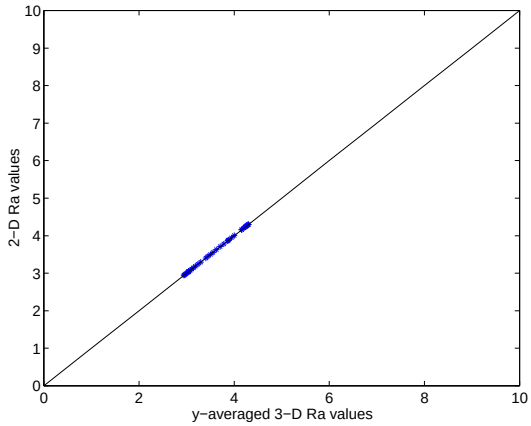

(c) Rayleigh Number

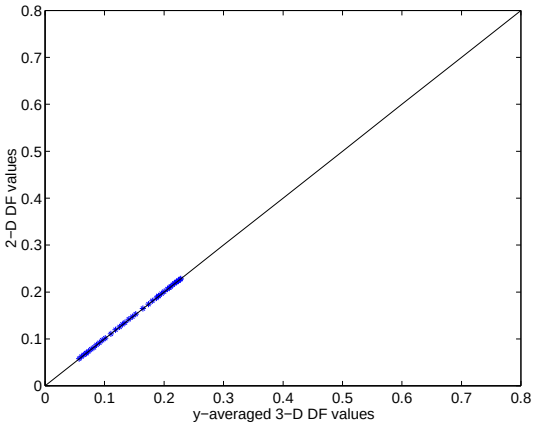

(d) Density Factor

Figure 7.6: Comparison of two- and three-dimensional metrics for Reservoir B.

Table 7.1: Comparison of CPU time for two- and three-dimensional grids for Reservoir C

Grid	CPU time
2D	30.64 hours
3D	166.85 hours

7.1 Discussion

Based on the results shown in Figures 7.1 to 7.5, it can be observed that the inclusion of a third dimension, though desirable, does not change the results significantly, in this particular case. The change in the Nusselt number is 1% or less. The same difference was observed for other reservoir and fluid properties, such as fluid composition. This negligible change in metrics and reservoir properties may be attributed to the fact that the reservoirs looked at are homogeneous in permeability and porosity. It would appear that the variation in fluid composition from point to point within the reservoir is more pronounced in three-dimensional grids.

The results obtained here are similar to the effect of grid refinement on velocity profiles (see Appendix C for details). Therefore in cases such as those used here, homogeneous permeability and porosity field and fluids comprising simple components, the use of more gridblocks appears to only require more CPU time (Table 7.1), although giving more output data points/values.

In heterogeneous reservoirs, there would be a more significant impact of the inclusion of the third dimension in representing the reservoir because there would be more alternative pathways for fluid to move within the reservoir and also because the variation of components may tend to follow the permeability profile. This is beyond the scope of this study.

Chapter 8

Sensitivity Studies

8.1 Compositional Variation as a Function of the Rayleigh Number

Various metrics have been used in previous chapters to characterize the effect convection and diffusion processes have on fluid distribution in reservoirs with horizontal and vertical temperature gradients. Equation 3.1 describes the Rayleigh number and its dependence on certain fluid and reservoir properties. The compositional variation within a reservoir is due to fluid movement which in turn is determined by convection and diffusion.

The dependence of compositional variation on Rayleigh number parameters is evident, but to what extent each parameter effects a change in fluid composition remains unknown. For example, is the effect of the doubling of permeability the same as that of doubling the temperature difference, although either would result in a doubling of the Rayleigh number. These issued are investigated in this section.

Table 6.4 lists the reservoir properties for Reservoir C which is used for this analysis. The reservoir properties that were changed are reservoir permeability, thickness and temperature difference. These properties were chosen because they can be changed without directly impacting the properties of fluid components, as parameters like heat capacity and viscosity would.

8.1.1 Results and Discussion

Figure 8.1 shows the metrics for the base case of Reservoir C with the value of Rayleigh number equal to 279. The first analysis was done by doubling the reservoir thickness to $2000m$, resulting in an increase in the Rayleigh number to 536. Figure 8.2 shows the comparison of metrics for this scenario to that of the base case. Here it is observed that the general processes within the reservoir are maintained, although there is a slower increase in the Nusselt number and a greater value of the separation factor at each timestep. This is due to a greater volume within which the fluid is able to convect and diffuse. This increase in volume affects the changes in the Nusselt number.

Figure 8.3 shows the comparison of metrics of the reservoir with an average permeability of $100md$ to that of the reservoir with a permeability of $200md$ which essentially has a Rayleigh number of 536, double that of the former reservoir. An increase in permeability shows a distinct increase in the separation factor in the reservoir, although this increase was not observed with a doubling of the reservoir height. This implies that a change in permeability may induce a corresponding change in the distribution of fluid within the reservoir.

Figure 8.4 shows the comparison of metrics with a doubling of the vertical temperature gradient, and hence again an increase in the Rayleigh number to 536. Along with the observation of an increase in separation factor, there is also a doubling of the density factor in the reservoir. This occurs because the fluid properties are directly dependent on the reservoir temperature. The changes in the Nusselt number remain the same, and this implies that although the fluid properties vary from the original case (Ra = 279), the changes in the thermal profile within the reservoir occur in the same manner.

It is important to note in Figures 8.2 to 8.4 that although the result of doubling these parameters (height, permeability and temperature gradient) is a doubling of the Rayleigh number in every case, the effect on the fluid distribution and thermal profiles is different, as readily observed in the comparisons. Hence, unlike the single-component problem, the Rayleigh number alone is not a sufficient parameter to deduce the state of the solution.

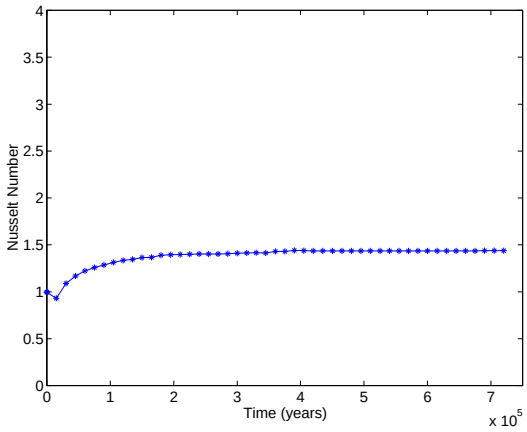

(a) Nusselt Number

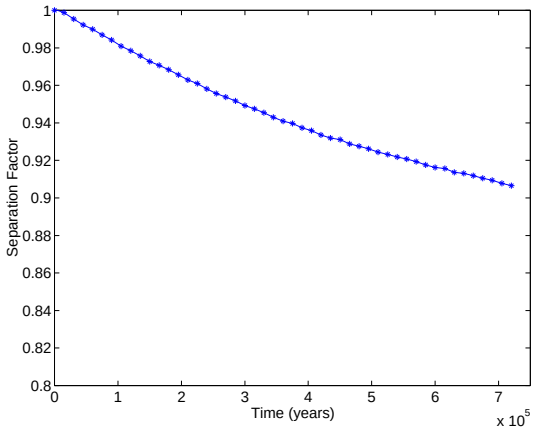

(b) Separation Factor

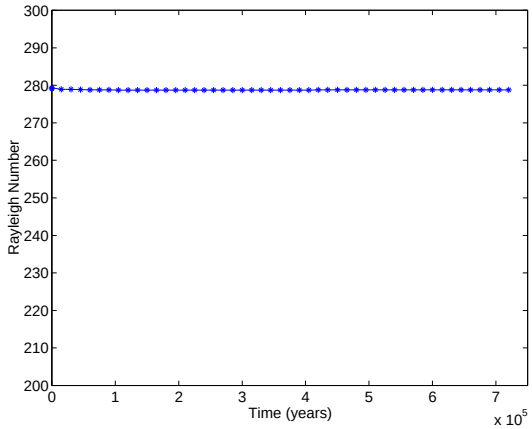

(c) Rayleigh Number

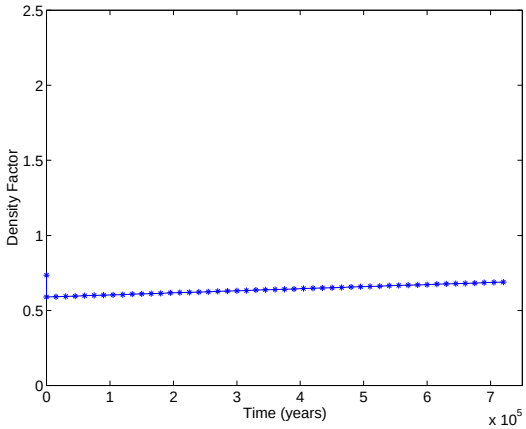

(d) Density Factor

Figure 8.1: Metrics for Reservoir C with Ra = 279.

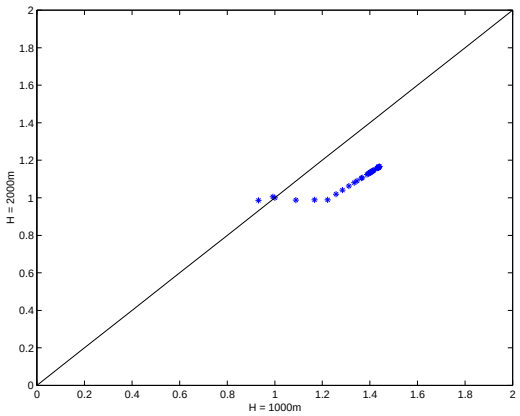

(a) Nusselt Number

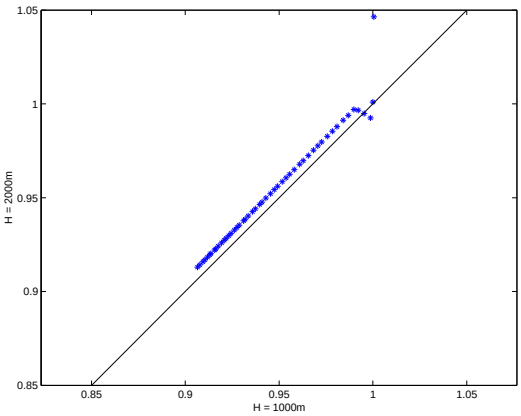

(b) Separation Factor

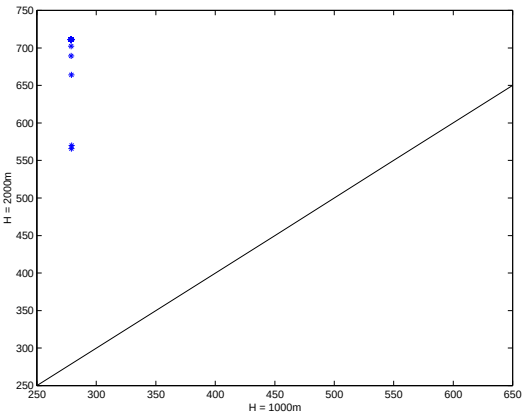

(c) Rayleigh Number

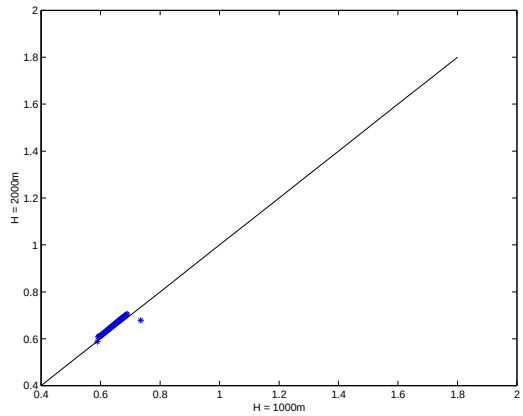

(d) Density Factor

Figure 8.2: Comparison of metrics with a doubling of reservoir thickness. [Reservoir C]

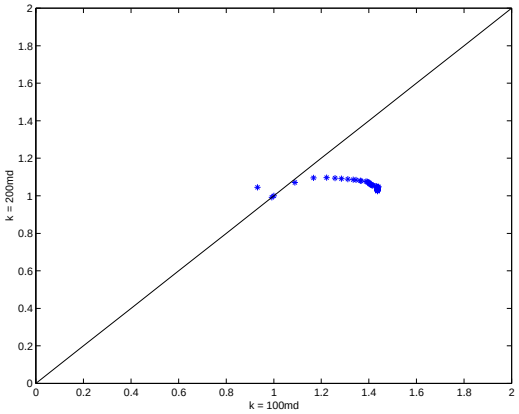

(a) Nusselt Number

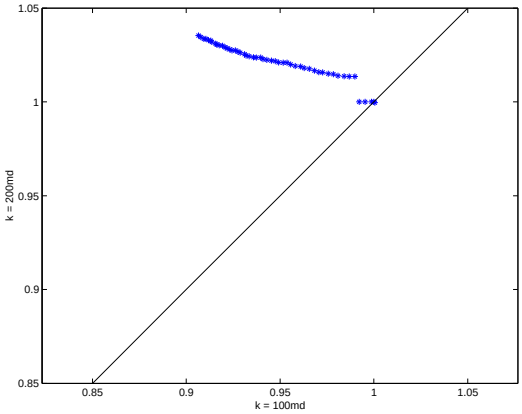

(b) Separation Factor

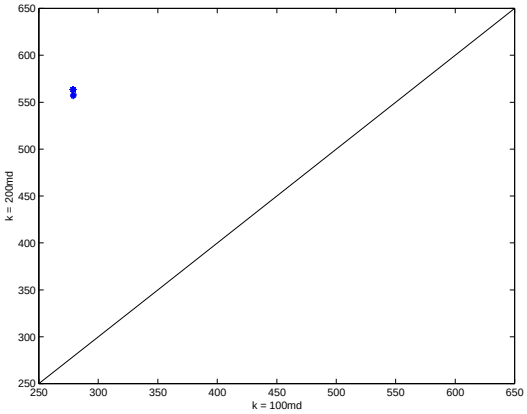

(c) Rayleigh Number

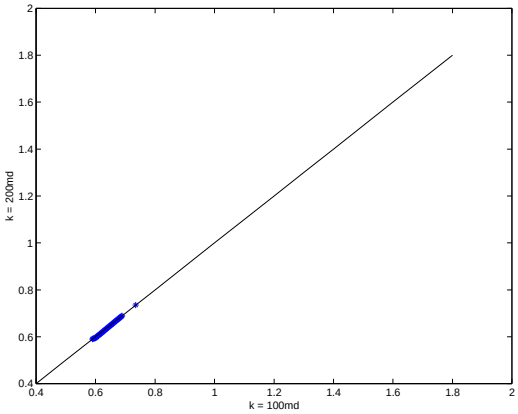

(d) Density Factor

Figure 8.3: Comparison of metrics with a doubling of reservoir permeability. [Reservoir C]

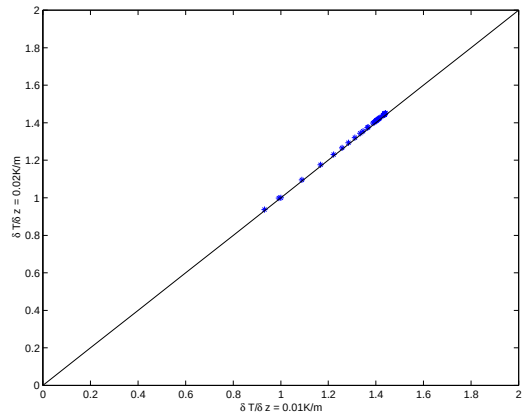

(a) Nusselt Number

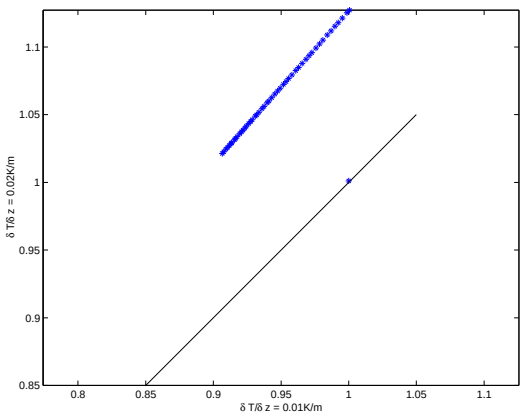

(b) Separation Factor

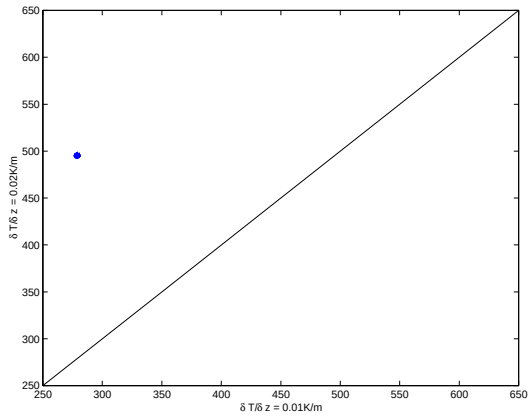

(c) Rayleigh Number

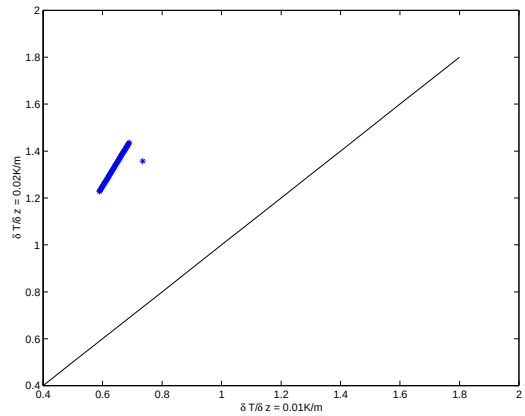

(d) Density Factor

Figure 8.4: Comparison of metrics with a doubling of temperature difference. [Reservoir C]

8.2 Effect of Variable Diffusion Coefficients

Generally, diffusion coefficients for thermal, pressure and molecular diffusion are assumed to be constant over a specific range of pressure and temperature. Due to the change in pressure, temperature and in particular composition over time, the diffusion coefficients change.

To investigate the effect of this change in coefficients on the compositional variation in the reservoir, diffusion coefficients were computed as functions of pressure, temperature and composition. The equations presented below may be found in Montel et al. (1992).

The generalized diffusion coefficients are defined as follows. For molecular diffusion, self-diffusion is defined as;

$$D^m_{i,i} = D^f_i \frac{M_i}{M} \Big/ \frac{\partial f_i}{\partial x_i} \tag{8.1}$$

where;

$$D^f_i = 7.410^{-12} \frac{T\sqrt{M}}{\mu V_i^{0.6}} \tag{8.2}$$

and diffusion is defined as;

$$D^m_{i,j} = -\frac{D^m_{i,i}}{n-1} - \frac{D^m_{j,j}}{n-1} + \sum_{k \neq i,j} \frac{D^m_{k,k}}{(n-1)(n-2)} \tag{8.3}$$

Equation 8.2 is Wilke's correlation for diffusion (Treybal, 1980). Fluid properties such as volumes and fugacity are computed within the equation of state, which in this study is the cubic equation of state using Peng-Robinson coefficients.

Thermal diffusion is defined as;

$$D^T_i = \alpha^T_i x_i (1 - x_i) \frac{D^f_i}{T} \tag{8.4}$$

where α^T_i is determined experimentally.

Sigmund's correlations (Sigmund, 1976) with da Silva and Belery extensions (da Silva and Belery, 1989) were used to correlate the coefficient at varying pressures and temperatures.

$$\frac{\rho_M D_{ij}}{\rho_M^o D_{ij}^o} = 0.99589 + 0.096016\rho_{pr} - 0.22035\rho_{pr}^2 + 0.032874\rho_{pr}^3 \tag{8.5}$$

For liquid systems, da Silva and Belery's extension for pseudoreduced densities less than 3;

$$\frac{\rho_M D_{ij}}{\rho_M^o D_{ij}^o} = 0.18839 \exp 3 - \rho_{pr} \tag{8.6}$$

In Chapter 4, it was shown that the effect of the pressure diffusion term is negligible with respect to compositional variation, therefore the pressure diffusion coefficient may be assumed constant.

8.2.1 Results and Discussion

Reservoir C (Table 6.4) was used for this analysis because with a ternary mixture, diffusion coefficients for two of the three components must be known. Two cases were run, the first with constant diffusion coefficients, and the second with variable diffusion coefficients. Figures 8.5 and 8.6 show the metrics for the two cases, constant and variable diffusion coefficients respectively. The differences in the metrics are negligible, of the order of 1x10^{-5}. Figure 8.7 shows the comparison of the metrics. Based on these results, it may be concluded that the effect of variable diffusion coefficients is negligible. This small impact that diffusion coefficients seem to have on compositional variation, may be due to the fact that the role of diffusion is small once convection dominates, and also that the magnitude of the diffusion term (based on the diffusion coefficients) is small compared to the other terms in the conservation equation, for example, molecular diffusion coefficients are of the order of 1x10^{-9} m^2/s .

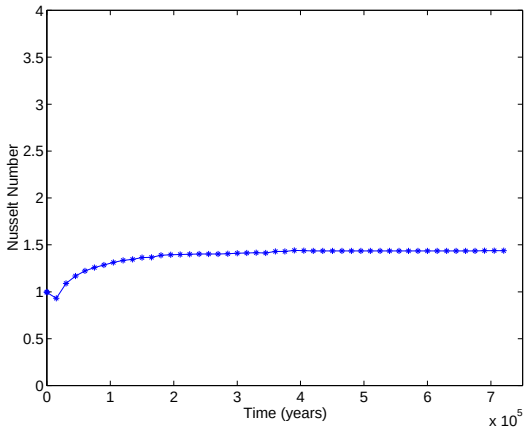

(a) Nusselt Number

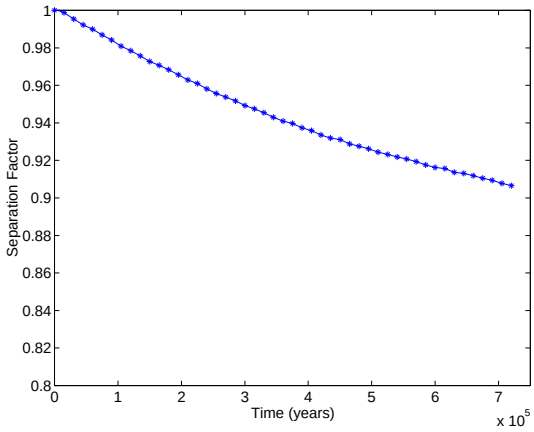

(b) Separation Factor

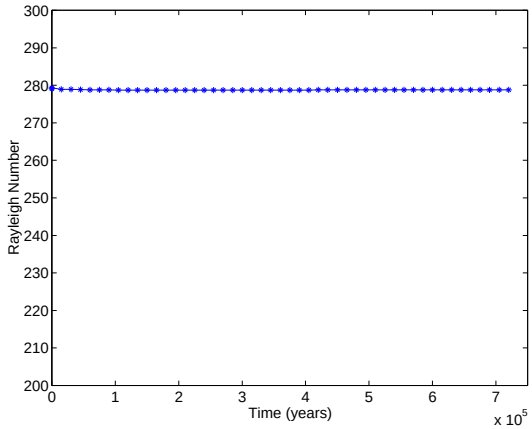

(c) Rayleigh Number

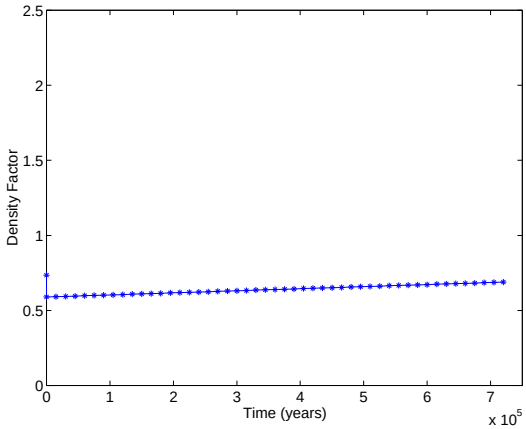

(d) Density Factor

Figure 8.5: Metrics for Reservoir C with constant diffusion coefficients.

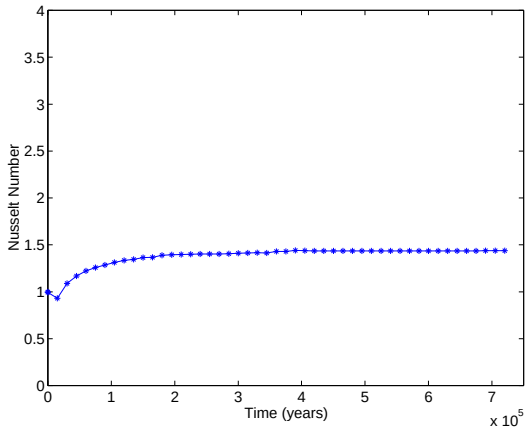

(a) Nusselt Number

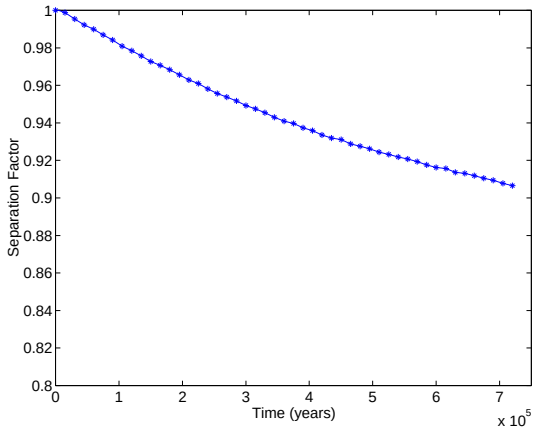

(b) Separation Factor

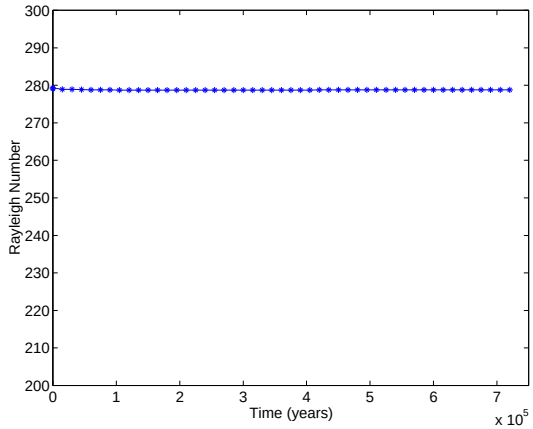

(c) Rayleigh Number

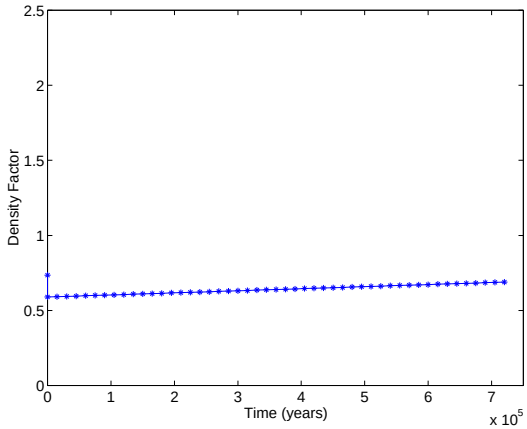

(d) Density Factor

Figure 8.6: Metrics for Reservoir C with variable diffusion coefficients.

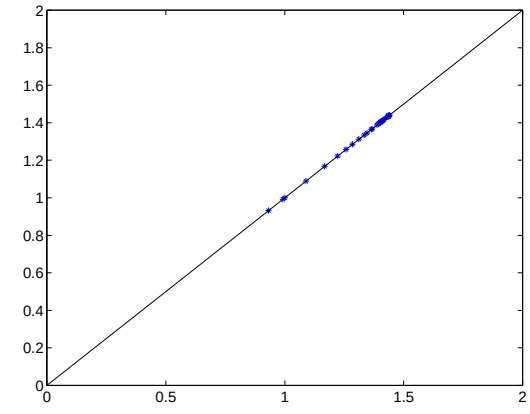

(a) Nusselt Number

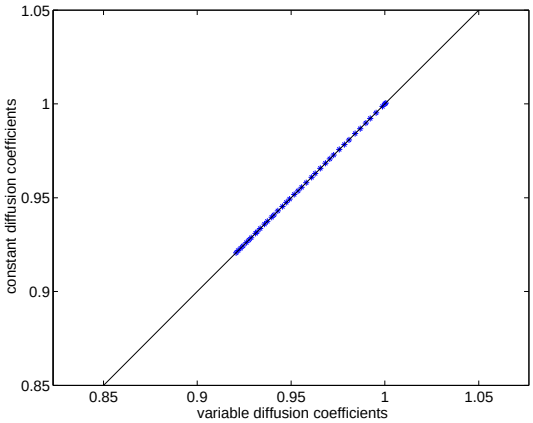

(b) Separation Factor

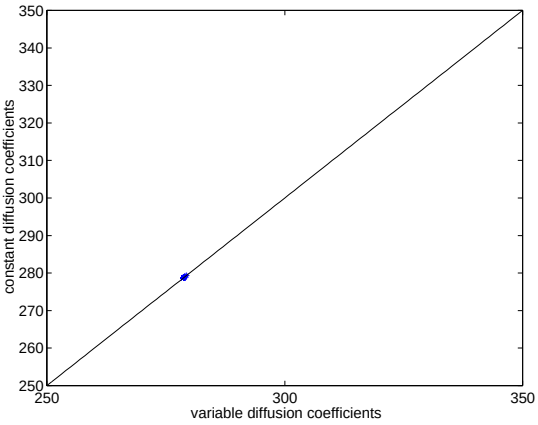

(c) Rayleigh Number

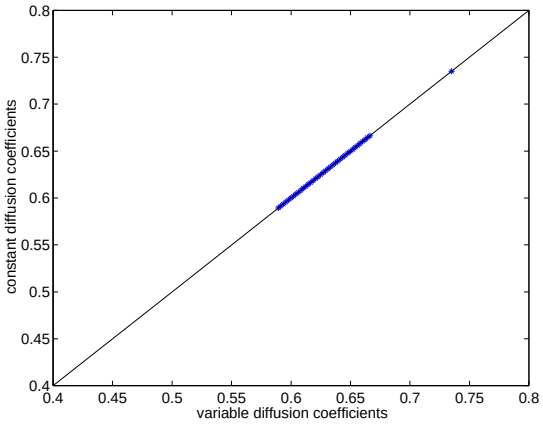

(d) Density Factor

Figure 8.7: Comparison of metrics for constant and fixed diffusion coefficients. [Reservoir C]

Chapter 9

The Effect of Heterogeneity

Reservoir permeability is known to have an important effect on the magnitude and direction of fluid flow. Although, the velocity at which fluid moves in nonproducing reservoirs is small compared to producing reservoirs, the effect of heterogeneity and/or anisotropy is nevertheless important.

Table 9.1 lists the scenarios that were studied, using the reservoir and fluid properties listed previously in Tables 6.2 and 6.3. The reservoirs represented are Reservoirs B and C, used previously for other runs.

9.1 Effect of Anisotropy

In this section of the study, the k_x/k_z ratios used were 1 and 0.1 respectively for the isotropic and anisotropic cases.

Figure 9.1 shows the metrics for Reservoir B with a homogeneous and isotropic permeability field while Figure 9.3 shows the metrics for the anisotropic case. As

Table 9.1: Key of cases to demonstrate the effect of anisotropy and heterogeneity.

Case	**Reservoir description**
A	Homogeneous and isotropic permeability field
B	Homogeneous and anisotropic permeability field
C	Heterogeneous and isotropic permeability field

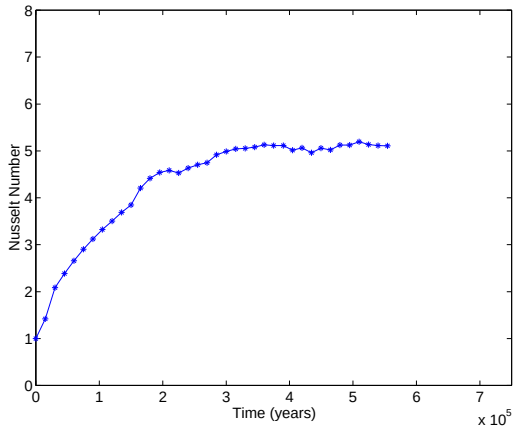

(a) Nusselt Number

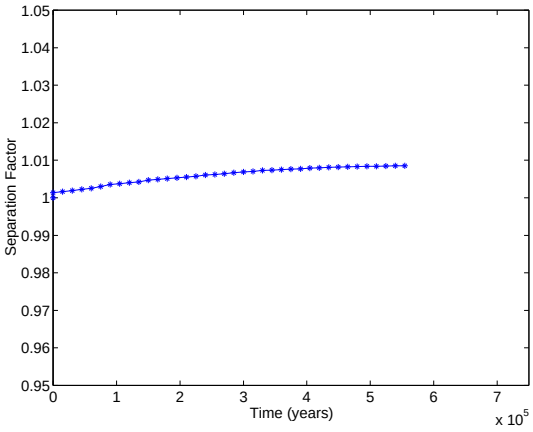

(b) Separation Factor

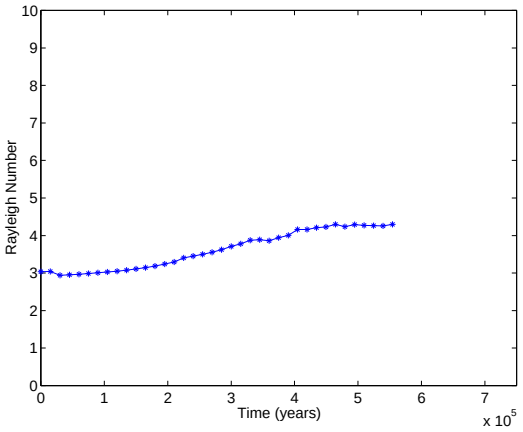

(c) Rayleigh Number

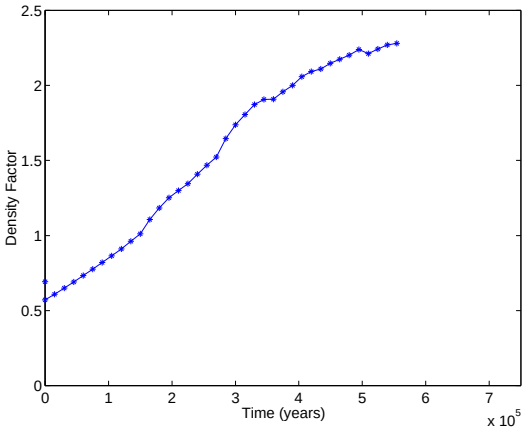

(d) Density Factor

Figure 9.1: Metrics for homogeneous and isotropic reservoir. [Reservoir B]

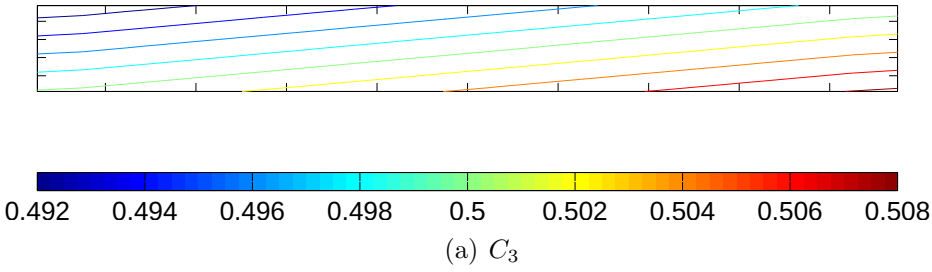

(a) C_3

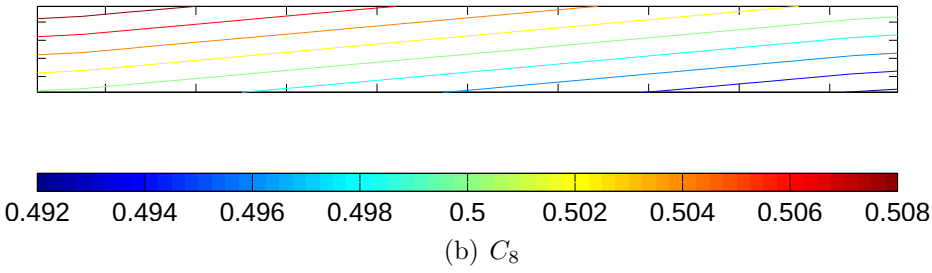

(b) C_8

Figure 9.2: Composition profile for homogeneous and isotopic reservoir. [Reservoir B]

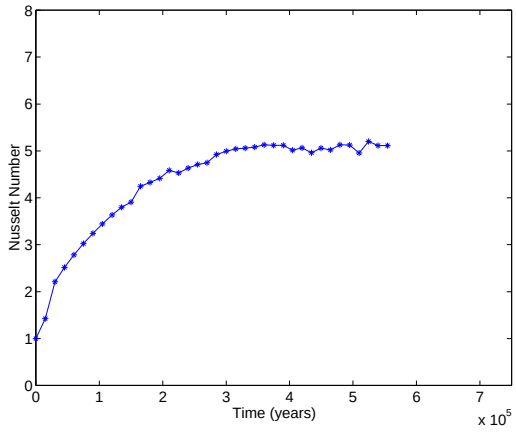

(a) Nusselt Number

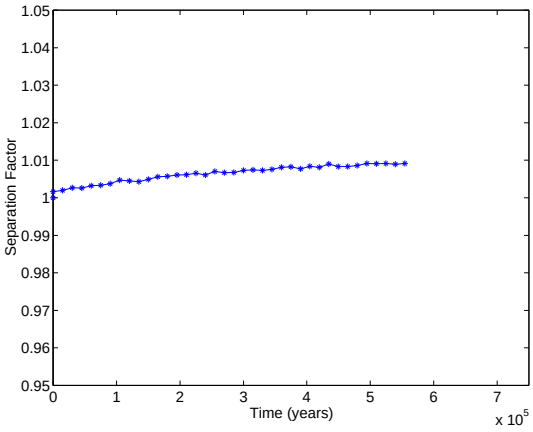

(b) Separation Factor

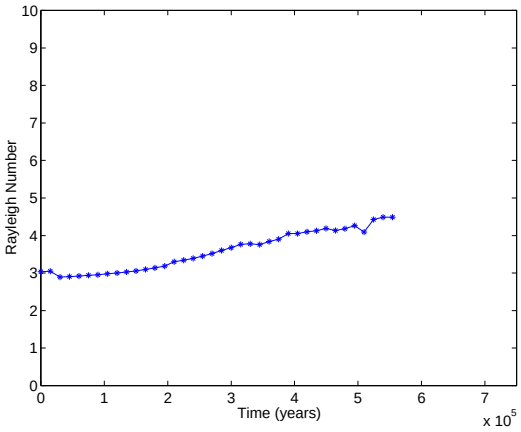

(c) Rayleigh Number

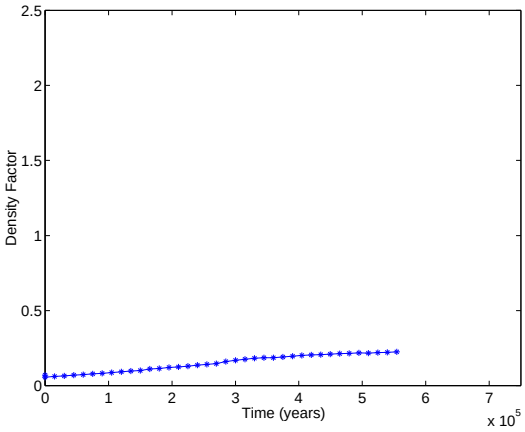

(d) Density Factor

Figure 9.3: Metrics for homogenous and anisotropic reservoir. [Reservoir B]

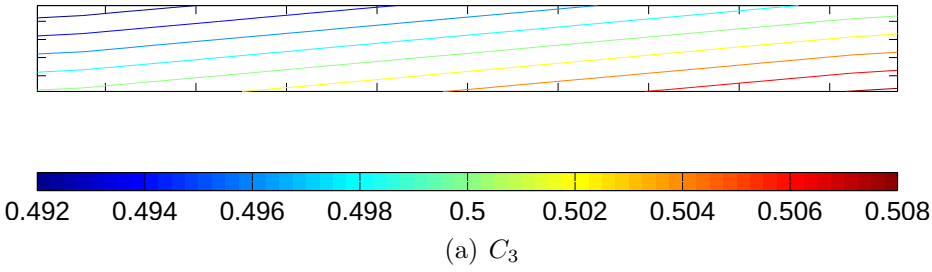

(a) C_3

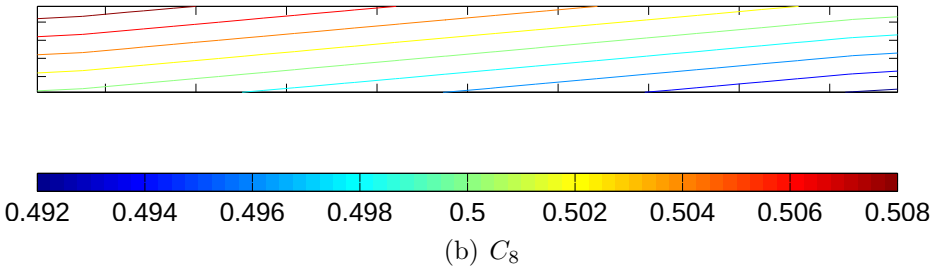

(b) C_8

Figure 9.4: Composition profile for homogeneous and anisotropic reservoir. [Reservoir B]

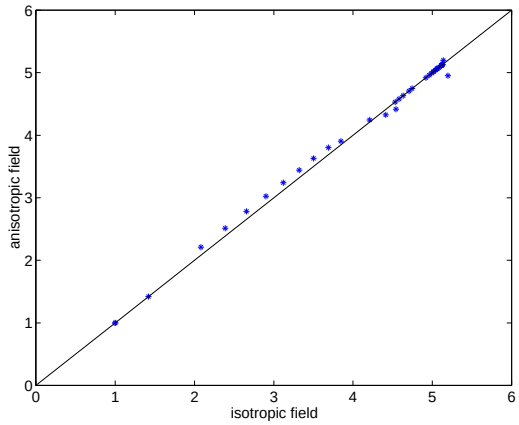

(a) Nusselt Number

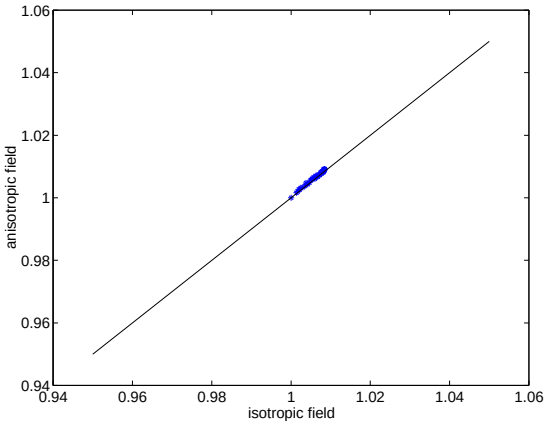

(b) Separation Factor

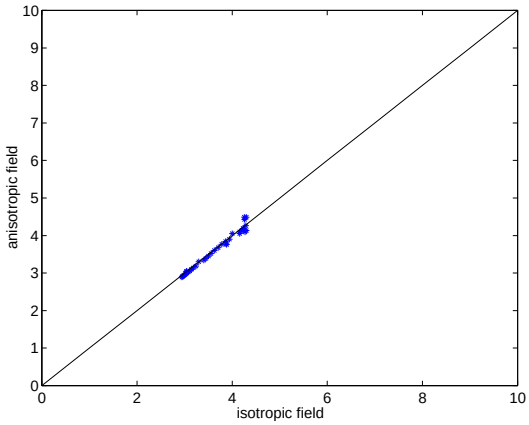

(c) Rayleigh Number

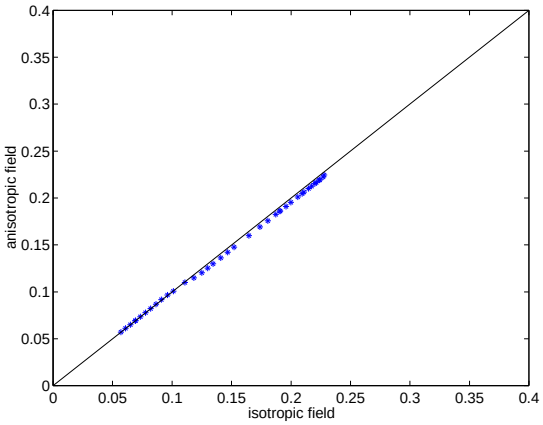

(d) Density Factor

Figure 9.5: Comparison of metrics for isotropic and anisotropic cases. [Reservoir B]

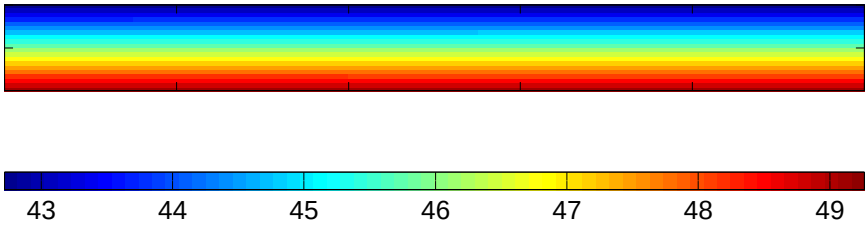

(a) Isotropic permeability field

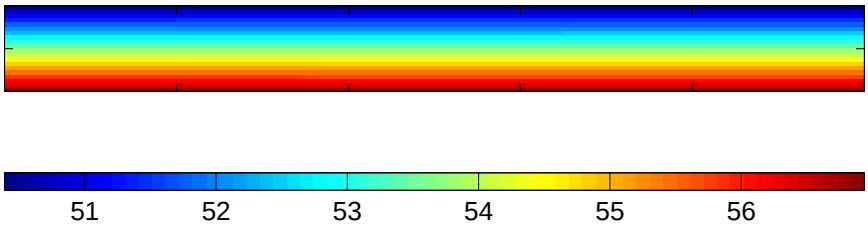

(b) Anisotropic permeability field

Figure 9.6: Pressure profiles in Reservoir B with isotropic and anisotropic permeability fields.

[Reservoir B]

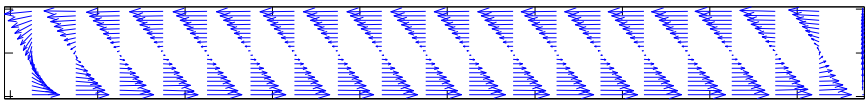

(a) Isotropic permeability field

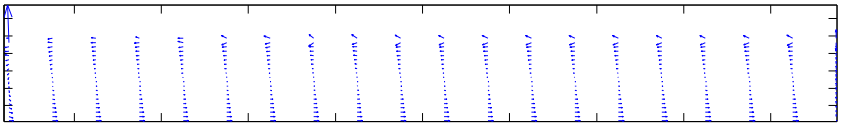

(b) Anisotropic permeability field

Figure 9.7: Velocity profiles for Reservoir B with isotropic and anisotropic permeability fields.

[Reservoir B]

expected, the Nusselt and Rayleigh numbers increase as convection of fluid becomes vigorous, while the composition profiles within the reservoir align in such a way as to compensate for the movement of heat and mass. Figures 9.2 and 9.4 show the composition profiles in the reservoirs. Figures 9.6 and 9.7 show the comparison of the pressure and velocity profiles for the two scenarios. Figure 9.6 shows that the pressure in the reservoir with an anisotropic permeability field (lower average permeability overall) is higher than in the reservoir with an isotropic field. Figure 9.7b is the most significant figure, as it shows that the effect of anisotropy is akin to that of the aspect ratio in a reservoir. As the permeability in one direction is changed, the fluid velocity changes to compensate for this reduction in permeability, as is expected.

To compare the values of the metrics to one another, Figure 9.5 was plotted. This figure shows that for an anistropic reservoir, as long as the initial Rayleigh number remains the same, there are variations in all metrics, but these variations may be assumed to be negligible.

Figure 9.8 shows the same comparison for Reservoir C. This analysis of the results is the same as those for Reservoir B. Of note here is that there is more scatter in these plots that in Figure 9.5. The Rayleigh number as well as temperature gradients in this case are much higher and these account for the greater spread in Rayleigh number.

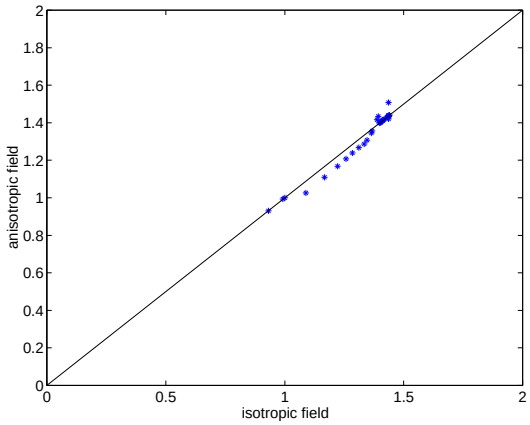

(a) Nusselt Number

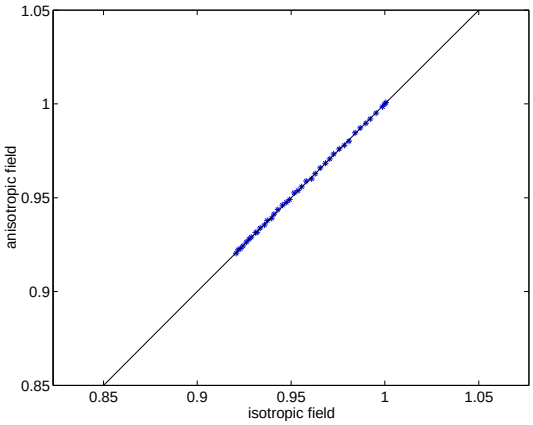

(b) Separation Factor

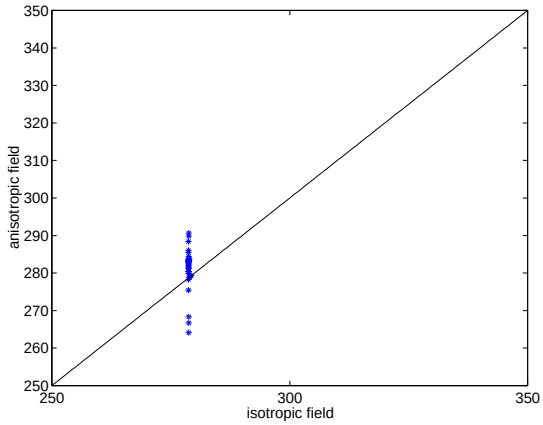

(c) Rayleigh Number

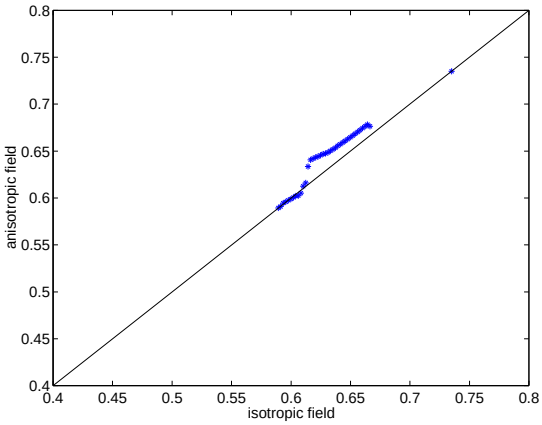

(d) Density Factor

Figure 9.8: Comparison of metrics for isotropic and anisotropic cases. [Reservoir C]

9.2 Effect of Heterogeneity

Figure 9.9 shows the heterogeneous permeability field used to investigate the effect of heterogeneity on compositional variation. This permeability field is a small section taken from the x-permeability field of dataset 1 of the tenth SPE comparative solutions project (Christie and Blunt, 2001), which can be found at http://www.spe.org/csp/. The average reservoir permeability is equal to the permeability used for the cases of the homogeneous reservoir, to allow for a uniform basis of comparison.

Figure 9.10 shows the metrics for Reservoir B with the heterogeneous permeability field. These figures show that for the heterogeneous reservoir, it takes longer for the fluid to stabilize within the reservoir and there are many more pathways for the fluid to take. Figure 9.13 shows that the velocity in the reservoir is aligned according to the permeability field, and therefore the permeability distribution is the dominant force when heterogeneous. For a clearer picture of how these results differ from those for the homogeneous case, Figure 9.11 shows the comparison of the metrics. There is a greater spread in the values for the heterogeneous case as is expected. Figure 9.14 shows the composition profile in the reservoir. This shows that the compositional variation is distorted by the heterogeneity. Instead of the components being distributed based on gravity and bouyancy, they are also distributed based on reservoir connectivity. Figure 9.15 shows the same comparison for Reservoir C. In this case there is an even greater difference in metrics, due to the fact that with an additional component, there are more variables to be taken into account. In particular, the Rayleigh number for the heterogeneous case is spread out from 250 to 350, while it remains mainly constant for the homogeneous case.

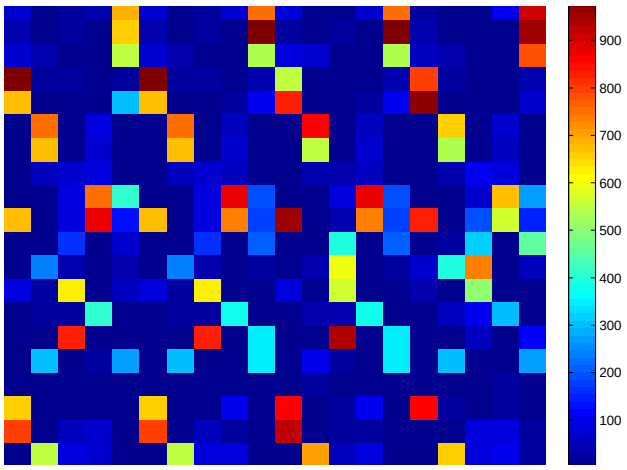

Figure 9.9: Heterogeneous permeability field (md).

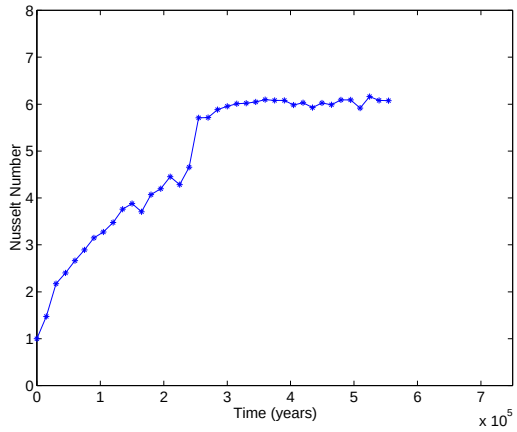

(a) Nusselt Number

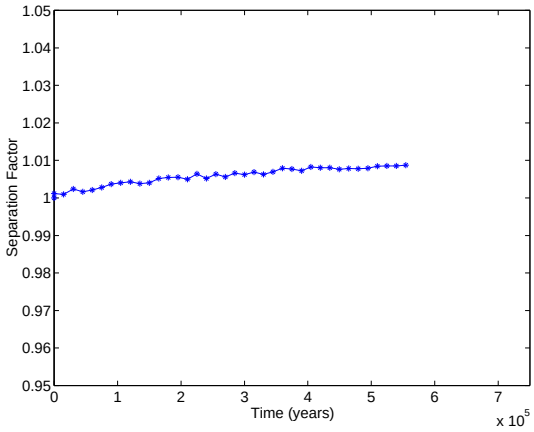

(b) Separation Factor

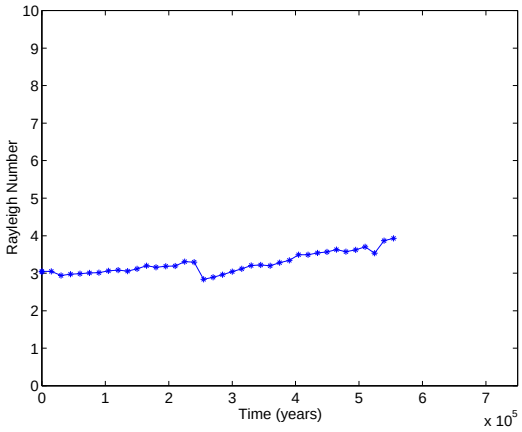

(c) Rayleigh Number

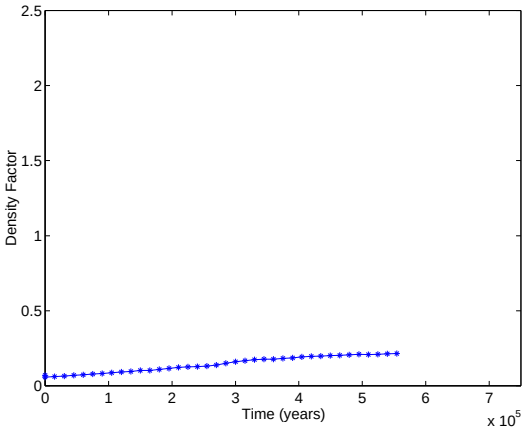

(d) Density Factor

Figure 9.10: Metrics for Reservoir B with a heterogenous permeability field.

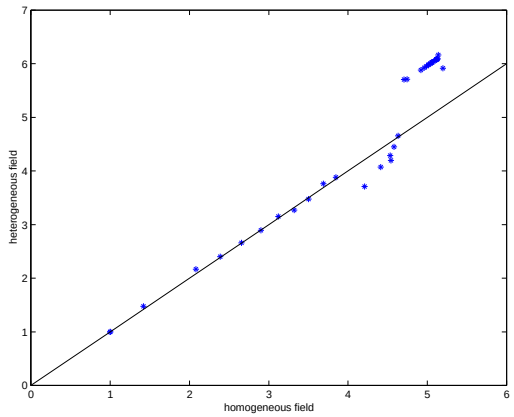

(a) Nusselt Number

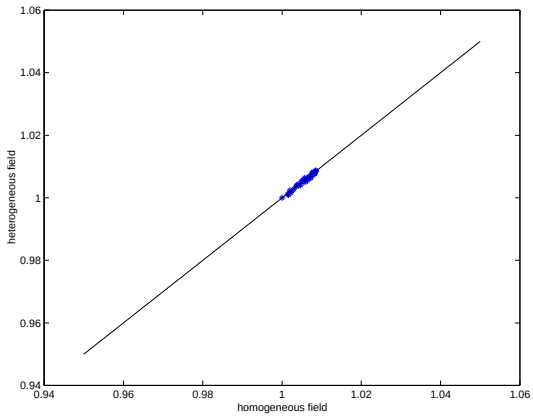

(b) Separation Factor

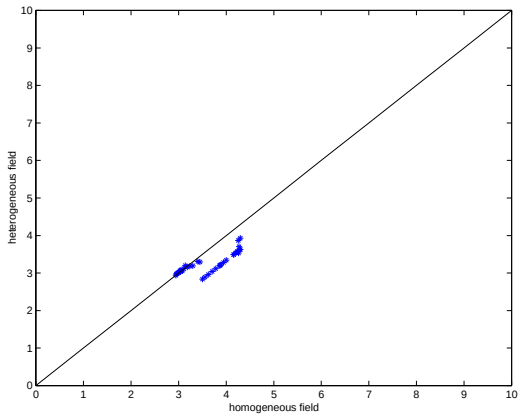

(c) Rayleigh Number

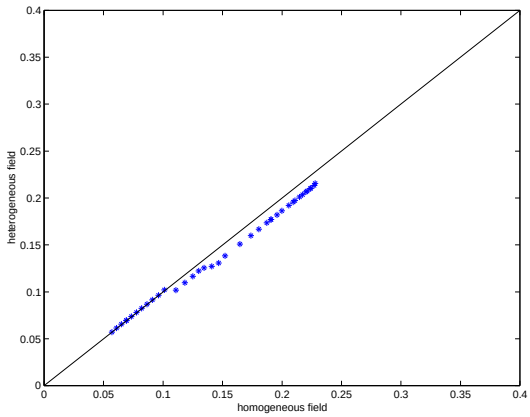

(d) Density Factor

Figure 9.11: Comparison of metrics for homogeneous and heterogenous cases. [Reservoir B]

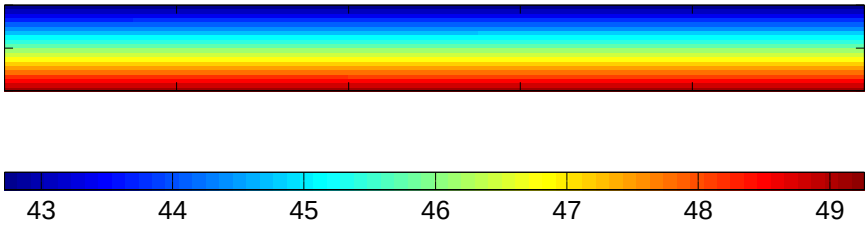

(a) Homogeneous permeability field

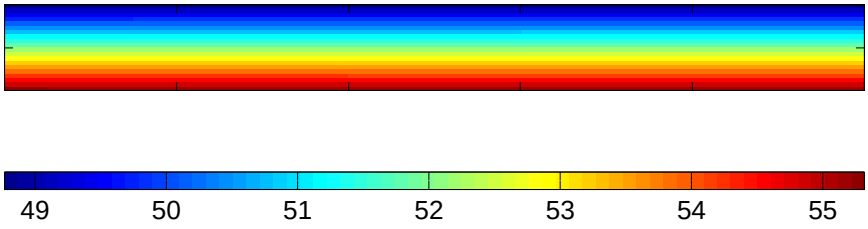

(b) Heterogeneous permeability field

Figure 9.12: Pressure profiles for Reservoir B with homogeneous and heterogeneous permeability fields.

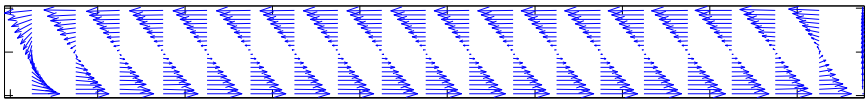

(a) Homogeneous permeability field

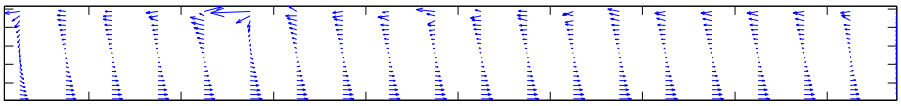

(b) Heterogeneous permeability field

Figure 9.13: Velocity profiles for Reservoir B with homogeneous and heterogeneous permeability fields.

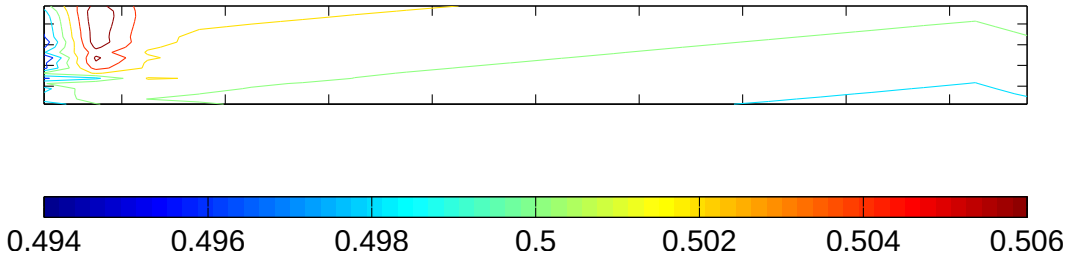

(a) C3

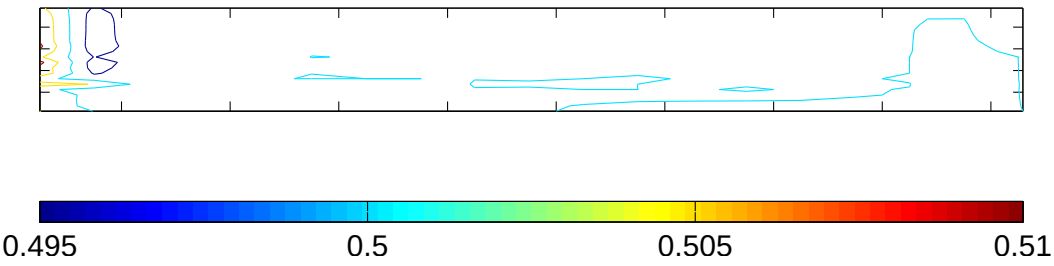

(b) C8

Figure 9.14: Composition profile for Reservoir B with a heterogeneous permeability field.

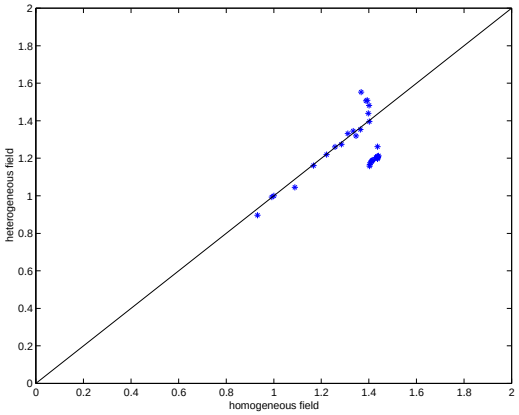

(a) Nusselt Number

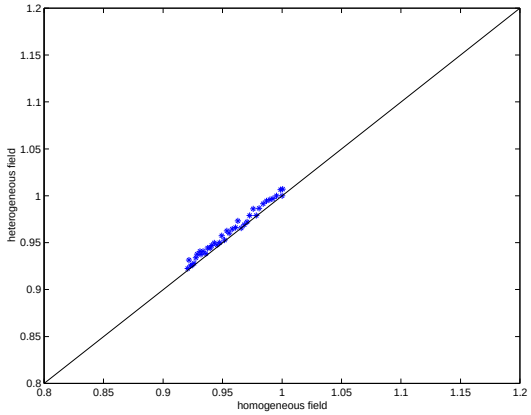

(b) Separation Factor

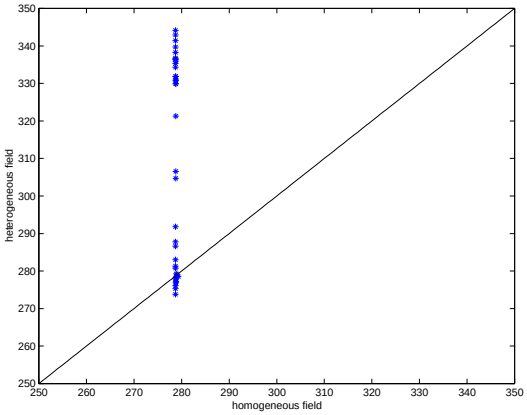

(c) Rayleigh Number

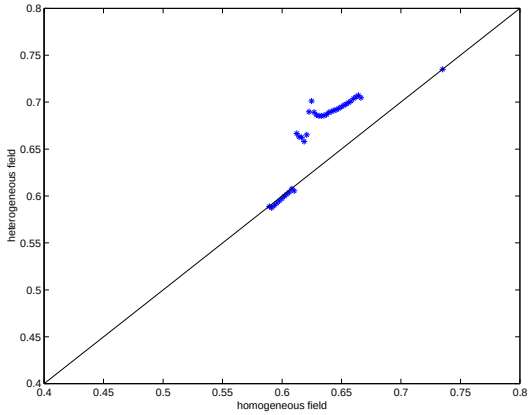

(d) Density Factor

Figure 9.15: Comparison of metrics for homogeneous and heterogeneous cases. [Reservoir C]

Chapter 10

Concluding Remarks

10.1 Conclusions

This study investigated compositional variations in hydrocarbon reservoirs with a view to using the information obtained from the analysis in the reservoir characterization process. The inclusion of an energy balance, the use of three-dimensional reservoirs, the effect of heterogeneity and anisotropy, sensitivity runs based on Rayleigh number parameters and the inclusion of composition-, temperature- and pressure-dependent diffusion coefficients were studied. Based on the analysis, the following conclusions were drawn;

1. Numerical analysis is required when dealing with multicomponent fluids because of the nonlinearity of the primary equations and the requirement to adequately describe fluid properties as functions of pressure, temperature and composition.

2. The energy balance is important when dealing with convection. The Nusselt number increases as convection becomes more vigorous, as shown in Chapter 6. For single-component fluids and by extension fluid mixtures with very similar components, the isotherms in the reservoir have been shown to change significantly over time. Multicomponent mixtures however exhibit compositional variations aligned to the pressure and temperature fields, still show a change in the Nusselt and Rayleigh number and the density and separation factors.

3. For multicomponent mixtures the change in the temperature field is less than 10%, but the change in fluid properties and heat transfer within the reservoir and between the reservoir and the over- and underburden is significant. Hence, a greater change in fluid density and Rayleigh numbers occurs.

4. The effect of an increase in the temperature gradient, or reservoir average permeability, or any of the Rayleigh number parameters differs from one parameter to the other, even though the resultant change in the Rayleigh number may be the same. Hence, the Rayleigh number alone is insufficient to characterize the solution.

5. In reservoirs with anisotropic permeability fields, the fluid velocities change in the ratio of the difference in permeability.

6. In reservoirs with heterogeneous permeability fields, the fluid velocities align in such a way as to honor the permeability field first and then follow the fluid convection due to the temperature gradients second.

7. Diffusion coefficients may be assumed to be constant. Although pressure, mass and thermal diffusion coefficients are functions of fluid composition, temperature and pressure, the effect of this variation on compositional variation is negligible. This is essentially because the coefficients are rather small in value and hence any changes in them would be inconsequential.

8. The use of three-dimensional grids to represent reservoirs is not always required when dealing with compositional variations, provided the convective motions are two dimensional. The reduction in the number of gridblocks and therefore the number of solution variables leads to a reduction in CPU time.

10.2 Future Work

Based on this study and others as listed in the literature review, there are other areas which are open to investigation that would broaden the use of compositional gradient analysis in reservoir engineering studies. These include;

1. Multiphase flow, including water.
2. Small-scale effects.
3. Practical applications.
4. Chemical reactions.
5. Heterogeneity.

Multiphase flow

Due to variations in temperature and pressure, the possibility of phase changes must be accounted for. The enthalpy associated with phase changes is much greater than fluid enthalpies alone and this will impact the energy transfer process within the reservoir and hence the extent to which convection occurs. This study will be useful particularly in condensate reservoirs where the effects of convection and diffusion have not been documented.

Small-scale effects

In studying how compositional variation begins in a reservoir, it would be useful to see how capillary pressure affects fluid replacement in the reservoir, such as oil displacing water in the process of forming an oil reservoir. Capillary pressure would be more significant in studies such as this because the reservoir is nonproducing. This effect may or may not be negligible due to the slow nature of natural convection and diffusion, but also due to the dominance of thermal diffusion and fluid buoyancy.

Practical applications

There are real reservoirs, such as the Ghawar Khuff reservoir in Saudi Arabia and others listed in Chapter 2, where compositional variations have been observed. The methodology developed here to predict the distribution of components in hydrocarbon reservoirs could be applied to these reservoirs. For example, over the producing life of the reservoir, pressure changes will result in changes in the fluid distribution in the reservoir. How do production, influx of water, and other processes affect compositional variations? Is this phenomenon more important in low permeability reservoirs (for example, chalk and diatomite formations) or in fractured reservoirs? These areas should be investigated.

Also the ability to map a composition profile from one reservoir to the other, where the main difference is a parameter like permeability or temperature gradient, would be a relevant application of this study.

Chemical reactions

Depending on the rock and fluid compositions, certain chemical reactions occur over the years within a reservoir. The distribution of fluid components in a reservoir under the effect of convection and diffusion processes takes place over thousands and/or millions of years and the slow production of certain compounds, for example, the production of sulphur dioxide in a reservoir with sulphur, could affect the distribution of fluid components in the reservoir.

Heterogeneity

It has been observed in this study that for heterogeneous reservoirs, the metrics defined here were not able to fully capture the compositional variation in the reservoir. More analysis is required to look fully into the effect of heterogeneity on fluid convection and diffusion, for example:

1. The use of three-dimensional grids would be more useful in capturing the effect of heterogeneity on compositional gradients.

2. The definition of a metric which would take into account the variation in composition as a function permeability and porosity.

Other areas

The boundary conditions imposed in this study were no-flow boundaries for the mass conservation equations and fixed temperature gradients (purely conductive) for the conservation of energy. Other boundary condition would make a difference in the profiles of composition obtainable in the reservoir, e.g. periodic boundary conditions.

Appendix A

Stability Analysis

This section contains a detailed description of the steps in the stability analysis of a convecting system. The reservoir here contains a single-phase fluid and has a vertical temperature gradient and a vertical concentration gradient as shown in Figure A.1.

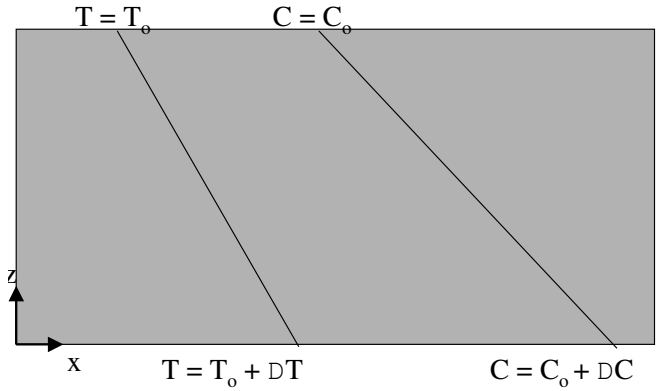

Figure A.1: Porous medium with vertical temperature and concentration gradients.

The governing equations are as follows:
The continuity equation:

$$\frac{\partial}{\partial t}(\phi\rho) = -\nabla \cdot (\rho \mathbf{u}) \tag{A.1}$$

Darcy's law:

$$\mathbf{u} = -\frac{k}{\mu}(\nabla p + \rho g) \tag{A.2}$$

The energy balance:

$$\rho c_{p_m} \frac{\partial T}{\partial t} + \rho c_{p_f} \mathbf{u} \cdot \nabla T = K \nabla^2 T + q_T \tag{A.3}$$

The solute balance:

$$\phi \frac{\partial C}{\partial t} + \mathbf{u} \cdot \nabla C = D_m \nabla^2 C + q_S \tag{A.4}$$

The boundaries are impermeable, hence the boundary condition is:

$$\underline{u} \bullet \underline{n} = 0 \tag{A.5}$$

In solving the governing equations the following assumptions were made:

- Darcy's law is valid.
- Local thermal equilibrium exists.
- Viscous dissipation results in negligible heating of the fluid.
- The effect of radiation is negligible.
- The fluid is incompressible.
- The Boussinesq approximation is valid.

The Boussinesq approximation states that density differences are negligible, with the exception of gravity force. This essentially means, with respect to this problem, that the changes of fluid density with pressure are neglected, except in the buoyancy term. Based on the Boussinesq approximation, the fluid density may be given as:

$$\rho = \rho_o[1 - \alpha_T(T - T_o) + \alpha_S(C - C_o)] \tag{A.6}$$

For this set of equations, the steady-state solution with $q_S = 0$ and $q_T = 0$ is given as:

$$\begin{aligned} \mathbf{u}_s &= 0 \\ T_s &= T_o + \Delta T(1 - \frac{z}{H}) \\ C_s &= C_o + \Delta C(1 - \frac{z}{H}) \\ p_s &= p_o - \rho_o g[(T_o + C_o)z + (\alpha_T \Delta T + \alpha_S \Delta C)(z - \frac{z^2}{2H})] \end{aligned} \tag{A.7}$$

At the onset of convection, the temperature difference is small, and so also are the components of the Darcy velocity, therefore perturbation variables may be defined as follows:

$$\begin{aligned} \mathbf{u} &= \mathbf{u}_s + \mathbf{u}^{'} \\ T &= T_s + T^{'} \\ p &= p_s + p^{'} \\ C &= C_s + C^{'} \end{aligned} \tag{A.8}$$

The dimensionless variables are:

$$\begin{aligned} \hat{x} &= \frac{x}{H} \\ \hat{t} &= \frac{\alpha}{\sigma H^2} t \\ \hat{u} &= u^{'} \frac{H}{\alpha} \\ \hat{T} &= \frac{T^{'}}{\Delta T} \\ \hat{C} &= \frac{C^{'}}{\Delta C} \\ \hat{p} &= \frac{k}{\mu \alpha} p^{'} \end{aligned} \tag{A.9}$$

Equations A.2, A.6 and A.9 are substituted into equation A.1. The perturbation variables are small quantities, hence the nonlinear terms which include perturbation variables may be neglected (Turcotte and Schubert, 2002, Chap. 9).
This gives:

$$-\hat{\nabla}\hat{p} - \mathbf{u} - Ra(\hat{T} + N\hat{C})_k = 0$$

where

$$N = \frac{\alpha_S \Delta T}{\alpha_T \Delta C} \tag{A.10}$$

The pressure perturbations are removed by taking the curl of the resulting equation. Taking only the z component, the resulting equation becomes:

$$\hat{\nabla}^2 \hat{w} = Ra \hat{\nabla}_H^2 (\hat{T} + N\hat{C}) \tag{A.11}$$

where

$$\nabla_H^2 = \frac{\partial^2}{\partial x^2} + \frac{\partial^2}{\partial y^2}$$

Substituting Equations A.9 into Equations A.4 and A.3 results in the following equations:

$$\frac{\phi}{\sigma}\frac{\partial \hat{C}}{\partial \hat{t}} - \hat{w} = \frac{1}{Le}\nabla^2 \hat{C}$$

$$\frac{\partial \hat{T}}{\partial t} - \hat{w} = \nabla^2 \hat{T} \tag{A.12}$$

$$\tag{A.13}$$

where the Lewis number is defined as:

$$Le = \frac{\alpha}{D_m} \tag{A.14}$$

The solution that will satisfy both the differential equation and the boundary conditions is:

$$\Phi(x, y, z, t) = \Phi^*(\hat{z}) exp(ilx + imy + i\omega t)$$

In terms of the variables of interest:

$$\hat{w} = w^* exp(\hat{z}) exp(ilx + imy + i\omega t)$$

$$\hat{T} = T^* exp(\hat{z}) exp(ilx + imy + i\omega t) \tag{A.15}$$

Substituting Equation A.15 into Equations A.11 and A.12 results in the following equations:

$$(D^2 - \alpha^2 - i\omega)T^* + w^* = 0$$

$$(D^2 - \alpha^2)w^* + \alpha^2 Ra(T^* + NC^*) = 0 \tag{A.16}$$

$$[\frac{1}{Le}(D^2 - \alpha^2) - i\omega\frac{\phi}{\sigma}]C^* + w^* = 0$$

where

$$D^2 = \frac{d^2}{dz^2}$$

In the case of marginal stability, $\omega = 0$.

$$\begin{aligned} (D^2 - \alpha^2)T^* + w^* &= 0 \text{ (a)} \\ (D^2 - \alpha^2)w^* + \alpha^2 Ra(T^* + NC^*) &= 0 \text{ (b)} \\ [\frac{1}{Le}(D^2 - \alpha^2)]C^* + w^* &= 0 \text{ (c)} \end{aligned} \tag{A.17}$$

Solving Equations A.17a and A.17b for T^* and C^* respectively and substituting into Equation A.17c gives an 8th-order system which will give eigensolutions of the form:

$$w* \sim sin(j\pi z) \tag{A.18}$$

with the condition:

$$Ra = \frac{j^2\pi^2 + \alpha^{2^2}}{\alpha^2}, for j = 1, 2, 3, ..., \tag{A.19}$$

By eliminating variables the critical Rayleigh number, Ra_c, is obtained from this set of equations with

$$\frac{\partial Ra}{\partial \alpha^2} = 0 \tag{A.20}$$

$$Ra_c = Ra(1 + NLe) = 4\pi^2 \tag{A.21}$$

See Nield and Bejan (1999) for a detailed analysis.

Appendix B

Description of Reservoirs

The following sets of reservoir and fluid properties were used to study the effect of reservoir properties, the inclusion on an energy balance, the effects of heterogeneity and variable diffusion coefficients on compositional variations in porous media, namely A, B, C and D.

Table B.1: Reservoir and fluid properties for Reservoir A

Dimensions	2000m x 100m x 2000m
Porosity	0.25
Permeability	200md
Datum reservoir pressure	55bars
Datum reservoir temperature	373K
Temperature gradients	0.01K/m and 0.003K/m

Table B.1 shows the properties for Reservoir A. This reservoir was used to show the effects of convection and the inclusion of the energy balance on a single-component fluid in a porous media. Table B.2 and B.3 show the details of Reservoirs B and C respectively. Reservoir B has contains a binary mixture fluid comprising propane and octane while Reservoir C contains a ternary mixture fluid comprising methane, ethane and butane. Reservoirs B and C are used to show not only the effect of the inclusion of an energy balance on compositional variations in porous media, but also

the effect of heterogeneity, variable diffusion coefficients and sensitivity analysis on the various reservoir properties.

Table B.2: Reservoir and fluid properties for Reservoir B

Dimensions	1000m x 100m x 100m
Porosity	0.25
Fluid composition	C_3 and C_8
Permeability	100md
Datum pressure	55bars
Temperature gradients	0.01K/m and 0.005K/m
Rock heat capacity	1800KJ/kgK
Rock conductivity	280KJ/kg

Table B.3: Reservoir and fluid properties for Reservoir C

Dimensions	1000m x 100m x 1000m
Porosity	0.25
Fluid composition	C_1, C_2 and C_4
Permeability	100md
Datum pressure	80bars
Temperature gradients	0.01K/m and 0.003K/m
Rock heat capacity	1800KJ/kgK
Rock conductivity	280KJ/kg

Table B.4 shows the reservoir and fluid properties used for the comparison to a field case. These properties were taken from the literature (**?**).

Table B.4: Reservoir and fluid properties for Reservoir D

Reservoir dimenstions	10km x 1.5km
Porosity	0.20
Fluid composition	CO_2, C_1, C_2, C_3-C_4, C_5-C_6, C_{7+}
Permeability	10md
Datum pressure	4.66 x 10^7Pa
Datum temperature	422K
Temperature gradients	0.0275 and 0.0015K/m
Fluid viscosity	0.075cp

Appendix C

Program Development

Methodology

To solve the system of nonlinear equations, a fully implicit formulation was used. In a fully implicit formulation, the coefficients of the unknowns, such as the transmissibilities, will be computed at the next time step; i.e. $n+1$ and therefore the solution will be obtained by solving a set of nonlinear equations. Newton's method was used to solve this set of nonlinear equations because of its fast convergence.

Description of the Simulator

The simulator comprises a main routine and various subroutines, all written in C++. There are three classes, namely;

- reservoir class
- gridcell class
- fluid class.

The subroutines are written around these three classes. A copy of the main routine and the various subroutine headers may be found in Appendix D. The nonlinear

solution for pressure, composition and temperatures in each grid block is done using an iterative solver GMRES. The steps involved are as follows;

Initialize reservoir and fluid objects - The data files are read in and simulation variables such as grid sizes and initial Δt are assigned.

Compute initial values for primary variables - Based on the initial temperature and pressure fields, fluid properties such as density and viscosity are computed.

Calculate primary variables at each time step - In order to do this a loop is computed at each time step which solves for the set of primary equations for all gridblocks for the primary variables.

Compute residual and Jacobian - Based on the primary variables at each iteration, the residual vector and the Jacobian matrix are computed.

Compute primary variables for each iteration until convergence - Using Newton's method a new set of primary variables is computed. Once the difference between sets of primary variables is less than the prescribed tolerance limits for each variable, the loop ends, otherwise iterations continue.

Compute next time step - The next time step is calculated based on the changes in the primary variables in the previous step.

End simulation - Once the total time for the simulation is reached, the simulation ends.

Figure C.1 is a flowchart of main routine of the program.

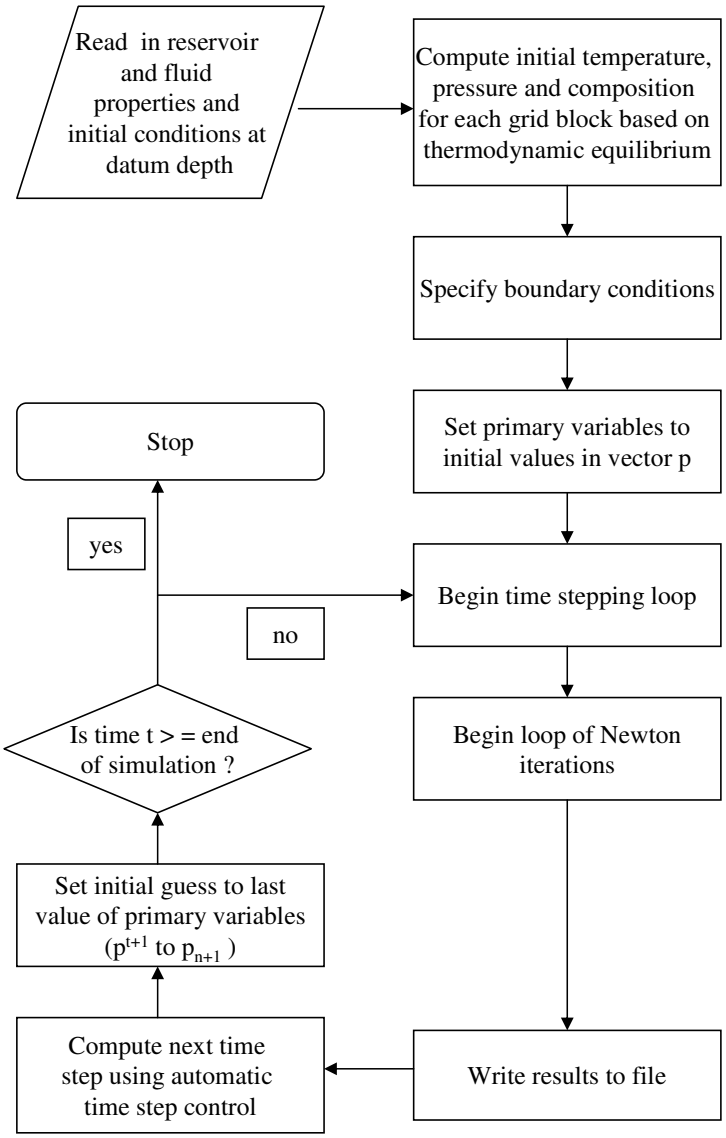

Figure C.1: General flow chart for the numerical simulator.

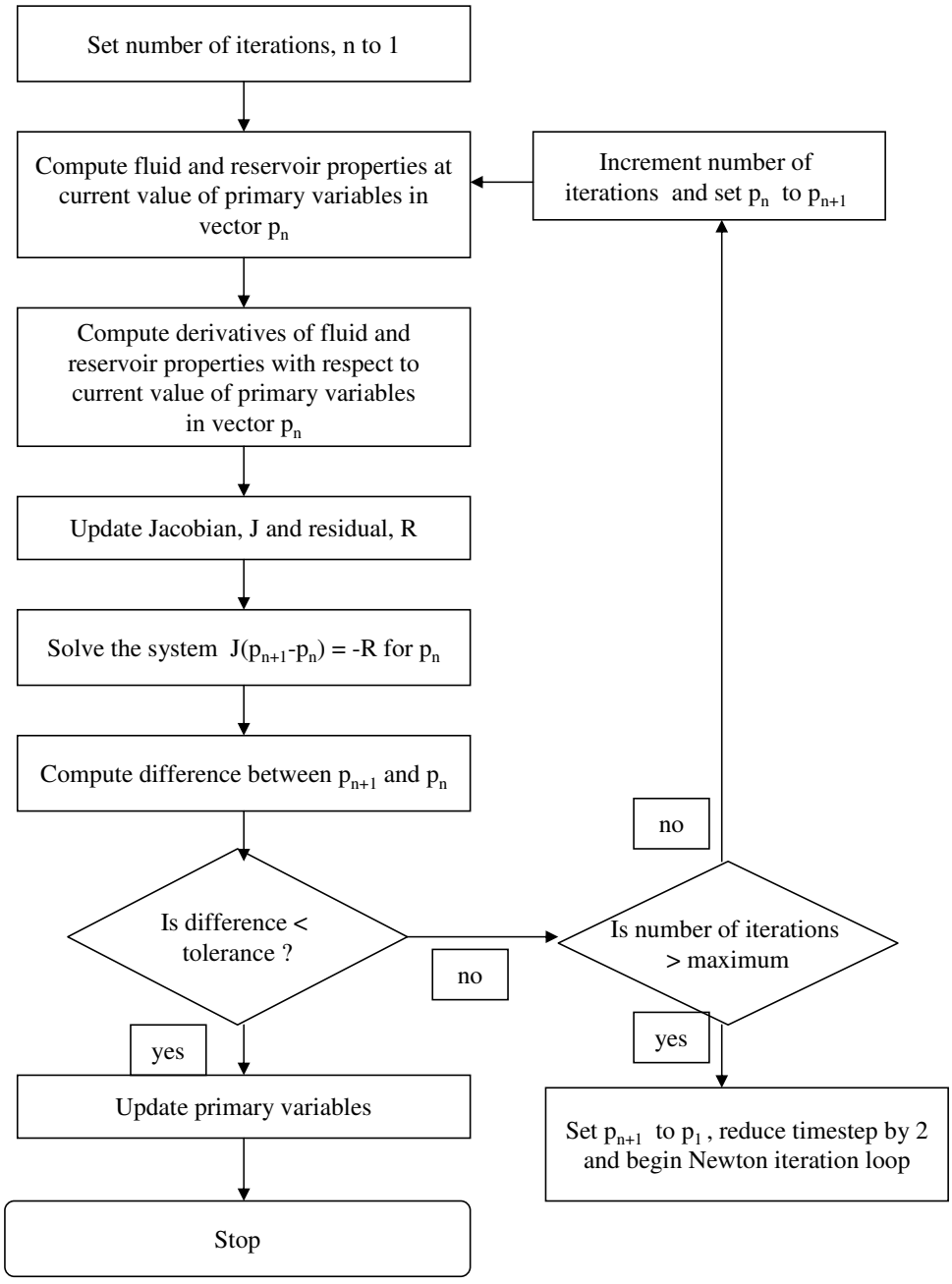

Figure C.2: Flow chart for Newton iterations

Test Cases

In order to test the routines as well as the accuracy of the simulator, various runs were made. It has been established in the literature, as reviewed in Chapter 2, that for systems with single-component, single phase incompressible fluids, the critical Rayleigh number is $4\pi^2$. Chapter 5 shows the results for a single-phase incompressible fluid. Those figures are shown again here for clarity.

Table C.1: Reservoir and fluid properties for Rayleigh number analysis.

Reservoir properties	
Dimensions	2000m x 100m x 450m
Grid	20x1x20
Porosity	0.25
Permeability	10 d
Thermal conductivity	120 kJ/kgK
Rock heat capacity	95 kJ/kg
Temperature difference across lower and upper boundaries	50 K
Fluid properties	
Average density	950 kg/m^3
Specific heat capacity	4.5 kJ/kgK
Molecular weight	18kg
Coefficient of thermal expansion	2E-04 K^{-1}
Oil viscosity	standard values of viscosity of liquid water as a function of temperature

Figure C.3 shows the composition profile at a Rayleigh number of 35, below the critical number of $4\pi^2$. When the Rayleigh number is greater that the critical value (44.3 in this case), Figure C.4 was obtained.

Tilted reservoirs, with horizontal and vertical hydrostatic pressure gradients, do not need additional forces or perturbations for convection to occur. Convection of fluids occurs readily in such reservoirs, as shown in Figure C.5.

The convection components of the simulator were also tested by adding a well to

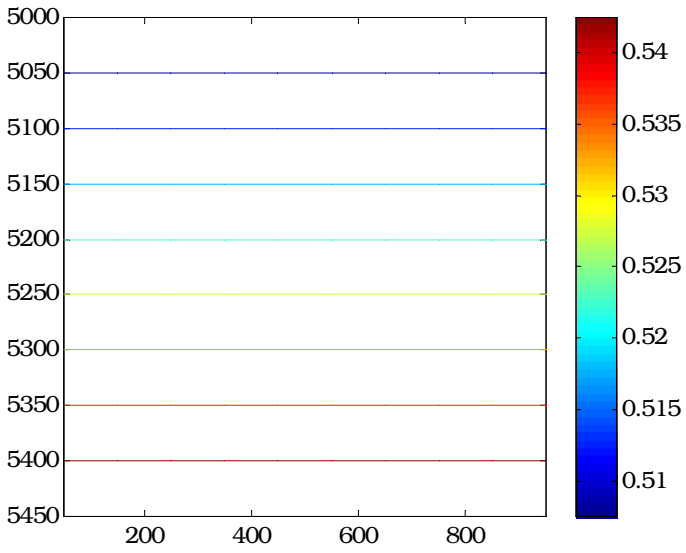

Figure C.3: Concentration profile for Ra = 35.
[Fluid in stable configuration, no motion]

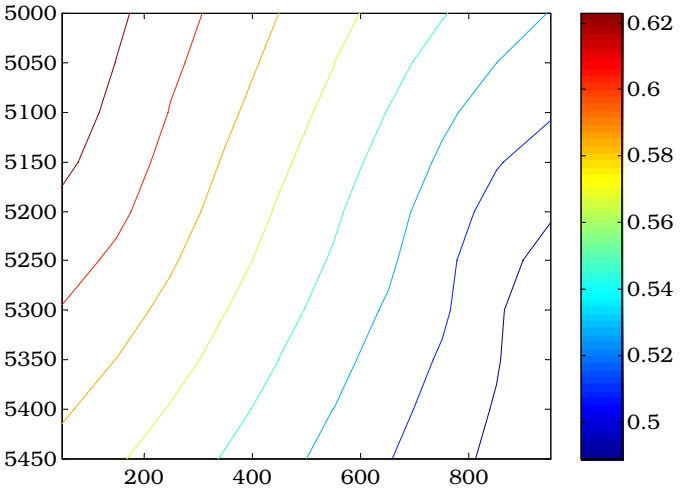

Figure C.4: Concentration profile for Ra = 44.3.
[Fluid motion occurring]

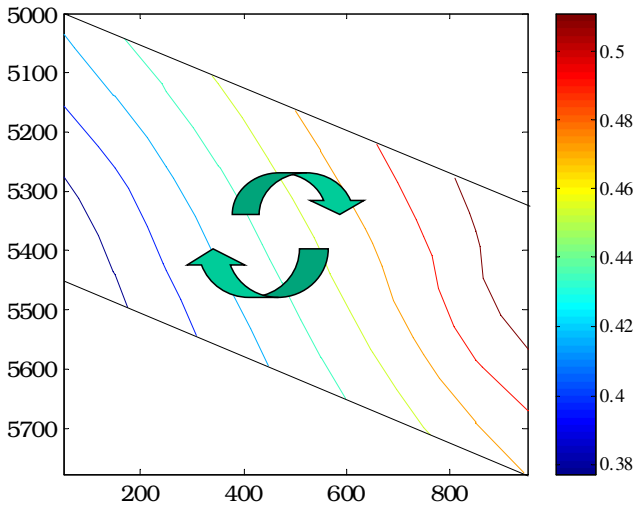

Figure C.5: Concentration profile in a tilted reservoir.
[Fluid motion occurs irrespective of value of Ra]

Table C.2: Reservoir and fluid properties for comparison to Eclipse.

Dimensions	1000m x 100m x 1000m
Porosity	0.25
Permeability	100md
Datum reservoir pressure	150bar
Datum reservoir temperature	1003K
Rock heat capacity	1800KJ/kgK
Rock conductivity	280KJ/kg
Components	C_3 and C_8
Oil production rate	$25m^3/day$

the program and comparing test runs including oil production to the same runs made in Eclipse, a commercial simulator. Table C.2 lists the reservoir and fluid properties. Figure C.6 shows a comparison of the well block pressure obtained using Eclipse to those of the program. These pressures match well in this case, as do the oil molar density and composition.

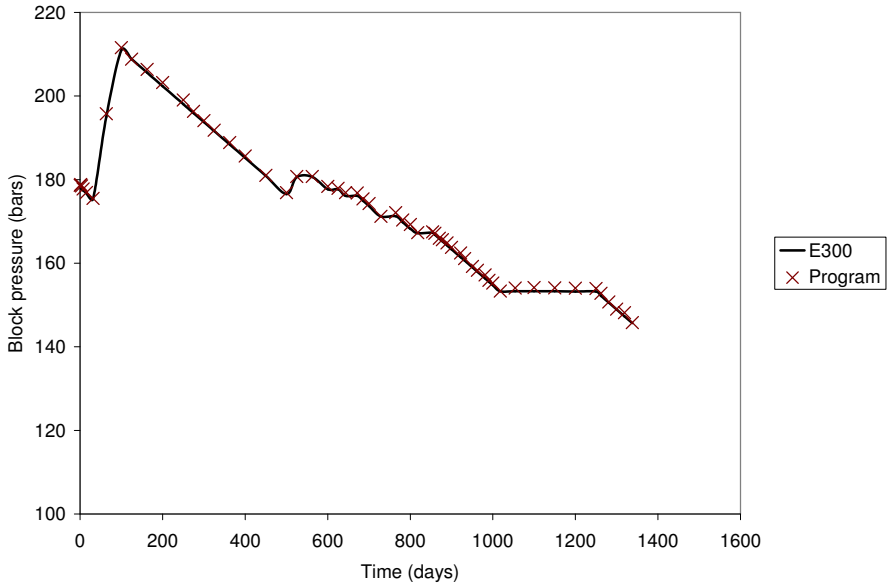

Figure C.6: Comparison of well block pressures
[Eclipse E300 thermal simulator]

Sensitivity Analysis on Grid Sizes

To check the consistency of the program, sensitivity analysis on grid sizes was also done. The results at a point or location within the reservoir are expected to be essentially the same irrespective of the amount of refinement applied to the grid, once a sufficiently fine grid is used. Table C.3 lists three grids and their dimensions that are used in the same reservoir. Figure C.7 shows the z-averaged absolute x-velocity. From this figure, the velocities at predefined locations within the reservoir are the same irrespective of the size of the gridblocks.

Table C.3: Grids and dimensions for consistency check.

25 x 25 x 25	20 x 20 x 20 m^3
50 x 50 x 50	10 x 10 x 10 m^3
100 x 100 x 100	5 x 5 x 5 m^3

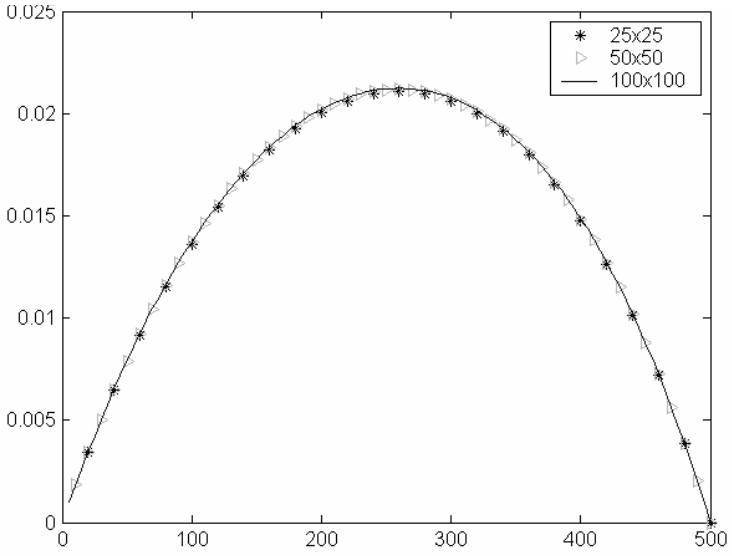

Figure C.7: Z-averaged velocities at predefined locations within the reservoir.

Appendix D

Program Interface

This chapter contains copies of the main routine and the headers for the various subroutines.

mainroutine.cpp

This is the central routine to the program. It shows how the program breaks down the routines as shows in Figure C.1.

```
#include "mainroutine.h"

int main(string file)
{
    clock_t start = clock();
    clock_t finish =0;

    reservoir A(file);
    reservoir& copyA = A;
    vector<double> POld(A.matSize, 0.0), Pk(A.matSize, 0.0);

    A.InitialGuess(POld);
    A.CompProp(POld);
```

```
if ((A.gibbs)&& (!A.boussinesq)){
    A.Gibbs(POld);
}else{
    A.Initialize(POld);
}
A.Metrics(POld);

double t = 0.0, normerr = 0.0, dt = 0.0005;
double lastT = 0.0; double& rlastT = lastT;
WriteOutput(POld, t, copyA, rlastT, file);
while (t<=A.tMax){
    int k=0; Pk = POld; vector<double> Pkk(A.matSize, 0.0);
    while (k < maxit){
        A.rhocp_av = A.kinvisc_av = A.totheight = A.dt_av = 0.0;
        A.visc_av = A.av_vel = 0.0;
        A.CompProp(Pk);
        int size = A.numPVar*(6*A.matSize -2*A.numPVar*
            (A.nx*A.ny +A.nz*A.ny + A.nx*A.nz));
        vector<double> mainD(A.matSize*A.numPVar, 0.0);
        vector<double> offD(size, 0.0), R(A.matSize, 0.0);

        ResJac(R, mainD, offD, Pk, POld, dt, copyA);
        Pkk = Solver(mainD, offD, R, Pk, copyA);
        bool negval = true; bool& rneg = negval;
        if (NormErr(Pkk, Pk, A, rneg)){
            break;
        }
        Pk = Pkk;
        k++;
        R.clear(); mainD.clear(); offD.clear();
    }
```

```
        if (k < maxit){
            if (A.firstStep) A.firstStep = false;
            t += dt;
            Velocity(Pkk, copyA);
            A.Metrics(Pkk);
            WriteOutput(Pkk, t, copyA, rlastT, file);
            dt = TimeStep(dt, Pkk, POld, A, t);
            POld = Pkk;
        } else {
            dt /=2;
            Pk = POld;
            if (dt <mindt){
                exit (-1);
            }
        }
    }
    finish = clock();
    double totalTime = (double)(finish-start)/CLK_TCK/60/60;
    unsigned int startrep = file.find(".txt");
    file.replace(startrep, file.size(), "_steps.txt");
    ofstream jFile(file.c_str(), ios::out|ios::app);
    jFile<<totalTime<<" hours"<<endl;
    return 1;
}
```

mainroutine.h

This is the main header file. It contains links to all the other headers files, and source files by extension, and also to the solvers and external programs that are used.

```
#ifndef _mainroutine_h
#define _mainroutine_h

// header files
#include <iostream>
#include <cstdlib>
#include <time.h>

// solver header files
#include "Solver\sparselib\headers\ilupre_double.h"
#include "Solver\sparselib\headers\compcol_double.h"
#include "Solver\sparselib\headers\iohb_double.h"
#include "Solver\sparselib\headers\spblas.h"
#include "Solver\sparselib\headers\mvm.h"
#include "Solver\sparselib\headers\mvvtp.h"
#include "Solver\sparselib\headers\mvblasd.h"
#include "Solver\sparselib\headers\gmres.h"

// cammva header file
#include "Solver\Cammva\headers\cammva.h"

// program header files
#include "reservoir.h"
#include "residual.h"
using namespace std;
```

```
/* Solver, Solve, Redo, Newx
 * ----------------------------------------
 * Subroutines for calling iterative solver and calculating
 * new values of primary variables.
 */
vector<double> Solver(const vector<double>& mainD,
    const vector<double>& offD, const vector<double>& R,
    const vector<double>& Pk, const reservoir& base);
void Solve(const vector<vector<double> >& J,
    const vector<double>& Pk, const vector<double>& R,
    vector<double>& Pkk);
CompRow_Mat_double Redo(CompRow_Mat_double J, int fixed_location);
VECTOR_double Redo(VECTOR_double y, int fixed_location);
VECTOR_double Newx(VECTOR_double y, int fixed_location);

#endif
```

reservoir.h

This header file lists the various classes that are defined, such as the fluid class, the reservoir class, the gridcell class and the component structure. These classes and structures form the basis for the entire program as all routines apart from the main routine were written around them.

```
#ifndef _reservoir_h
#define _reservoir_h

#pragma warning(disable: 4786)

// header files
#include <iostream>
#include <cstring>
#include <cmath>
#include <string>
#include <vector>
#include <algorithm>
#include <fstream>
#include <iomanip>
#include "eosutilities.h"
using namespace std;

typedef vector<vector<double> > matrix;

// enumerations
typedef enum{xcoord = 1, ycoord, zcoord} coord;
typedef enum{b = 1, c, f, e, m, n}cube;
typedef enum{oilphase =1, gasphase, waterphase} phase;
typedef enum{compbal = 1, totalbal, waterbal, energybal} equation;
typedef enum{presvar = 1, compvar, satvar, tempvar} variable;
```

```
// class gridCell: individual cellblock properties
class gridCell
{
public:
    double overT, underT, nusselttop, nusseltbot, Nuf;
    double dip, cpmix;
    double Uo, Uw, Ug, Uo_old, Uw_old, Ug_old, dUo_dp, dUg_dp;
    double dUo_dT, dUw_dT, dUg_dT, dUw_dp;
    double phi, phinot, phi_old, kx, ky, kz, lx, ly, lz, depth;
    double T, Tnot, p, pnot, po, pg, pw, pcog, pcow, dpcog_dsg;
    double dpcow_dsw;
    double mrhoo, mrhog, mrhow, sgo, sgg, sgw, muo, mug, muw, k;
    double entho, enthg, enthw, dentho_dp, dentho_dT, denthg_dp;
    double denthg_dT, denthw_dp, denthw_dT;
    double entho_old, enthw_old, enthg_old;
    double volo_old, volg_old, volw_old, So, Sg, Sw;
    double dmrhoo_dp, dmrhoo_dT, dsgo_dp, dsgo_dT, ux_oil;
    double uy_oil, uz_oil;
    double dmrhog_dp, dmrhog_dT, dsgg_dp, dsgg_dT, ux_gas;
    double uy_gas, uz_gas;
    double dmrhow_dp, dmrhow_dT, dsgw_dp, dsgw_dT;
    double dlambdao_dp, dlambdao_dT, dlambdag_dp, dlambdag_dT;
    double dlambdaw_dp, dlambdaw_dT;
    double dlambdao_dS, dlambdag_dS, dlambdaw_dS;
    double dphi_dp, kro, krg, krw, lambdao, lambdag, lambdaw;
    double dkrw_dsw, dkro_dsw;

    vector<double> dmrhoo_dx, dsgo_dx, dmrhog_dy, dsgg_dy;
    vector<double> dlambdao_dx, dlambdag_dy;
    vector<double> dentho_dx, denthg_dx, dUo_dx, dUg_dx;
```

```
    vector<double> x, y, z, Kyx, volx_old, voly_old;
    // live oil composition and relative permeabilities

    gridCell();
    setToZero(int num);
    ~gridCell();
};

struct component
{
public:
    double visc, heatcap, mw, tc, tboil, pc, vc, zc, omega;
    double sg, dP, dT;
    double k, fl, fv, phil, phiv;
    double cpA, cpB, cpC, cpD, Hvap, Tvap, cpgas, cp_dT;
    double muA, muB, muC;
    double rhoref, cref, thermref;
    vector<double> dX; // diffusion coefficients
    string name;
};

class fluid
{
public:
    //vector of data for each component
    vector<component> compData;
    vector<vector<double> >Kij;
    vector<double> x, y, z, K, znot;
    vector<double> betax, xnot;
    double dz_dp, dz_dT;
    vector<double> dz_dx, df_dp, dphi_dp;
```

```
vector< vector<double> > df_dx, dphi_dx;
double amv, bmv, aml, bml;
vector<double> a_comp, b_comp;
double L, zL, zV, vV, vL, R;
double liq_mdens, liq_visc, liq_sg, liq_enth;
double vap_mdens, vap_visc, vap_sg, vap_enth;
double Tnot, pnot, rhonot, viscnot, betaT;;
double T_std, Moil, Mgas;
int numComps;

/* VLE subroutines
* -------------------------------------
* Subroutines to calculate fluid properties based
* on compositions obtained from flash routine.
*/
void EOSSolve(double T, double p, vector<double> &roots,
          int& num, bool vapour);
void EOS(double T, double p, bool vapour);
void Vol(double t, double p);
void Deriv(double T, double p, bool liquid);
void Rounds(double t, double p, int numHCPhases);
bool Converged(void);
void KEstimate(double t, double p);
void Flash(int numHCPhases);
void Feval(double& func, double& deriv, double L) const;
void CalcFug(double t, double p, bool vapour);
void GibbsFug(double T, double p);
void Enth(double T);
void HeatCapacity(double T);
fluid();
~fluid();
```

```
};

struct well{
public:
    int wellx, welly, wellz;
    double flowrate, pres, rw;
    bool bhp;
};

// class reservoir: reservoir properties and component properties
class reservoir
{
public:
    bool thermal, molDiff, pDiff, TDiff, metric, firstStep;
    bool wellPI, gibbs;
    bool boussinesq, fixed, deadoil;
    bool oil, water, gas;
    double g, alpha, p_atm, pRef, TRef;
    double T_kel, stdT, stdp;
    bool ktemp, kporo, kperm;
    int nx, ny, nz, matSize, fixed_block;
    int numComps, numPVar, numPhases, numHCPhases;
    double dimx, dimy, dimz;
    double pDatum, tops, dDatum, TDatum, k_r, cp_r, cr_r;
    double cr_water;
    double pnot, fixed_val;
    double dip;
    double tMax, dtMax;  // time for simulation
    int numOutput;
    double gradX, gradY, gradZ;
    double Nusselt, Rayleigh, RhoFac, RhoFac1, av_vel;
```

```
double phi_av, k_av, rhocp_av, kinvisc_av, totheight;
double dt_av, visc_av;

well prod;

// vector of data for each grid cell
vector<gridCell> gridData;

// fluid mixture
fluid mixture;

// constructor, destructor
//reservoir();
reservoir(string datafile);
~reservoir();

/* subroutines to initilaize reservoir properties and
 * unknowns, calculate fluid and rock properties
 */
void SetToZero(void);
void InitializeFluid(string pvtfile, string kijfile);
int Loc(int i, int j, int k, int &locMat) const;
void CompProp(const vector<double>& P);
void Gibbs(vector<double>& P);
void Viscosity(double T, double pres, int a);
void Porosity(double p, int pos);
void Enthalpy(double T, int a);
void Initialize(vector<double>& POld);
void InitialGuess(vector<double>& POld);
void MolarDensity(double T, double p, bool vapour, int a);
void Boussinesq(double T, int a);
```

```
    void reservoir::Vogel(int a, double T);
    int vlength();
    double Capillary(int loc, phase B);
    void RelPerm(int a);
    double Visc_ratio(double tr, double pr, double sg);

    /* Accum, MatTJ
     * ---------------------------
     * Subroutines to populate Jacobian matrix and unknown vector
     */
    void Accum(const vector<double>& P, const vector<double>& POld,
        int a, int b, double dt, vector<double>& R,
        vector<double>& mainD) const;
    void MatTJ(const vector<double>& P, vector<double>& R,
        vector<double>& mainD, vector<double>& offD, int a, int a1,
        int b, int b1, coord axis, double dt, int offDloc) const;
    void Metrics(const vector<double>& P);
    void GridblockCentres(vector<double>& centrex,
        vector<double>& centrey, vector<double>& centrez) const;
    void VelCalcLocs(vector<double>& centrex,
        vector<double>& centrey, vector<double>& centrez) const;
    void HeatLoss(int a, int b, const vector<double>& P,
        double dt, cube side, int i, vector<double>& mainD,
        vector<double>& R) const;
};

//viscosity
int viscosity_ratio(double tpr, double ppr, double spgr, double& val);


#endif
```

gridloc.h

This header file contains functions that write the output from the code, calculate averages and other geometric functions required. Also listed are the functions for calculating the timesteps and errors for the Newton iterations.

```
#ifndef _gridloc_h_
#define _gridloc_h_

#include "reservoir.h"

/* Valid, ThermalBoundary
 * ----------------------
 * Ensures that the grid blocks i+1, j+1, k+1 are within the reservoir
 */
bool Valid(int i, int j, int k, cube subMatrix, const reservoir& base);
bool ThermalBoundary(int i, int j, int k, cube subMatrix,
    const reservoir& base);

/* Loc
 * ----
 * Returns the location of the grid cell with coordinates i, j, k
 * in the vector of grid cell properties in the reservoir.
 */
int Loc(int i, int j, int k, int &locMat, const reservoir& base);

/* Geometric
 * ----------
 * Computes the geometric component of the transmissbility term.
 */
double Geometric(int a, int b, const reservoir& base, coord axis);
```

```
/* DiffGeom
 * --------
 * Computes the geometric component of the diffusion term.
 */
double DiffGeom(int a, int b, const reservoir& base, coord axis);

// conduction part
double GeomCond( int a,  int b, const reservoir& base,coord axis);

double Average_perm(int a, int b, const reservoir& base, coord axis);

/* Norm
 * ----
 * Computes the 2 norm of a vector R, with the pressure and the
 * component mass fraction weighted differently.
 */
bool NormErr(const vector<double>& PNew, const vector<double>& POld,
    const reservoir& base, bool& rneg);

/* Timestep
 * ---------
 * Computes the next time step to be taken based on the changes
 * in the proimary variables
 */
double TimeStep(double dt, const vector<double>& PNew,
    const vector<double>& POld, const reservoir& base, double t);
```

```
/* GibbsErr
 * --------
 * Computes the mean squared error in the vector P
 */
double GibbsErr(vector<double> PNew, vector<double> POld,
    int numComps);

/* Vel
 * ---
 * This function computes the bulk velocity based on darcy's law
 * between two gridblocks
 */
double Vel(const reservoir& base, const vector<double>& P, int a,
    int ab, int n, int nb, coord axis);

/* Velocity
 * ---------
 * This is the wrapper function for the computation of the bulk
 * velocity for every grid block in the reservoir.
 */
void Velocity(const vector<double>& P, reservoir& base);

/* WriteOutput
 * -----------
 * Writes the data to file, temperature, pressure, molar density
 * and velocity
 */
void WriteOutput(const vector<double>& P, double t,
    const reservoir& base, double& lastT, const string file);

#endif
```

residual.h

This file contains references to routines that are called directly to compute the Jacobian matrix and the residual vector. Apart from the routines that are functions of the reservoir class, all other routines computing parts of the accumulation and flow terms, including differentials are listed under the residual.h file.

```
#ifndef _residual_h_
#define _residual_h_

#include "gridloc.h"


/* ResJac
 * ------
 * Wrapper function for the residual and jacobian.  Loops over
 * the possible directions with active cells around a gridblock.
 * The accumulation and thermal conductivity are computes for
 * each grid block later.
 */
void ResJac(vector<double>& T, vector<double>& mainD,
    vector<double>& offD, const vector<double>& P,
    const vector<double>& POld, double dt,
    const reservoir& base);

/* Subroutines to compute the differential of various terms
 * with respect to the primary variables
 */
double TotalDp(const gridCell& base, double g, double delZ,
    double thou, phase B);
```

```
double TotalDT(const gridCell& base, double g, double delZ,
    double thou, phase B);

double TotalDS(const gridCell& base, double g, double delZ,
    double thou, phase B);

double TotalDx(const gridCell& base, double g, double delZ,
    double thou, phase B, int k);

double EnergyDp(const gridCell& base, double g, double delZ,
    double thou, phase B);

double EnergyDT(const gridCell& base, double g, double delZ,
    double thou, phase B);

double EnergyDx(const gridCell& base, double g, double delZ,
    double thou, phase B, int k);

#endif
```

Nomenclature

C	solute concentration
c_p	constant pressure heat capacity
c_r	rock compressibility
D	diffusion coefficient
D_m	mass diffusivity
f	fugacity
g	acceleration due to gravity
H	enthalpy
h	convection heat transfer coefficient
J	diffusion flux
$\bar{k}$	interaction parameter
k	permeability
k_f	thermal conductivity of fluid
k_r	relative permeability
K_{rrT}	rock thermal conductivity
L	characteristic length

Le	Lewis number
N	buoyancy ratio
Nu	Nusselt number
p	pressure
q_S	rate of solute production
Q_T	rate of heat production
R	universal gas constant
Ra	Rayleigh number
Ra_S	Solutal Rayleigh number
S	saturation
T	temperature
t	time
U	internal energy
$\mathbf{u}$	Darcy velocity
x	distance
$\mathbf{x}$	coordinates
y	component mole fraction
Z	compressiblity factor
	GREEK
α	thermal diffusivity
α	volumetric thermal expansion coefficient

α_S	concentration expansion coefficient
α_T	thermal expansion coefficient
Δ	difference
λ	effective thermal conductivity of fluid-filled medium
μ	dynamic viscosity
ν	kinematic viscosity
ω	acentric factor
ϕ	porosity
ρ	density
	SUPERSCRIPTS
$'$	perturbation variable
$\hat{}$	dimensionless variable
m	molar
c	component
	SUBSCRIPTS
c	critical value
f	fluid
p	phase
p	pressure
pr	pseudoreduced
r	reduced value

rr	reservoir rock
S	solute
T	thermal

Bibliography

G.H. Alani. Volumes of Liquid Hydrocarbons at High Temperature and Pressures. *Petroleum Transactions, AIME*, 219:288–292, August 1960.

M.A. Christie and M.J. Blunt. Tenth SPE Comparative Solution Project: A Comparison of Upscaling Techniques. *paper 66599 presented at the SPE Reservoir Simulation Symposium held in Houston, Texas*, 11-14 February 2001.

K.H. Coats. In-Situ Combustion Model. *SPE Journal*, pages 533–554, December 1980.

R.E. Cunningham and R.J.J. Williams. *Diffusion in Gases and Porous Media*. Plenum Press, New York, 1980.

F.V. da Silva and P. Belery. Molecular Diffusion in Naturally Fractured Reservoirs: A Decisive Recovery Mechanism. *paper 19672 presented at the SPE Annual Technical Conference and Exhibition, San Antonio, Texas*, October 1989.

B. Faissat, K. Knudsen, E.H. Stenby, and F. Montel. Fundamental Statements about Thermal Diffusion for a Multicomponent Mixture in a Porous Medium. *Fluid Phase Equilibria*, 100:209–222, 1994.

K. Ghorayeb and A. Firoozabadi. Modeling Multicomponent Diffusion and Convection in Porous Media. *SPE Journal*, 2(5):158–1710, June 2000a.

K. Ghorayeb and A. Firoozabadi. Molecular, Pressure and Thermal Diffusion in Nonideal Multicomponent Mixtures. *AIChE Journal*, 46(5):883–900, May 2000b.

K. Ghorayeb and A. Firoozabadi. Numerical Study of Natural Convection and Diffusion in Fractured Porous Media. *SPE Journal*, 1(5):12–20, March 2000c.

A.N. Hamoodi, A.F. Abed, and J. Grabenstetter. Modeling of a Large Gas-Capped Reservoir with Areal and Vertical Variation in Composition. *paper SPE 28937 presented at the 69th Annual SPE Technical Conference and Exhibition*, 25-28 September 1994.

R.N. Horne. *Transient Effects in Geothermal Convective Systems*. PhD thesis, School of Engineering, Department of Theoretical and Applied Mechanics, Univerisity of Auckland, March 1975.

D. Jacqmin. Convection of a Gravity Segregating Fluid Forced by a Horizontal Temperature Gradient. In D.A. Drew and J.E. Flaherty, editors, *Mathematics Applied to Fluid Mechanics and Stability: Proceedings of a Conference Dedicated to Richard C. DiPrima*, pages 263–273, Philadelphia, 1985. SIAM Press.

D. Jacqmin. Interaction of Natural Convection and Gravity Segregation in Oil/Gas Reservoirs. *SPE Reservoir Engineering*, pages 233–238, May 1990.

A. Kovseck. *PEN 251: Petroleum Hydrocarbon Thermodynamics*. Stanford University, September 2001.

J.L. Lage and D.A. Nield. Convection Induced by Inclined Gradients in a Shallow Porous Medium Layer. *Journal of Porous Media*, 1(1):57–69, 1998.

E.R. Lapwood. Convection of Fluid in a Porous Medium. *Proc. Cambridge Phil. Soc.*, 44:508–521, 1948.

J. Lohrenz, B.G. Bray, and C.R. Clark. Calculating Viscosities of Reservoir Fluid from Their Compositions. *Journal of Petroleum Technology*, 16:1171–1176, October 1964.

D.M. Manole. *Theoretical and Numerical Analysis of Mono and Double Diffusive Convection in Porous Media*. PhD thesis, School of Engineering and Applied Sciences, Southern Methodist University, May 1995.

D.M. Manole, J.L. Lage, and D.A. Nield. Convection Induced by Inclined Thermal and Solutal Gradients, with Horizontal Mass Flow in a Shallow Horizontal Layer of a Porous Medium. *International Journal of Heat and Mass Transfer*, 37(14): 2047–2057, 1994.

R.S. Metcalfe, J.L. Vogel, and R.W. Morris. Compositional Gradients in the Anschutz Ranch East Field. *SPE Reservoir Engineering*, 3(3):1025–1032, August 1988.

F. Montel, J.P. Caltagirone, and L. Pebayle. A Convective Segregation Model Predicting Reservoir Fluid Compositional Distribution. In P.R. King, editor, *The Mathematics of Oil Recovery*, pages 85–113. Clarendon Press, Oxford, 1992.

R.D. Moser. Mass Transfer by Thermal Convection and Diffusion in Porous Media. *Presented at the 10th International Conference on Applied Mathematics held in Austin, Texas*, June 1986.

D.A. Nield. Convection in a Porous Medium with Inclined Temperature Gradient. *International Journal of Heat and Mass Transfer*, 34(1):87–92, 1991.

D.A. Nield and A. Bejan. *Convection in Porous Media*. Springer-Verlag, New York, 2nd edition, 1999. ISBN 0-387-98443-7.

K.G. Padua. Non-Isothermal Gravitational Composition Variation in a Large Deep Water Field. *paper SPE 38854 presented at the Annual SPE Technical Conference and Exhibition held in San Antonio, Texas*, 5-8 October 1997.

K.G. Padua. Nonisothermal Gravitational Equilibrium Model. *SPE Reservoir Evaluation and Engineering*, 2(2):211–216, April 1999.

Z. Qiao and P.N. Kaloni. Convection in a Porous Medium Induced by an Inclined Temperature Gradient with Mass Flow. *Journal of Heat Transfer*, 119:366–370, May 1997.

M.F. Riley and A. Firoozobadi. Compositional Variation on Hydrocarbon Reservoirs with Natural Convection and Diffusion. *AIChE Journal*, 44(2):452–464, Feb 1998.

A.M. Schulte. Compositional Variations within a Hydrocarbon Column Due to Gravity. *paper SPE 9235 presented at the 55th Annual SPE Technical Conference and Exhibition, held in Dallas, Texas*, 21-24 September 1980.

A.A. Shapiro. Evaluation of Diffusion Coefficients in Multicomponent Mixtures by means of the Fluctuation Theory. *Physica A: Statistical Mechanics and its Applications*, 320:211–234, March 2003.

P.M. Sigmund. Prediction of Molecular Diffusion at Reservoir Conditions. Part I - Measurements and Prediction of Binary Dense Gas Diffusion Coefficients. *Journal of Canadian Petroleum Technology*, pages 48–57, 1976.

K.O. Temeng, M.J. Al-Sadeg, and W.A. Al-Mulhim. Compositional Grading in the Ghawar Khuff Reservoirs. *paper SPE 49270 presented at the Annual SPE Technical Conference and Exhibition held in New Orleans, Louisiana*, 27-30 September 1998.

R.E. Treybal. *Mass-transfer Operations*. McGraw-Hill Book Company, Singapore, 3rd edition, 1980.

D.L. Turcotte and G. Schubert. *Geodynamics: Application of Continuum Physics to Geological Problems*. Cambridge University Press, Cambridge, NewYork, 2nd edition, 2002.

J.S. Turner. Double-diffusive Phenomena. *Annual Review of Fluid Mechanics*, 6: 37–56, 1974.

J.S. Turner. Multicomponent Convection. *Annual Review of Fluid Mechanics*, 17: 11–44, 1985.

J.R. Wood and T.A. Hewett. Fluid Convection and Mass Transfer in Porous Sandstones- A Theoretical Model. *Geochimica et Cosmochimica Acta*, 46:1707–1713, May 1982.